Spring 5-8-2021

Characterization of Di-Aryl Urea Compounds Against Acute and Chronic Toxoplasma Gondii

Austin Sanford
University of Nebraska Medical Center

CHARACTERIZATION OF DI-ARYL UREA COMPOUNDS AGAINST ACUTE AND CHRONIC *TOXOPLASMA GONDII*

By

Austin Gregory Sanford

A DISSERTATION

Presented to the Faculty of The University of Nebraska Graduate College in Partial Fulfillment of the Requirements for the Degree of Doctor of Philosophy

Pathology & Microbiology Graduate Program

Under the Supervision of Professor Paul H. Davis

April 2021

Supervisory Committee

Paul Fey, Ph.D.

Corey Hopkins, Ph.D.

Guangshun Wang, Ph.D.

Paul H. Davis, Ph.D.

ACKNOWLEDGMENTS

I would first like to thank my mentor Dr. Paul H. Davis. He has been instrumental in my development as a scientist from my first day in his laboratory seven years ago as an undergraduate sophomore at The University of Nebraska at Omaha. The opportunities that he has provided me gave me the chance to explore a career in infectious disease research in multiple labs and meet peers who I now consider my closest friends. His mentorship allowed for my growth as a researcher, be able to think critically, how to lead a team, and learn vital skills on how to teach others in the lab. Going forward, I will always be thankful for where I am in my career as a scientist because of Dr. Davis.

Secondly, many thanks go to my fellow current and past lab members of the Davis lab. Especially my peers and close friends: Matthew Martens, Thomas Schulze, Elyssa Darner, Ryan Hemsley, Ryan Grove, and LeeAnna Lui. From assisting me with *in vivo* and bioinformatic experiments that would have taken exponentially more time to complete without their help to being my fellow peers and providing their feedback, they all were instrumental to my research.

Many thanks go to Dr. Jonathan Vennerstrom and his previous graduate student Dr. Derek Leahs at the University of Nebraska Medical Center. Their research was instrumental in the development of the experimental compounds that were the foundation of my dissertation work. Without their support, my project would not have been possible.

I would like to thank my family. My mother and father John and D'lisa Sanford have provided their constant support throughout my graduate career which allowed me to truly focus on my studies and research. Throughout primary school, to my undergraduate career, and finally my graduate career they have always been there for me. As parents, they raised me to always put my best foot forward and to keep my head

held high. These life skills have proved to be exemplary to my development as a scientist. My older brothers, John and Zachery Sanford, have always lent their brotherly advice and have dealt with many of my ramblings regarding my research.

Lastly, I would like to thank my wife Hailee Sanford. She entered my life as I just began my graduate career. The countless hours she has lent her support and ear during my lows and her praise when truly encouraged me to work as hard as possible day to day. Not only do I love her, but I owe her my deepest gratitude for supporting me emotionally.

CHARACTERIZATION OF DI-ARYL UREA COMPOUNDS AGAINST ACUTE AND CHRONIC *T. GONDII*

Austin Sanford, Ph.D.

University of Nebraska Medical Center, 2021

Supervisor: Paul H. Davis, Ph.D.

Toxoplasma gondii is an obligate intracellular parasite that has infected nearly 60 million individuals in the United States alone. Acute infection causes ill effects to the fetus *in utero* when mothers are primarily infected, and to immunocompromised individuals. Chronic infection consists of quiescent tissue cysts located primarily in brain tissue and is capable of reverting back to the acute stage causing severe toxoplasma encephalitis in immunocompromised individuals. Current treatments for acute infection are lacking while there are no approved treatments for the clearance of chronic infection. The aim of this research was to evaluate a family of di-aryl urea compounds that had previously been shown to be active against a panel of apicomplexan, kinetoplastid, and helminth parasites for activity against *T. gondii* acute and chronic infection. *In vitro* models were utilized to determine activity against both acute and chronic *T. gondii* infection as well as possible host cellular toxicity. Compounds that exhibited selectivity in our *in vitro* assays were selected for further analysis in an *in vivo* murine model for activity against lethal acute infection in mice. One of the four compounds tested, U21, was successful at achieving 100% survival with no apparent toxicity in mice. Tested compounds did not have any effect on chronic *T. gondii* in a murine model. In efforts to identify a possible mode of action of U21 random mutagenesis, electron microscopy imaging, and differential expression analysis of treated *T. gondii* was utilized. Through these assays, it was found that U21 treatment may be causing dysregulated *T. gondii* lipid synthesis. Further investigation into dysregulated lipid synthesis caused by U21 is currently underway to confirm if it is indeed a possible mechanism of action.

Table of Contents

LIST OF FIGURES

LIST OF TABLES

LIST OF ABBREVIATIONS

AIDS	Acquired Immunodeficiency Syndrome
IFN	Interferon
TNF	Tumor Necrosis Factor
IL	Interleukin
FDA	Federal Drug Administration
DHFR	Dihydrofolate Reductase
HIV	Human Immunodeficiency Virus
CNS	Central Nervous System
BBB	Blood Brain Barrier
FAS	Fatty Acid Synthesis
HTS	High throughput Screen
SAR	Structural Activity Relationship
IC_{50}	Concentration that Inhibits 50% of Growth
PSA	Polar Surface Area
PPB	Plasma Protein Binding
CL_{int}	Intrinsic Clearance Ratio
LC-MS	Liquid Chromatography – Mass Spectrometry:
SNPs	Single Nucleotide Polymorphisms
RCM	Random Chemical Mutagenesis
NGS	Next Generation Sequencing
GO	Gene Ontology
EM	Electron Microscopy
SEM	Scanning Electron Microscopy

TEM	Transmission Electron Microscopy
WBR	Worm Burden Reduction
DMSO	Dimethyl Sulfoxide
PMA	Phorbol 12-Myristate 13-Acetate
M-CSF	Macrophage Colony Stimulating Factor
MEP	Methylerythritol Phosphate
EMS	Ethylmethane Sulfonate
qPCR	Quantitative Polymerase Chain Reaction
TgPIS	*Toxoplasma gondii* Phosphatidylinositol Synthase
TgPSS	*Toxoplasma gondii* Phosphatidylserine Synthase
P-gp	P-gylcoprotein

INTRODUCTION

I: *Toxoplasma gondii* Background

Toxoplasma gondii is an obligate intracellular protozoan parasite capable of infecting warm-blooded hosts that has infected approximately a third of the world's population [1]. Infection is characterized by the biological stage of the parasite notated as: tachyzoites, bradyzoites, and sporozoites [2]. In warm blooded animals, such as humans, infection is caused by acutely infecting tachyzoites capable of infecting any nucleated cell which subsequently stage convert to the chronic stage through the conversion of tachyzoites to bradyzoites within tissue cysts primarily residing in deep muscle, cardiac, and brain tissue. Once formed, these tissue cysts cause life-long infection that is unable to be cleared by the host immune system. Humans and other warm-blooded animals only serve as intermediate hosts with members of the Felidae family acting as definitive hosts [2]. The life cycle of *T. gondii* is centered around the definitive host where *T. gondii* can undergo sexual division in the feline's gut. One to two weeks after infection, the infected feline begins to shed parasites in their feces in the form of extremely environmentally stable oocysts containing sporozoites capable of infecting warm-blooded organisms [3]. Humans are commonly infected through the ingestion of contaminated fruits and vegetables as well as drinking contaminated water that contain infective oocysts. Livestock that have an established chronic infection can serve as an additional reservoir for infection and cause subsequent horizontal transmission [3].

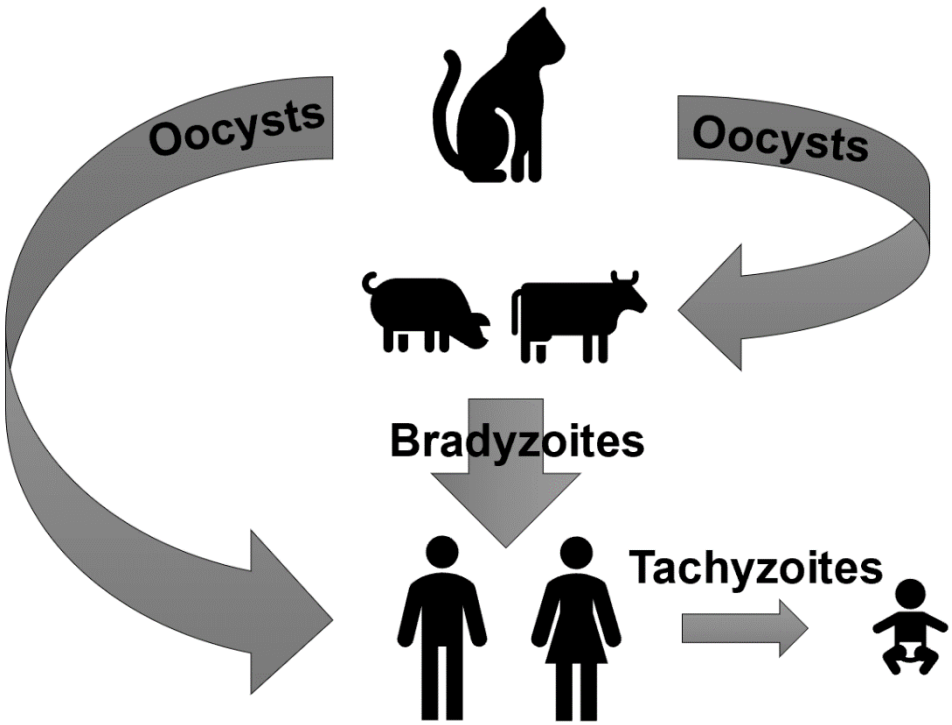

Figure 1: Life Cycle of *Toxoplasma gondii.*

Infection in healthy individuals is usually asymptomatic in approximately 80% of cases [4]. In the remaining 20% of cases, the most common symptoms include: fever, rash, sore throat, and cervical lymphadenopathy [5]. Individuals with severely compromised immune systems such as cancer patients, autoimmune deficiency syndrome (AIDS) patients, and organ transplant recipients can develop much more severe symptoms. If left untreated in these individuals, infection can prove to become life altering and possibly lethal. In these patients, quiescent chronic *T. gondii* infection can revert to the acute stage causing subsequent clinical symptoms. In 30% of *T. gondii* infected and untreated AIDS patients that present with <100 CD4+ T Cells/μL [4], the reversion of bradyzoites to the acute stage, tachyzoites, in brain tissue causes cerebral toxoplasmosis. The decrease in CD4+ T-cells and subsequent decreases in production of IFN-γ is postulated to be the cause of stage reversion [4]. Clinical manifestations of

cerebral toxoplasmosis include severe brain lesions and encephalitis. Patients that are diagnosed with cerebral toxoplasmosis tend to present with headaches, visual abnormalities, behavior changes, and fever [6]. Symptoms in some patients with cerebral toxoplasmosis do not adhere to the listed symptoms and must be properly diagnosed with appropriate brain scans. While epidemiological studies focusing on mortality rates of cerebral toxoplasmosis are scarce, Mboera et. al 2019 reported that 52.9% of *T. gondii* associated deaths in Tanzania were untreated human AIDS patients by cerebral toxoplasmosis and subsequent encephalitis [7].

In pregnant females that are infected for the first time, tachyzoites can cross the placental barrier causing subsequent vertical transmission and congenital infection of the fetus. It is estimated that 1.5 in 1,000 pregnancies and births are affected by congenital toxoplasmosis [8]. Infection during the early stages of pregnancy, first and second trimester, can cause abortions and stillbirth of the fetus. During the later stages of pregnancy, third trimester, it has been shown that infection can cause hydrocephalus, blindness, deafness, and mental/physical retardation of the affected fetus [8]. In some cases, infection can establish in the retina causing toxoplasma retinitochoroiditis with an incidence of 0.6% leading to scarring of the retina and possible degenerative blindness [9].

II: Acute & Chronic *T. gondii* Infection

Acute infection is caused by unicellular crescent shaped tachyzoites that can infect virtually any nucleated cell through host cell mediated phagocytosis or active penetration of the host cell membrane. Upon active infection, tachyzoites form a parasitophorous vacuole in the host cell cytosol and undergo rapid replication by endodyogeny causing eventual lysis and subsequent infection of neighboring host cells [10]. In a healthy host, the adaptive immune response mounts a Th1 type response

following acute infection causing tachyzoites to convert to the quiescent chronic stage [11]. Here, tachyzoites convert to bradyzoites within tissue cysts located primarily in deep skeletal muscle, cardiac, and brain tissue. Once formed, bradyzoites within tissue cysts are unable to be cleared by the host's adaptive immune system therefore causing a life-long infection [2].

It is hypothesized that tissue cysts cannot be cleared by the host immune response due to the expression of bradyzoite specific surface proteins and down-regulation of tachyzoite surface proteins that subsequently modulate host IFN-γ production. Tachyzoite specific surface proteins are known immunodominant antigens and it is postulated that *T. gondii* has evolved to express differentiated surface proteins during chronic infection to circumvent host immune surveillance [12]. Thus far, all identified bradyzoite antigens are poor immuno-stimulators further suggesting that bradyzoites within tissue cysts are actively circumventing the host's immune system to establish a life-long infection [12].

The molecular mechanisms that cause the conversion from acute to chronic *T. gondii* infection have yet to be completely defined. Through *in vitro* studies, it has been shown that depleting nutrients and causing significant biological stresses to tachyzoites can induce tachyzoites to convert to the chronic stage [13]. Through exposure to an alkaline environment *in vitro*, tachyzoites convert to bradyzoites within cysts. Thus, it can be concluded that causing outward stresses on tachyzoites *in vitro* causes the conversion of tachyzoites to the chronic stage of infection. Additionally, through *in vivo* studies it has been shown that the production of IFN-γ has clear effects on stage conversion of *T. gondii* [13]. Acutely infected mice that are unable to produce IFN-γ succumb to acute infection and are unable to form tissue cysts. Additional work has identified other cytokines, tumor necrosis factor (TNF)-alpha and interleukin (IL)-6, that may cause stage conversion [13]. While it is believed that *T. gondii* cysts are unable to

be identified by the hosts' adaptive immune response, recent work suggests that memory CD8+ T-cells can control the number of *T. gondii* cysts located in brain tissue and in the future may serve as a method to clear tissue resident cysts [14]. Therefore, the host immune response to acute infection has a clear part to play in the formation of chronic infection.

III: Treatment of *T. gondii* Infection & The Need for Novel Therapeutics

Therapeutics utilized in clinics to combat acute infection are lacking due to adverse reactions caused by current treatment options. Prescribed anti-Toxoplasma medications in the United States that are approved by the Federal Drug Administration (FDA) to treat acute toxoplasmosis include pyrimethamine and sulfadiazine, commonly administered as a combination therapy [15]. Pyrimethamine targets *T. gondii* DNA replication through inhibition of dihydrofolate reductase (DHFR). While pyrimethamine is highly effective, it can cause severe bone marrow suppression when given for a prolonged period due to folic acid antagonism and is commonly administered with folic acid supplementation [16]. Additionally, pyrimethamine is only provided as Daraprim in the American market causing it to be financially expensive for patients [17]. Through combination treatment, sulfadiazine acts synergistically with pyrimethamine to target *T. gondii* dihydrofolate reductase (DHFR) [15]. As a sulfa based drug, it has the propensity to cause severe allergic reactions in some patients [18]. In addition, sulfadiazine is administered at high dosages up to 375 mg/kg [15] which can be detrimental to the patient causing disruptions in their natural gut flora and requiring further probiotic supplementation [19]. While these treatments are effective against acute toxoplasmosis, they have clear limitations and do not inhibit the transition of tachyzoites to the chronic stage of infection or exhibit activity against already formed tissue cysts containing bradyzoites [20].

Other clinically available medications that exhibit activity against *T. gondii* infection include anticoccidials used in veterinarian medicine. Coccidian agents treated include *Neospora, Sacrocystis,* and *Eimeria.* Veterinarian anticoccidials including toltrazuril, aprinocid, and diclazuril have been shown to be effective *in vitro* against acute *T. gondii* infection with respective concentrations that inhibit 50% of growth (IC_{50}s) of 0.94, 7.2, 0.006 μM [15]. Through *in vivo* survival analysis of mice infected with a lethal amount of *T. gondii* tachyzoites aprinocid (100 μg/day) allowed for 100% survival and diclazurl (1 mg/day) allowed for 100% survival as well [15]. Neither have been investigated for activity against chronic *T. gondii* infection. Toltrazuril administered for 14 days allowed for significant reductions in cyst burden in muscle and heart tissues [15]. For future use in treatment of human *T. gondii* infections, safety analysis must be completed to ensure that there are no severe off target effects. To date, no molecular drug target has been identified for these anticoccidial compounds.

Antibacterial agents have also been extensively investigated for activity against *T. gondii* infection. Unlike anticoccidial veterinary drugs, antibacterial drugs are utilized in clinics for the treatment of acute or recrudescent *T. gondii* infections in humans. Clarithromycin and azithromycin, both macrolide antibiotics, are the most administered antibiotics utilized for *T. gondii* infections in humans [15]. The lincosamide antibiotic, clindamycin, is not as commonly used for the treatment of toxoplasmosis but still is utilized in clinics. No antibacterial drugs to date have been identified to have activity against the chronic stage of *T. gondii* infection [15]**.**

To inhibit recrudescent cysts causing toxoplasma encephalitis in AIDS patients, prolonged treatment of trimethoprim-sulfadiazine is commonly utilized [15]. While effective once prophylactic treatment is suspended, viable *T. gondii* bradyzoites within tissue resident cysts have been observed to recrudesce and cause subsequent acute infections. Interestingly, retroviral therapies are hypothesized to directly affect *T. gondii*

infection in treated patients. *In vitro* activity has been reported with no clear mechanisms yet identified. Didanosine, a known reverse transcriptase inhibitor of human immunodeficiency virus (HIV), at 100 mg/kg in mice allows for a 65% decrease in *T. gondii* cysts located in brain tissue. In AIDS patients that received didanosine treatments a decrease in recrudescent infection is observed suggesting that didanosine may have activity in humans as well as mice. Further work is warranted to characterize how these antiretroviral therapies directly affect both acute and chronic *T. gondii* infections [15].

While clinicians have various options for treating acute *T. gondii* infection, there are no FDA approved medications to prevent or clear the chronic stage of *T. gondii* infection potentially due to the quiescent nature of bradyzoites as well as the structural biology of *T. gondii* cysts. Chronic infection is responsible for recrudescent infection in immunocompromised individuals and is hypothesized to cause adverse physiological effects such as anxiety, schizophrenia, obsessive compulsive disorder, and an increase in risk taking behavior [21]. Previous work with the antimicrobial miltefosine has been shown to significantly reduce cyst numbers by 78% in chronically infected mice [22]. Miltefosine is approved by the United States Centers for Disease Control and Prevention for the treatment of *Naegleria fowleri*; a pathogenic amoeba that infects the central nervous system (CNS) and causes severe inflammation of the CNS and death if not treated appropriately [23]. The chemical profile of miltefosine allows for the treatment of CNS infections due to the ability of the drug to cross the blood-brain-barrier (BBB) [23]. Crossing the BBB is also imperative for the treatment of chronic *T. gondii* because of cysts residing in brain that have the potential to revert to the acute stage thus causing cerebral toxoplasmosis. Drugs and compounds that are unable to cross the BBB due to their chemical profile are likely to be ineffective against tissue cysts residing in brain tissue [24]. Another major hurdle for drug discovery against the chronic stage is penetrating the cyst wall itself to reach the bradyzoites within [13]. Identifying

compounds that can penetrate both the BBB and the cyst wall is imperative for the discovery of potential therapeutics to clear the tissue resident cysts.

To address the issue of the lack FDA approved compounds that are highly effective with limited side effects against acute *T. gondii* infection and the complete lack of drugs that are effective against chronic infection, thousands of compounds have been synthesized for identification of novel compounds that may serve as potential future therapeutics. These include compounds that affect DNA synthesis, steroid synthesis, fatty acid synthesis, transcription, virulence factors, egress, and invasion processes of *T. gondii* [25]. Adequate toxicity screening, *in vitro* and *in vivo*, is lacking for a number of these chemotypes. Activity in *in vivo* models is also lacking with only *in vitro* efficacy data available against acute *T. gondii* infection. Little to no experimental compounds have been screened for activity against chronic *T. gondii* infection in *in vitro* and *in vivo* based assays [25]. The impressive number of compounds that have been screened for activity against *T. gondii* give much needed insight in what chemotypes are effective and what future compounds should be synthesized for the eventual discovery of a novel anti toxoplasma therapeutic.

It is not uncommon for compounds/drugs that are effective against *T. gondii* to be effective against other protozoan species. *Plasmodium*, the causative agent of malaria, is a close relative to *T. gondii* due to both being apicomplexan parasites. Pyrimethamine, a known *DHFR* inhibitor in *T. gondii*, is known to target *DHFR* in Plasmodium as well and causes dysregulated DNA synthesis [26]. Additionally, due to the shared apicoplast organelle, compounds and drugs that target the apicoplast organelle are generally effective in both parasites [27]. Inhibitors of prokaryotic DNA synthesis such as quinolone-based compounds and drugs have been reported to be effective in both Toxoplasma and Plasmodium through hypothesized dysregulated DNA synthesis in the apicoplast organelle [27]. Fatty Acid Synthesis II (FASII) inhibitors shown to be effective

against both gram positive and gram-negative bacteria are also seen to be highly effective against both apicomplexans. Supplementation and genetic based assays suggest that FASII is an essential pathway operational in the apicoplast in most apicomplexans [27]. Thiolactomycin and triclosan, known FASII inhibitors, are effective against both *T. gondii* and *P. falciparum* in *in vitro* assays [27]. It is important to note that antiparasitic drugs and compounds can be effective against a broad panel of parasites, including Plasmodium and Toxoplasma, with others being primarily effective in one species of protozoa.

Thus, the discovery of novel compounds that effectively clear both acute and chronic *T. gondii* infection is of utmost importance to add to the limited arsenal of therapeutics. The discovery of novel antiparasitic compounds can either focus on screening a large library of compounds through a high throughput screen (HTS) or designing a compound to bind to a specific target such as a known essential enzyme of *T. gondii* [28, 29]. For this work and dissertation, the HTS method will be utilized for novel anti-toxoplasma compound discovery.

IV: Discovery and Development of Anti-Toxoplasma Compounds

Once a singular compound, or a family of compounds, has been identified to be effective against *T. gondii* through HTS or other screening, derivatives can then be synthesized. This is a commonly used method for the discovery of novel compounds for therapeutic discovery and focuses on screening many compounds in a high throughput-based assay to identify top compounds. Once a compound is discovered to be effective in an HTS, said compound can be altered through the synthesis of derivatives to screen for improvements made during derivatization. Once improvements have been identified to cause an increase in activity or safety, structural activity relationship (SAR) analysis can be utilized to further optimize future derivatives [30]. Focusing on derivatives of a

previously discovered active compound allows for the discovery of novel compounds that would not have been screened and discovered in classical HTS model.

Characterizing the safety profile of experimental compounds is a major step towards the discovery of a novel anti-Toxoplasma therapeutic followed by quantifying the activity against *T. gondii* in a HTS (Figure 2). Safety is generally determined through screening compounds for any activity against host cell lines through *in vitro* cellular viability assays. These can include assays that measure host cell respiration such as an Alamar Blue Assay [30]. Similar to screening for safety, quantifying any potential mutagenic effects that can be caused by compound treatment is essential for drug discovery. Proving that a compound lacks the ability to cause point mutations in the host through established *in vitro* assays, such as the Ames assay, allows for screening prior to an *in vivo* experiment for mutagenic effects caused by treatment [30].

Another major hurdle of discovering novel anti parasitic compounds is quantifying the selectivity of compounds against *T. gondii*. A compound that does not exhibit activity towards the host and exhibits significant activity against *T. gondii* is generally accepted as being selective. Both selectivity and overall safety is commonly first determined through *in vitro* assays by determining concentrations that inhibit 50% of growth (IC_{50}) via host cell viability assays and determining activity against *T. gondii* (Figure 2). For activity against acute *T. gondii* infection, an IC_{50} based *in vitro* assay is commonly used to determine the relative activity of compounds against tachyzoites to determine overall activity [30].

Along screening compounds in an HTS, compounds must be analyzed through physicochemical profiling and metabolic stability to select future candidates that qualify for further characterization in an *in vivo* model (Figure 2). Physicochemical profiling includes determining the lipophilicity, solubility, and absorption characteristic of a compound. Lipophilicity is quantified to determine the compounds' ability to permeate

phospholipid bi-layer membranes of host cells and of *T. gondii* (or other pathogens) [31]. To determine lipophilicity, *in silico* modeling such as ChemAxon software can be utilized to measure the polar surface area (PSA) of compounds. Compounds that have poor lipophilicity, PSA values greater than 140 angstroms, are too hydrophilic to be considered to allow for membrane permeation. PSA values also give an indication if compounds may be able to effectively cross the blood-brain barrier (BBB) with PSA values less than 90 angstroms [31]. For this dissertation BBB penetration is of key importance due to the interest of identifying compounds that can effectively clear *T. gondii* cysts harboring bradyzoites residing in brain tissue. An additional measure for determining lipophilicity of a compound is determining the physical LogD value. While PSA values can be determined via *in silico* modeling, LogD values represent the partition of a compound between the aqueous and lipid phases at a desired pH, commonly at a physiological pH of 7.4, through liquid chromatography analysis [31].

Anti-parasitic drugs that are orally bioavailable have a clear advantage over drugs that are administered through injection or intravenous administration. Having the ability to administer a compound orally allows for compounds to be administered as tablets, capsules, or a formulation. Meaning that patients do not have to rely on medical facilities personnel for proper treatment. This is of utmost importance in developing countries where medical facility access is severely limited [32]. Assessing aqueous solubility allows for the identification of compounds that are potentially orally bioavailable. Compounds that are found to be poorly soluble are generally not as orally bioavailable due to low absorption rates in the digestive system [33]. To compensate for this, poorly soluble compounds may have to be administered at higher doses to compensate for this effect. Additionally, proteins that are present in the sera of the host can directly affect the amount of compound that is able to reach the desired target site(s). This effect can be measured as plasma protein binding (PPB) [34]. Compounds

that are found to have higher PPB values tend to have lower efficacy against the intended disease/pathogen due to the binding of proteins in the sera inactivating the compound [35].

Lastly, quantifying overall metabolic stability allows for the identification of compounds that may serve as novel anti-parasitic compounds (Figure 2). Compounds that have significantly low metabolic stability must be given at an increased rate to allow for adequate amounts to be present in the sera and the desired target site [35]. Stability of compounds can be assessed in both *in vitro* and *in vivo* models. *In vitro* models include the use of *ex vivo* liver microsomes from either mice or human liver samples. From microsome based experiments, the intrinsic clearance ratio (CL_{int}) is quantified and is correlated to the overall stability [35]. Half-life of compounds, the amount of time that it takes for 50% of the compound to be metabolized, can be determined with *in vivo* murine models through the administration of a compound of interest and collecting blood over an extended period of time. Followed by liquid chromatography – mass spectrometry (LC-MS) based experiments to determine relative amounts of compound in periphery blood [35]. Compounds that are identified to exhibit high rates of metabolic stability are of particular interest for anti-parasitic drug discovery due to the amount of active respective compound being present in the serum versus compounds that are metabolized at an accelerated rate are of limited interest. Shorter half-lives indicate that a compound is rapidly metabolized into respective metabolites that may not be active against the pathogen of interest [35]. While longer half-lives allow for treatment regiments of anti-parasitic compounds to include fewer administrations for the patient.

Once a novel anti-Toxoplasma compound is identified to exhibit selective activity through *in vitro* assays and is observed to have drug like qualities by physicochemical and metabolic analysis, mouse models are then utilized to determine efficacy against *T. gondii* infection in an *in vivo* model (Figure 2). Survival based assays are utilized to

determine efficacy of a compound of interest against acute *T. gondii* infection since mice succumb to acute infection if infected with a lethal number of tachyzoites. Route of administration of compound is based on physicochemical and metabolic properties. Oral administration is ideal for the discovery of novel antiparasitic compounds as previously discussed. Along with acute infection, activity of compounds in an *in vivo* model against chronic *T. gondii* infection is observed through a murine model. Infecting with a sub-lethal amount of tachyzoites allows for the formation of tissue resident cysts. Infection can also be established by oral administration of isolated *T. gondii* cysts from infected mouse brain tissue. Once cysts are formed, compound administration followed by quantification of tissue resident cysts determines how effective the compound of interest is at clearing tissue resident *T. gondii* cysts.

V: Approaches to Evaluate the Mechanism of Action of Novel Anti-Toxoplasma Compounds

The discovery of novel compounds to combat *Toxoplasma* infection has been extensively explored for the last two decades. To date, there has been a large undertaking from multiple groups to identify compounds that are effective against *T. gondii* for potential future use in clinics [36]. These include both the discovery of novel compounds and the screening of previously published compounds or known drugs for activity against *T. gondii*. Most of this work has focused on the activity against the acute stage of *T. gondii* infection. Yet, there is still a clear gap in the effort to discover novel therapeutics for the clearance and prevention of the chronic stage of *T. gondii*. This is possibly due to the difficulty in screening compounds and drugs for activity against the chronic stage of *T. gondii*.

Once a compound has been discovered to exhibit activity against *T. gondii* in both *in vitro* and *in vivo models*, concluded to be safe through the previously mentioned

experiments, profiled for physicochemical properties, and confirmed to be metabolically stable; the next step is to determine a possible molecular mechanism on how the compound affects the parasite (Figure 2). There are multiple methods that can be used to determine a molecular mechanism of a compound, a common method in the *Toxoplasma* field is random chemical mutagenesis (RCM). RCM allows for random single nucleotide polymorphisms (SNPs) mutations to be induced throughout the *T. gondii* genome by exposure to a known mutagen [37]. If an induced SNP constitutes a potential target, it will be selected through screening for resistance to the compound of interest. Once resistance is established, downstream next generation sequencing (NGS) is utilized, and SNPs investigated for potential targets [37]. Verification of the target can then be performed with complementation and knock-out genomic based experiments.

RCM does have its own limitations due to the design of the assay. Targets that can be identified are those that are enzymes that are encoded by the nucleus of *T. gondii* due to the assay design of RCM. These include enzymes that catalyze multi-step reactions that when disrupted cause parasite death. If a compound is targeting a DNA product derived from the apicoplast, metabolites of an essential pathway, an essential gene needed for parasite survival, or causing a phenotypic defect including growth, invasion, motility; RCM would be unable to identify the target. Additionally, if the compound of interest is modulating the host cell in some way that causes parasite death, RCM would be unable to capture that target. Methods to circumvent this issue through genetic manipulation of *T. gondii* are currently being developed by other groups [38, 39, 40]. These methods have yet to be widely used in the field possibly due to internal complications with respective assay designs. In recent years, analysis of the transcriptome of treated parasites has been utilized to determine pathways changes caused by treatments [41].

Differential expression (DE) analysis of the transcriptome of treated parasites versus untreated parasites allows for the identification of pathways that might be affected by compound treatment (Figure 2). Previous work by Zhai et. al 2020 utilized RNA-seq technology for differential expression of treated parasites [41]. Through DE and gene ontology (GO) analysis, biological pathways that are upregulated or downregulated can be identified [42]. This method allows for the identification of pathways that RCM would be unable to identify such as pathways that include essential genes, non-DNA encoded targets, and changes in parasite morphology causing dysregulated motility, invasion, or division.

Any physical changes to *T. gondii* itself caused by treatments can be quantified using electron microscopy (EM) imaging (Figure 2) [43]. Scanning electron microscopy (SEM) allows for the capture of any phenotypic abnormalities of the surface of *T. gondii* tachyzoites caused by compound treatment. While transmission electron microscopy (TEM) allows for the capture of any ultrastructure phenotypes caused by treatment(s). Ultrastructure phenotypic abnormalities include any changes to organelle structures and organelle distribution that are observed through ultra-thin sectioning of samples and subsequent TEM imaging. Both SEM and TEM allow for the image analysis of treated samples in much higher magnification versus other methods including light, confocal, and fluorescence microscopy [43].

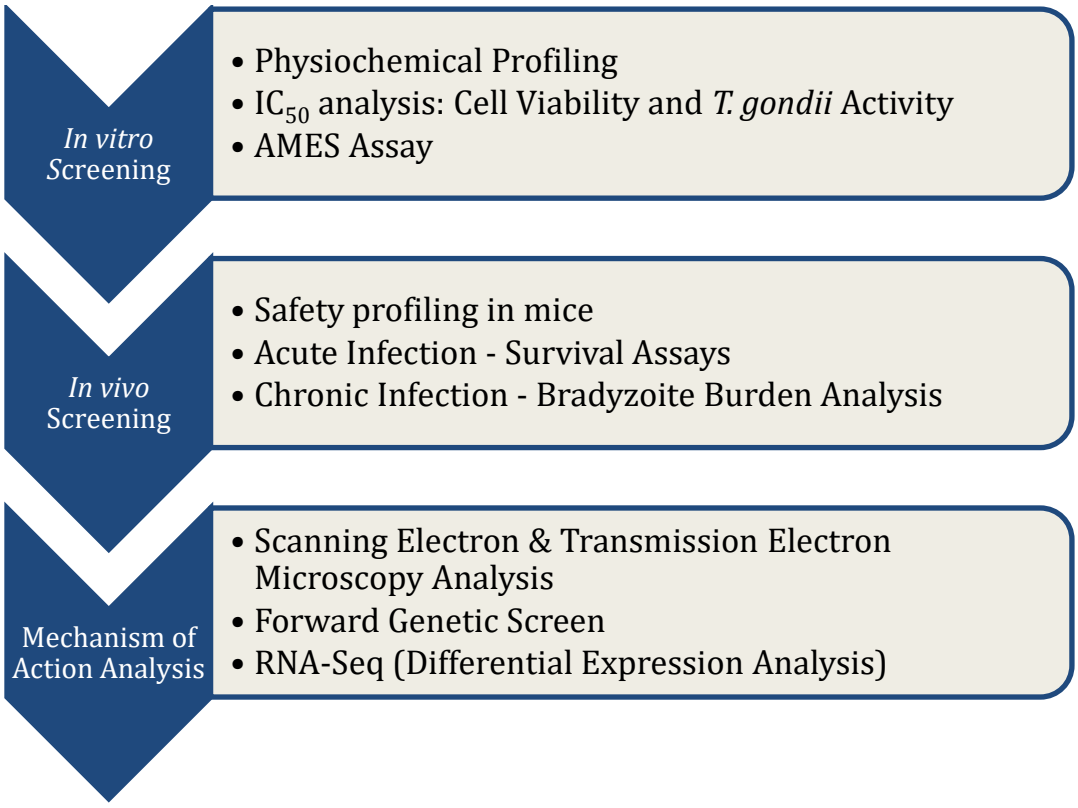

Figure 2: Discovery of Novel Anti-Toxoplasma Compounds. Novel compounds are initially screened *in vitro* for physiochemical profiling, IC_{50} analysis, and potential to induce mutations in an AMES assay. Following *in vitro* screening, most promising compounds are selected for *in vivo* screening in a murine model for safety, activity against acute *T. gondii* infection as well as chronic infection. Lastly, compounds that exhibit selective activity in both *in vitro* and *in vivo* screens move onto mechanism of action analysis. In this dissertation work electron microscopy, forward genetic screening, and differential expression analysis are utilized in hopes of identifying a molecular target of a top compound.

VI: Di-Aryl Urea Compounds

The aim of this work is to characterize a family of *N,N* di-aryl urea chemotypes for activity against *T. gondii*. Di-aryl urea chemotypes have been previously investigated for activity against human cancers. These include drugs that are in current clinical use and clinical trials such as sorafenib and regorafenib [44]. Sorafenib is a protein kinase inhibitor, notably an inhibitor of RAF kinases, and is currently approved by the FDA for the treatment of thyroid cancer and exhibits activity against renal cell and hepatocellular carcinomas [44].

The focus of this work is on compounds that were initially discovered from a HTS screen of 400 compounds for activity against *Plasmodium falciparum* [45]. Compound MMV665852 (Figure 3), or MMV52, was identified to have an *in vitro* IC_{50} against the asexual erythrocytic stage of *P. falciparum* of 1160 nM [45]. For reference, a frontline anti-malarial that is currently utilized in endemic regions known as chloroquine has a respective IC_{50} ranging from 0.2-283.4 nM [46]. The parent structure of MMV52 is triclocarban, a known antibacterial that is primarily effective against gram positive and some gram-negative bacteria [47]. It was previously hypothesized to effect FASII synthesis in bacteria, but recent work has shown that triclocarban most likely does not target the FASII pathway [48]. Up until 2016, triclocarban was utilized in hand soaps as an antibacterial agent. Due to recent research suggesting that triclocarban can cause dysregulated estrogen production after extended usage, the FDA has prohibited the use of triclocarban in personnel use products [49].

Following the initial screening of MMV52, it was then characterized for activity against the helminth *Schistosoma mansoni*. *S. mansoni* is a water borne parasite that infects humans as a blood fluke and is responsible for the disease schistosomiasis [50]. In this work, MMV52 was found to be effective against the juvenile and adult stages of the worm through *in vivo* and *ex vivo* assays with respective IC_{50}s of 4.7 and 0.8 μM [50]. In a murine model, MMV52 was able to reduce worm burden (WBR) by 53% [51]. Additionally, the overall safety of MMV52 was quantified in human MRC-5 fibroblasts with an IC_{50} of 12.8 μM leading to MMV52 having a somewhat poor selectivity index in regard to *S. mansoni* activity [50]. Physicochemical analysis determined that MMV52 exhibited poor solubility and absorption due to its non-polar nature. Metabolic stability analysis determined that the projected half-life was only 4.7 hours, suggesting that MMV52 could be optimized through the synthesis of derivatives and subsequent screening for further characterization [50].

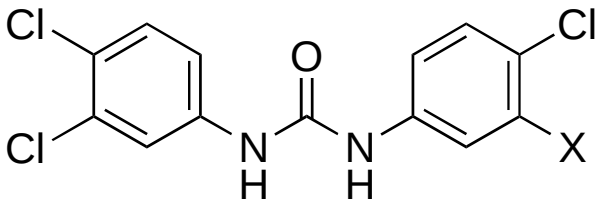

MMV665852 (**4**), X = Cl
Triclocarban (**5**), X = H

Figure 3: Chemical Structure of MMV665852

Synthesis of MMV52 derivatives were based on SAR analysis of the previously screened *N,N* di-aryl urea chemotypes, including compound MMV52, to optimize efficacy and stability. A total of 20 derivatives were synthesized. Most derivatives were found to be effective against *ex vivo* juvenile and adult *S. mansoni* worms with over half exhibiting sub micromolar IC_{50} values [51]. Safety was analyzed against a panel of human cell lines *in vitro* including human foreskin fibroblasts (HFF), osteosarcoma (U-2OS), embryonic kidney (HEK-293), and hepatic carcinoma (HC-04) cells. All 20 derivatives did not cause any detrimental effects to host cells up to 50 µM [51]. Compared to MMV52, all derivatives' PSA values were elevated from 41.1 angstroms to at least 54.0 angstroms up to 84.2 angstroms [51]. Through increasing PSA values of derivatives, the aqueous solubility also increased as well as the oral bioavailability. Overall half-lives of compounds increased compared to MMV52. Two compounds exhibited shorter half-lives than MMV52 while the remaining 18 derivatives' half-lives ranged from 10 hours to >48 hours (could not be determined) [51]. WBR values for all 20 derivatives were lower than MMV52 value of 53% WBR [51]. These poor WBR values could be attributed to the fact that these derivatives are quite lipophilic and exhibit relatively high PPB values. Which could lead to low amounts of compound being delivered to the desired therapeutic site of infection thus reducing the WBR values [51].

Activity of compound #20 [52], identification code: AR33, against *P. falciparum* was quantified *in vitro* and was found to be active at an IC_{50} value of 96 nM. Compared to the parent of AR33, MMV52, with a respective IC_{50} of 1160 nM [41]. Proving that through synthetization of derivatives, AR33 exhibited greater activity against an apicomplexan parasite compared to the parent, MMV52. Thus, AR33 was selected for further optimization based on the high metabolic stability (could not be determined half-life, >48hrs), safety profile, and decreased lipophilicity shown by Wu et. al 2019 [52] and the increased activity against *P. falciparum*. Over 40 of these *N,N* di-aryl urea compounds, notated henceforth as “U” compounds, were synthesized (Table 1). Of these compounds, only compound U21 showed an increase in activity against *P. falciparum* at an IC_{50} value of 0.042 µM (Table 2) [52]. In this dissertation, U04 through U30 will be investigated further for characterization against *T. gondii* (Table 1). Of important note, compounds and drugs that exhibit *in vitro* activity the *P. falciparum* are commonly found to be effective against *T. gondii* due to their shared targets, pathways, and apicoplast organelle. Additional screening against kinetoplastid parasites, *Trypanosoma bruci, Trypanosoma cruzi,* and *Leishmania donovani*, identified that these U compounds were effective against all tested protozoans through *in vitro* based IC_{50} analysis (Table 2). These U compounds, U04 – U30, will be the focus of this dissertation work.

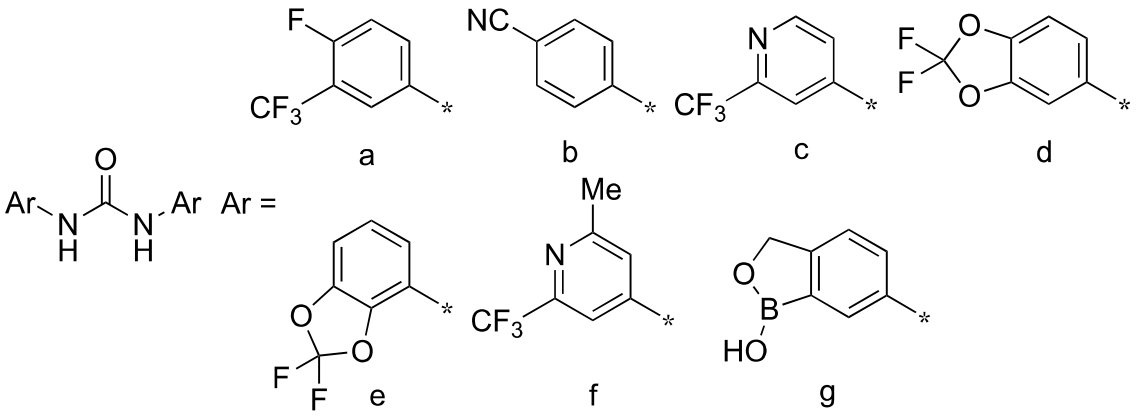

Compound Identification	Aromatic Ring (Ar) Identification
AR33	A, A
U04	C, C
U14	A, B
U19	A, C
U21	C, D
U26	C, E
U28	A, G
U30	D, F

Table 1: Structures of N,N di-aryl urea compounds. Compounds were synthesized and chemical structure verified as described in [52].

	IC_{50} (μM)			
Cmpd	***P. falciparum* NF54**	***T. b. rhodesiense* STIB 900**	***T. cruzi* Tulahuen C4**	***L. donovani*[b] MHOM-ET 67/L82**
AR33	0.096	2.3	1.6	1.3
U04	0.34	5.3	7.2	9.0
U14	0.45	6.2	1.7	0.58
U19	0.22	6.5	4.5	0.65
U21	0.042	4.5	3.2	0.41
U26	0.70	14	2.9	1.0
U28	3.1	0.52	6.6	0.97
U30	0.29	5.1	1.1	0.13
Drug Standards[a]	0.0042	0.0070	1.2	0.99

Table 2: Activity of *N,N* di-aryl Urea Compounds Against a Panel of Protozoans. The following protozoans were screened against *N,N* di-aryl urea compounds for activity through IC_{50} analysis. The following protozoans were tested: *Plasmodium falciparum* NF54, *Trypansoma brucei rhodesciense* STIB 900, *Trypanosoma cruzi* Tulahuen C4, and *Leishmania donovani* MHOM-ET 67/L82. Drug standards[a] utilized are as listed: choloroquine for *P. falciparum*, melarsoprol for *T. t. rhodesiense*, benznidazole for *T. cruzi*, and miltefosine for *L. donovani* [49, 52].

,

VII: Aim of Dissertation Work

The aim of this work is to characterize a subset of these U compounds against *Toxoplasma gondii*. Based on the work showing that both MMV52 and AR33 exhibited activity against the apicomplexan *P. falciparum* [49, 52], **we hypothesize that these compounds will be effective in clearing *T. gondii* infections**. In Chapter 1, I aim to characterize the activity against the acute of *T. gondii* and profile the safety indexes of these *N,N* di-aryl urea U compounds through *in vitro* based assays. I then will select the most efficacious compounds from this screen for activity in a mouse model for activity

against both acute *T. gondii* infection with the use of a lethal infection model and quantification of survival rates of treated mice. These compounds will also be screened for any cytotoxic effects in mice prior to these murine *in vivo* assays. In Chapter 2, the molecular target of U21 is explored. RCM and supplementation experiments will be utilized in attempts to characterize a possible mode of action of the most efficacious compound from Chapter 1. To answer further explore how these *N,N* di-aryl urea compounds are affecting *T. gondii*, EM and differential expression analysis through RNA-seq is utilized in Chapter 3. Additionally, the activity of *N,N* di-aryl urea compounds are investigated against the chronic stage of *T. gondii* is quantified through a novel *in vitro* assay and in a mouse model for inhibiting cyst formation and clearing cysts from mouse brain tissue. In context to FDA approved anti-Toxoplasma therapeutics and novel compounds that exhibit activity against *T. gondii*, these *N,N* di-aryl urea compounds present with attractive chemical profiles for a potential future orally bioavailable anti *Toxoplasma* therapeutics. In addition, by characterizing these compounds for activity against both the acute and chronic stage in *in vitro* and *in vivo* based assay, identification of novel compounds with anti-toxoplasma activity can be identified to add to the limited arsenal of FDA approved therapeutics. Mechanism of action analysis is imperative for understanding how anti-toxoplasma drugs and compounds directly affect the parasite to assess if any cross reactivity may be possible due to the possibility of shared targets between the host and parasite.

CHAPTER I: *In vitro* & *In vivo* Characterization of Di-Aryl Urea Compounds against *Toxoplasma gondii*

I.I Introduction

Acute toxoplasmosis poses a severe health risk for immunocompromised individuals due to the risk of cerebral toxoplasmosis [4]. Current therapeutics are effective in controlling infection but can cause detrimental effects to the patient such as allergic reactions and severe bone marrow toxicity [16]. While there are with no approved options for the treatment and clearance of life-long chronic *T. gondii* infection [25]. Due to the lack of current therapeutic options for controlling acute toxoplasmosis and the complete lack of therapeutics to clear chronic infection, novel *N,N* di-aryl urea compounds that exhibit activity against *Plasmodium* and other protozoa were screened for activity against both acute *T. gondii* infection through *in vitro* based assays and against an *in vivo* murine model for treatment of acute *T. gondii* infection.

The family of di-aryl urea compounds that will be discussed in this dissertationwere initially discovered in a HTS screen against *P falciparum*, an apicomplexan like *T. gondii*. In this screen, compound MMV52 was discovered to have nanomolar IC_{50} activity, 1160 nM, against *P. falciparum* in an *in vitro* screen [45]. Further studies characterized MMV52 in other protozoan species including *S. mansoni*, leading to the synthesis of the derivative AR33 [51]. AR33 was further investigated against *P. falciparum* and found to have an increase in activity at an IC_{50} of 96 nM [52]. Based on the activity of MMV52 and AR33 against *P. falciparum* from *in vitro* IC_{50} analysis it was hypothesized that the derivatives of AR33, notated as U compounds, would have activity against *T. gondii* infection. As previously discussed, it is not uncommon for compounds to be effective against both apicomplexans due to shared pathways and the apicoplast organelle serving as a potential target.

Due to the clear lack of current therapeutics to treat acute toxoplasmosis and no approved treatment for clearing chronic infection the derivatives of AR33, U04-U30, underwent rigorous *in vitro* HTS and *in* vivo screening for the identification of active anti-Toxoplasma compounds. Prior to HTS analysis of U04-U30 physicochemical properties and metabolic stability were measured through PSA, LogD, solubility, intrinsic clearance ratios, and PPB analysis. Compared to AR33, U04-U30 were measured to be less lipophilic than AR33 and relatively more soluble in an aqueous solvent. Additional *in vitro* metabolic stability analysis, intrinsic clearance ratios, identified that many of the tested U compounds were more stable than AR33. This was confirmed in an *in vivo* model through half-life analysis in mice treated with a single dose of U compound through oral gavage administration.

To explore if U Compounds exhibited similar activity to AR33 against *T. gondii*, an *in* vitro HTS method was utilized to assess activity against acute *T. gondii* infection and for cell viability analysis against host cell lines. U04-U30 were found to not cause any detrimental effects against tested host cell lines and not cause mutagenic effects in an Ames assay. *In vitro* IC_{50} analysis against acute toxoplasmosis of U04-U30 confirmed that all tested compounds were active against acute *T. gondii* at similar or improved IC_{50} values compared to AR33. Further analysis in a murine model confirmed that these di-aryl urea compounds were safe *in vivo* at all tested concentrations, up to 100 mg/kg, through oral gavage administration. Through a lethal acute *T. gondii* infection in mice, U21 was identified to perform at concentrations similar to pyrimethamine levels against acute *T. gondii* infection while other tested compounds were not as effective.

I.II Methods

Physicochemical & Stability Analysis

Polar surface areas (PSA) were calculated through ChemAxon JChem Software for Excel. Partition values, gLogD, were estimated with a modified gradient HPLC method and comparing chromatographic retention properties to known compounds. Solubility of compounds was determined through dissolving in DMSO and spiking in phosphate buffer (pH 6.5) as well as 0.01 M HCl. Concentration ranges were then determined through nephelometry. For the estimation of *in vitro* clearance ratios, compounds were incubated with either mouse or liver *ex vivo* microsomes and clearance ratios determined as described previously [52]. Half-lives in CFW mice were determined through single administration of 100 mg/kg of respective compound. Blood was then collected through tail vein bleeds over the course of 48 hours. Relative abundance of compounds was then determined by HPLC analysis.

Cell Line Maintenance

Human foreskin fibroblasts (HFF), human osteosarcoma cells (U-2OS), human embryonic kidney cells (HEK-293), human liver cells (HC-04), murine macrophages (RAW264.7A), and THP-1 monocytes were all obtained from ATCC. HFF, U-2OS, HEK-293, HC-04, and RAW264.7A cells were all cultured in DMEM media (Gibco) with 10% heat inactivated bovine serum (GE Healthcare Life Sciences), 2mM L-Glutamine (GE Healthcare Life Sciences), 100 ug/mL penicillin and streptomycin (Corning), 100 ug/mL gentamicin sulfate, and 10% Medium 199 (Corning). THP-1 monocytes were cultured in RPMI-1640 with the addition of 0.05 mM 2-mercaptoethanol and 10% heat inactivated bovine serum (GE Healthcare Life Sciences). All cell lines were cultured at 37C with 5% CO_2.

Murine bone marrow derived macrophages were obtained through sacrificing female CFW mice through CO_2 induced euthanasia and isolation of monocytes from bone marrow for further differentiation *ex vivo* into macrophages. Femurs were flushed with 1X PBS with a 28G needle and flow through was collected. After centrifuging at 250G for 10 minutes, pellets were resuspended in RPMI-1640 media supplemented with 20% heat inactivated bovine serum plus 20mM penicillin and streptomycin. 2 ng/mL of rmGM-CSF was added to allow for differentiation to macrophages in a tissue grade sterile 96 well plate at 20,000 cells/mL. After 3 days at 37C + 5% CO_2, increasing concentration of compounds (0 – 100 µM) was added and tested in duplicate. 24 hours after initial compound addition, an Alamar Blue assay was conducted as discussed below to determine any detrimental effects caused by compound exposure.

In vitro Host Cellular IC_{50} Analysis and Mutagenicity

Human foreskin fibroblasts (HFF) cells were plated in a tissue grade sterile 96 well plate and allowed to grow to confluence. Once confluent, 2000 RH-dTom *T. gondii* tachyzoites were then added to each well and allowed to infect over 24 hours at 37C with 5% CO_2. After 24 hours, media was then replaced and increasing concentration of compounds dissolved in DMSO were added (0 – 100 µM) in duplicate. Concentrations of DMSO did not exceed 1% in any well to prevent any toxicity caused by solvent. Fluorescent readings were taken daily for a total of 5 days with a BioTek Snergy plate reader at 530/25 excitation and 590/25 emission. Pyrimethamine was included as a positive control for *T. gondii* IC_{50} analysis against tachyzoites. IC_{50}s were calculated after day 5 post-infection.

For host cell viability analysis, host cells were plated in tissue grade sterile 96 well plates and allowed to grow to confluence. Host cells tested included: HFF, U-2OS, HEK-293, HC-04, THP-1, J774, and RAW264.7. Once confluent, compounds at

increasing concentrations (0 – 100 µM) were added in duplicate. After 24 hours of treatment, an Alamar blue assay was utilized to measure cell viability. Briefly, 0.5mM of resazurin salt was added to each well and allowed to incubate for at least 4 hours at 37C with 5% CO2 away from light. Fluorescent readings were then taken at 520/25 excitation and 590/25 emission with a BioTek Snergy HT plate reader. Viability was determined after 24 hours by comparing treated cells with untreated cells to determine percent viability and respective IC_{50} values.

Mutagenic effects caused by compound administration was quantified through detecting DNA single point mutagenicity using a modified Ames assay (Environmental Bio-Detection Products Inc.) with *Salmonella typhimurium* (TA100 strain). Briefly, compounds were tested at 3X their respective *T.* gondii IC_{50} values in a total of 48 replicates. Revertant colonies were counted and compared to a natural revertant control. Statistical analysis between the two was performed through an unpaired Student's t-test.

Pre- and Post-Exposure Analysis of *Toxoplasma gondii* Tachyzoites

Pre-cellular treatment analysis of *N,N* di-aryl urea compound included plating HFF cells in sterile tissue grade 96 well plates and allowing cells to grow to confluency. Once confluent, host cells were then treated with 10 µM of respective compound (U21, U26, or U28) for 24 hours. After 24 hours, compound was removed via washing the host cells twice with sterile 1X PBS, and cells were infected with 2000 *T. gondii* RH-dTom tachyzoites isolated from HFF cells. 5 days post-infection, tachyzoite growth and survival was then quantified through fluorescent readings from a BioTek Syngergy plate reader at 530/25 excitation and 590/25 emission and comparing treated to untreated (DMSO) tachyzoites.

Pre-parasitic treatment analysis entailed isolating untreated 2e6 RH-dTom tachyzoites/mL from HFF cells and treating with 10 µM of respective compound (U21,

U26, or U28) at 37C for 4 hours. After treatment, tachyzoites were then counted and 2000 tachyzoites/mL were transferred to confluent uninfected HFF cells in sterile tissue grade 96 well plates. Tachyzoite growth and survival was quantified 5 days post-infection through fluorescent readings utilizing a BioTek Synergy plate reader at 530/25 excitation and 590/25 emission and comparing treated to untreated (DMSO) tachyzoites. Statistical analysis of both pre-treated host cells and parasites included the use of a one-way ANOVA test to determine if decreases in *T. gondii* growth was significant or not.

In vivo Safety and Lethal Acute *Toxoplasma gondii* Survivability

To assess potential toxicity of *N,N* di-aryl urea compounds, female CFW mice (n=5) were administered 100 mg/kg through oral gavage administration dissolved in 47.5% propylene glycol, 47.5% Kollisolv, and 5% DMSO. Compounds were administered every third day for a total of 3 doses. Mice were monitored and weighed daily. All mouse studies were performed and approved under the IACUC number 18-075-07.

Activity of *N,N* di-aryl urea compounds against alveolar macrophages in mice was assessed through administering 100 mg/kg of U21 through oral gavage CFW female mice (Jackson Laboratories, n=3). 48 hours after initial administration, treated mice were sacrificed through CO_2 euthanasia and lungs were extracted. Extracted lungs were inflated and fixed in formalin for 24 hours. Fixed lung tissue was then sectioned, hematoxylin and eosin (H&E) stained, and imaged under light microscopy to visualize any toxic effects to lung tissue and more importantly alveolar macrophages. CFW mice treated with only solvent (n=3) were included as a control for analysis. Images were sent to HistoWiz for professional analysis of alveolar macrophages in treated versus untreated samples. Sectioning and staining of samples were performed at the University of Nebraska Medical Center Tissue Science Facility.

Activity of *N,N* di-aryl urea compounds against acute *T. gondii* infection *in vivo* was investigated through a lethal acute infection in a murine model. 8-week-old female CFW mice (n=10) were infected with *T. gondii* 5,000 ME49 tachyzoites. Simultaneously, *N,N* di-aryl urea compound administration began at respective dosage (100, 75, 50, or 25 mg/kg) through oral gavage administration every three days for a total of three dosages. A pyrimethamine group (n=10) treated through intraperitoneal (IP) injection every day for 10 days was included as a positive control dissolved in 47.5% propylene glycol, 47.5% Kollisolv, and 5% DMSO. Mice were monitored daily and weighed. After 28 days post-infection, survival was plotted on a Kaplan-Meir (KM) survival curve through IBM STSS Statistics 22 software. To confirm infection of surviving mice, an ELISA was utilized to confirm *T. gondii* specific antibodies from isolated sera 21 days post-infection. Statistical analysis was performed through IBM SPSS Statistics Software through a log-rank test to determine overall significance of *N,N* di-aryl urea compound treatment versus solvent treated mice.

I.III Results

I. Physicochemical & Metabolic Stability Analysis

Prior to characterizing *N,N* di-aryl urea compounds for activity and safety, U04-U30 were first analyzed for physicochemical properties. All tested U compounds (U04-U30) were found to exhibit higher polarity (PSA) and LogD (gLogD7.4) values compared to AR33. U04, U19, U21, and U26 all had an increase in solubility due to the increased PSA and LogD values (Table 3). U26 and U28 exhibited an increase in intrinsic clearance ratios compared to AR33 while U04, U14, U19, U21, and U30 did not allow for a measured intrinsic clearance ratio in mice suggesting an increase in metabolic stability (Table 3). Lastly, U04-U30 PPB values were all recorded as >95% similar to AR33 (Table 3).

Previous work characterized these *N,N* di-aryl Urea compounds for *in vivo* stability through half-life analysis (51). Compared to the parent compound of AR33, MMV552, a clear increase of stability was observed. Importantly, U21's half-life was unable to be determined even after 48 hours after a single administration of 100 mg/kg via oral gavage.

Compd	$gLogD_{7.4}$[a]	PSA ($Å^2$)[b]	$Sol_{2.0}/Sol_{6.5}$ (µg/mL)[c]	h/m CL_{int} (µL/min/mg protein)[d]	cPPB (%)[e]	Half-Life T ½ (Hours)[f]
AR33	4.5	41.1	<1.6/<1.6	10/7	98.7	4.0
U04	3.0	66.9	12.5-25/12.5-25	<7/<7	95.2	11
U14	3.8	64.9	<1.6/<1.6	<7/12	98.4	2.7
U19	3.8	54.0	3.1-6.3/3.1-6.3	<7/<7	98.7	18
U21	3.7	72.5	3.1-6.3/3.1-6.3	<7/16	98.5	c.n.d
U26	3.6	72.5	3.1-6.3/3.1-6.3	14/92	97.0	-
U28	2.5	70.6	<1.6/<1.6	13/34	96.7	-
U30	4.3	72.5	<1.6/<1.6	<7/36	98.5	-

Table 3: Physicochemical Analysis of N,N di-aryl urea compounds. LogD values of compounds were quantified through their chromatographic retention properties via a HPLC method [52] [a]. PSA values were calculated through ChemAxon JChem Software for Excel [b]. Solubility of compounds dissolved in DMSO was determined through spiking them in phosphate buffer (pH 6.5) of 0.01 M HCl (pH 2.0). Concentration ranges were then calculated through nephelometry [52] [c]. *In vitro* clearance ratios were measured in both mouse and liver microsomes as described in [52] [d]. PPB values were measured through a gradient HPLC method as described in [52]. Briefly, N,N di-aryl urea compound chromatographic retentions were compared to a set of standard compounds on a human albumin column. [e] Murine in vivo half-lives were determined through administering a single dosage of compound at 100 mg/kg to female CFW mice. Treated mice were then bled over a course of 48 hours through tail vein bleeding. Relative amounts of compound were determined through LC-MS analysis [f] [52].

II. *N,N* Di-aryl Urea Compounds: Host Cell Viability & Acute *Toxoplasma gondii* Activity

U04-U30 exhibited similar or improved activity against *T. gondii* tachyzoites through *in vitro* IC_{50} analysis compared to their parent compound, AR33 (Table 4). U26 was found to be the most effective against *in vitro* tachyzoites at an IC_{50} of 0.42 µM. U04

had the lowest amount of activity at an IC_{50} of 4.3 µM. As a point of reference pyrimethamine, current anti-toxoplasma therapeutic utilized in clinics, has an IC_{50} value on average of 2.0 µM (Table 4).

To assess any adverse effects of *N,N* di-aryl urea, an Alamar Blue cell viability assay was utilized to measure IC_{50}s of compounds against a panel of host cell lines. AR33 only exhibited activity against HFF cells at 57 µM with no activity in any of the other tested cell lines (U-2OS, HEK-293, and HC-04). U04, U14, U26, U28, and U30 did not have any measured activity in any host cell line (>100 µM) (Table 4). Additionally, there was no measured mutagenic effects of *N,N* di-aryl urea compounds in an Ames assay (Table 4).

	IC50 (uM)					
Compd	***T. gondii* RH-dTom Tachyzoites**	**HFF**	**U-2OS**	**HEK-293**	**HC-04**	**Ames Assay**
AR33	1.7	57	>100	>100	>100	NEGATIVE
U04	4.3	>100	>100	>100	>100	NEGATIVE
U14	1.7	60	>100	>100	>100	NEGATIVE
U19	1.8	71	>100	48	>100	NEGATIVE
U21	2.0	80	>100	72	>100	NEGATIVE
U26	0.42	>100	>100	>100	>100	NEGATIVE
U28	2.6	>100	>100	>100	>100	NEGATIVE
U30	1.5	42	>100	>100	>100	NEGATIVE
Pyr	2.0	>100	>100	>100	>100	NEGATIVE

Table 4: Activity of N,N di-aryl Urea Compounds Against acute *T. gondii* and Host Cells. IC_{50} analysis was performed on the *Toxoplasma gondii* RH-dTom tachyzoites through in vitro culturing and fluorescent readings at increasing concentration of compound (0 – 100 µM) for 5 days. For cell viability analysis all host cells tested (HFF, U-2OS, HEK-293, and HC-04) were cultured with respective compound for 24 hours and an Alamar Blue assay was then utilized to quantify viability of host cells at increasing concentration of compound (0 – 100 µM) and respective IC_{50}'s calculated. For all IC_{50} experiments, compounds were tested in duplicate. Mutagenic capacity of compounds was assessed with an Ames Assay and revertant colony counts. [52]

Cell viability screening was then expanded to include *in vitro* immortalized macrophage and *ex vivo* murine macrophages based on the work of a collaborator showing activity of *N,N* di-aryl urea compounds against macrophage cell lines [52]. U21 and U30 were screened against: J774 and RAW264.7A immortalized murine macrophages, THP-1 human monocytes, THP-1 human monocytes differentiated to macrophages through phorbol 12-myristate 13-acetate (PMA) exposure, and murine bone marrow derived macrophages (BMDM). In J774 cells, both U21 and U30 exhibited activity at 48 and 57 µM respectively (Table 5). No activity was seen against RAW264.7A. In both non-differentiated and differentiated THP-1 cells, U21 had significant effects at 16 µM (Table 5). Similar to U21, U30 exhibited activity at 17 and 16 µM respectively. Surprisingly, U21 presented with even higher activity against murine BMDM at 11 uM while U30 had similar activity to THP-1 at 17 µM (Table 5) suggesting that *N,N* di-aryl urea compounds may be acutely toxic to macrophages.

	IC_{50} (µM)				
Cmpd ID	**J774**	**RAW264.7A**	**THP-1**	**THP-1 + PMA**	**Murine BMDM**
U21	48	>100	16	16	11
U30	57	>100	17	16	17

Table 5: IC_{50} Analysis of N,N di-aryl urea compounds in Macrophages. Relative IC_{50}s were calculated for all tested macrophages: J774, RAW264.6, THP-1, and murine bone marrow derived macrophages. THP-1 monocytes were also differentiated to macrophage-like-cells via 15 ug/mL of PMA. Murine monocytes were isolated from mouse femurs and differentiated to macrophages via M-CSF. [52]

To further investigate effects of U21 against macrophages, outbred female CFW mice were treated with either U21 at 100 mg/kg or solvent (n=3). Following treatment lungs were isolated, fixed, sectioned, and stained for histopathology analysis. Expert

analysis indicated that there were no noticeable phenotypes of alveolar macrophages or lung tissue seen in U21 treated mice suggesting that U21 does not cause any visible toxicity to *in vivo* murine macrophages based on H&E analysis (Figure 4).

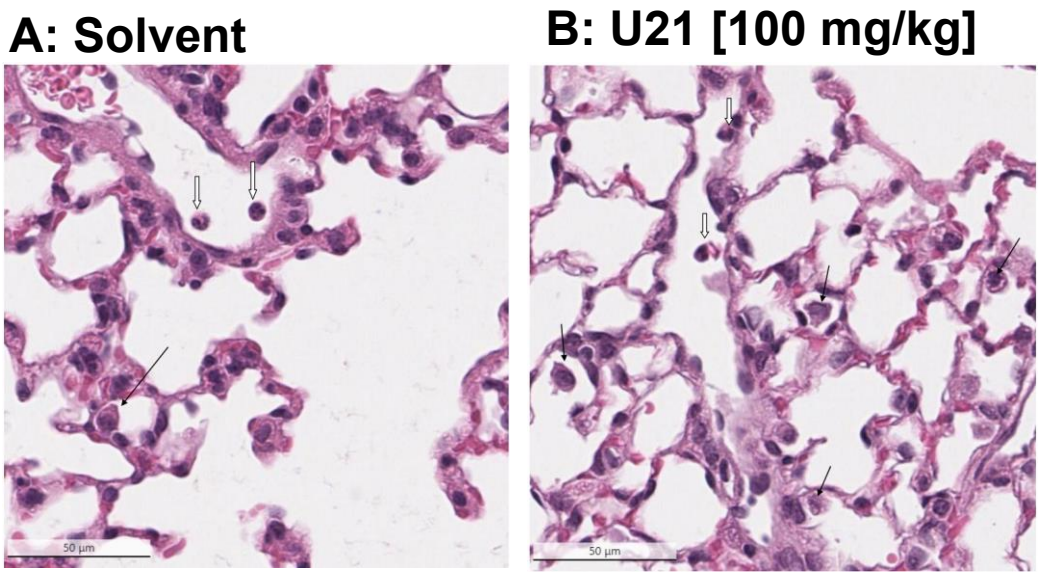

Figure 4: Immunohistochemistry Staining of Murine Lung Tissue following U21 Treatment. CFW mice (n=3) were treated with 100 mg/kg of U21. Solvent treated mice were utilized as a negative control (n=3). Two days after initial treatment, mice were sacrificed, lungs extracted, and then fixed in formalin. Tissue was then sectioned, H&E stained, and then slides submitted for expert analysis. It was concluded that U21 treatment did not cause any detectable pathology to lung tissue or alveolar macrophages. [52]

III. Pre-parasitic & Pre-cellular Exposure Analysis of *Toxoplasma gondii* Tachyzoites

To validate the physicochemical properties outlined in Chapter 1, *in vitro* pre-host and pre-tachyzoite activity was measured. The ability of *N,N* di-aryl urea compounds to pass through the cell membrane of host cells can be assessed by the treatment of uninfected host cells followed by *T. gondii* infection [53]. In addition, the ability of compounds to pass through the cell membrane of tachyzoites can be assessed through the pre-treatment of tachyzoites and the subsequent addition of treated parasites to host cells [53]. Based on the physicochemical properties presented in Table 3, it was initially

hypothesized that both pre-treated host cells and tachyzoites would allow for significant decreases in *in vitro* tachyzoite survival.

Pre-exposure analysis of both host cells and extracellular tachyzoites treated with U21, U26, or U28 was conducted to determine if *N,N* di-aryl urea could pass the cell membrane of host cells and tachyzoites. All compounds tested (U21, U26, and U28) were seen to have significant activity against extracellular tachyzoites (p value < 0.05). All treatments caused ~20% reduction in parasite viability when treated extracellular tachyzoites were placed on uninfected HFF cells, allowed to infect, and viability quantified via fluorescent values (Figure 5, p value < 0.05). Pre-exposed HFF cells that only allowed for a significant reduction in tachyzoite growth when treated with U28. Interestingly, U21 treatment caused a slight increase in parasite viability when HFF cells were pre-treated but was not found to be statistically significant.

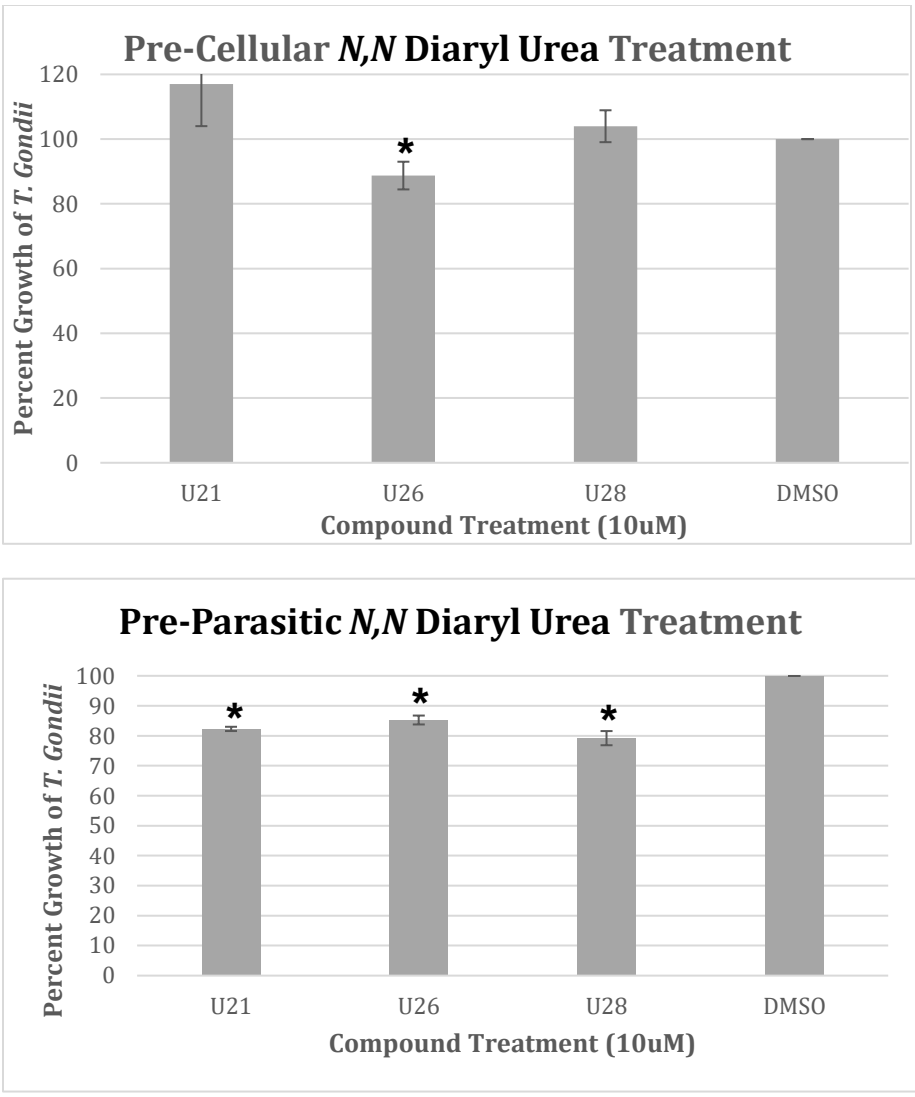

Figure 5: Pre-cellular and Pre-parasitic *N,N* Diaryl Urea Compound Treatment Analysis. (A) HFF cells were plated in a 96 well plate and allowed to grow to confluency. Compounds were then added at 10uM and allowed to incubate at 37C for 24 hours. Cells were then washed to remove compound and infected with 2000 RH-dTom *T. gondii* tachyzoties. (B) Isolated RH-dTom *T. gondii* tachyzoites from untreated HFF cells were treated with 10uM for 4 hours at 37C. 2000 of the treated RH-dTom *T. gondii* tachyzoites were then used to infect untreated HFF cells. For both assays (A & B), tachyzoite growth was quantified through fluorescent readings at 530/25 excitation and 590/25 emission. Percent growth was calculated on day 5 post infection (*p value < 0.05).

IV: *N,N* Di-aryl Urea Compounds: *In vivo* Activity

Activity of *N,N* di-aryl urea compounds *in vivo* was quantified through a lethal acute infection model in mice. Following a lethal acute infection of *T. gondii* tachyzoites, mice began to receive treatment with respective *N,N* di-aryl urea compounds. Based on physicochemical, metabolic stability, cell viability, and activity against *T. gondii* the

following *N,N* di-aryl urea compounds for further *in vivo* analysis (n=10): U21, U26, U28, and U30. U21 allowed for pyrimethamine levels of survival (100%, p value < 0.05) while both U28 and U28 only allowed for 10% and 20% survival, respectively (Figure 5). U30 treated mice allowed for half of pyrimethamine levels of survival at 20% (Figure 6).

To assess if lower concentrations of U21 exhibited pyrimethamine levels of survival as well, infected mice were treated with 75, 50, or 25 mg/kg via oral gavage (n=10). At 75 mg/kg, 40% of mice survived with 50 mg/kg (p value < 0.05) and 25 mg/kg treated mice survival rates only at 20% and 0% respectively (Figure 7). Suggesting that U21 allows for a dose dependent survival in a lethal acute *T. gondii* infection model with 100 mg/kg allowing for pyrimethamine levels of survival. In all mouse models, surviving mice were bled 21 days post-infection and were confirmed to be infected due to the presence of *T. gondii* antibodies in sera that were measured through an indirect ELISA (data not shown).

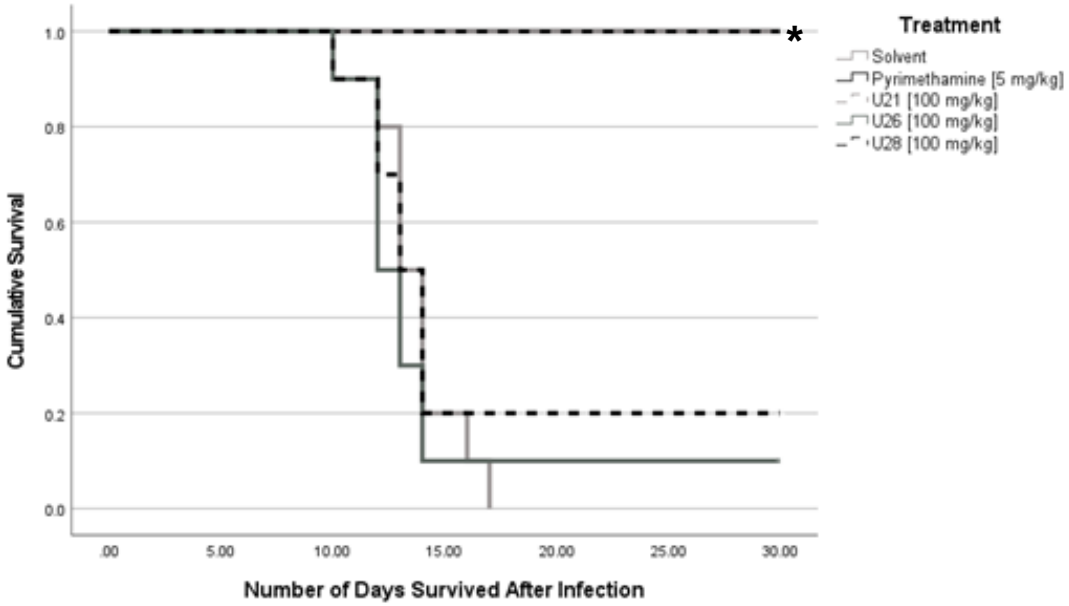

Figure 6: Survival of mice lethally infected with *T. gondii* treated with N,N'-diarylurea compounds. . CFW mice were infected with 5,000 *T. gondii* ME49 tachyzoites. Following infection, compound treatment (U21, U26, U28) began via oral gavage at 100 mg/kg given every three days. Pyrimethamine was given at 5 mg/kg via IP injection once per day as a positive control. 100% survival was seen in both pyrimethamine (n=10) and U21 (n=10, p < .005), while 20% survival was seen in U28 (n=10) and ~10% seen in U26 (n=9). 0% survival was seen in solvent treated which was used as a negative control (n=13). (*p value < 0.05) [52]

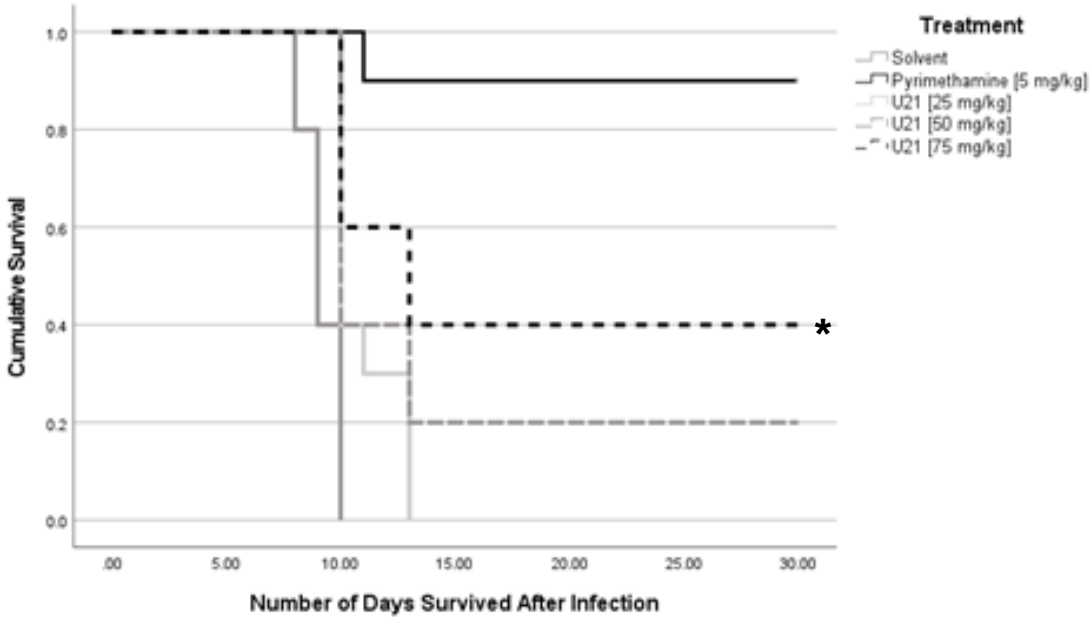

Figure 7: Survival of mice lethally infected with *T. gondii* treated with varying U21 doses. CFW mice were infected with 5,000 *T. gondii* ME49 tachyzoites. Following infection, U21 treatment began via oral gavage at 25, 50, or 75 mg/kg given every three days. Pyrimethamine was given at 5 mg/kg via IP injection once per day as a positive control. 40% survival was seen in the 75 mg/kg treatment group (n=10) while only 20% survived in the 50 mg/kg group (n=10)., 0% survival was seen in infected solvent treated (n=10) and 25 mg/kg (n=10). (*p value < 0.05) [52]

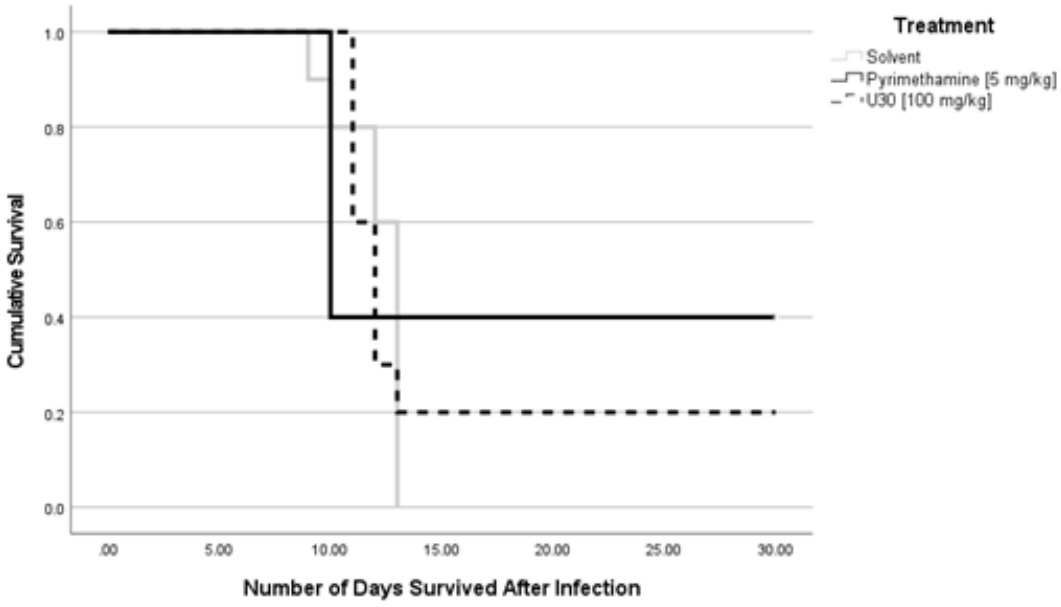

Figure 8: Survival of mice lethally infected with *T. gondii* treated with U30. CFW mice were infected with 5,000 *T. gondii* ME49 tachyzoites. Following infection, U30 treatment began via oral gavage 100 mg/kg given every three days. Pyrimethamine was given at 5 mg/kg via IP injection once per day as a positive control. 20% survival was seen at 100 mg/kg of U30 treatment group (n=10). 0% of solvent treated mice survived and 40% of pyrimethamine treated mice survived infection. [52]

I.IV Discussion

AR33 and its derivatives, U04 – U30, were found to have similar or improved physicochemical properties regarding the solubility, stability, LogD, and PPB values (Table 3). In addition, U04-U30 exhibited activity to *T. gondii* tachyzoites through *in vitro* IC_{50} analysis. U04-U30 exhibited similar activity to AR33 with U26 being the most effective at 0.40 µM and U04 being the least effective at an IC_{50} of 4.3 µM (Table 4). All *N,N* di-aryl urea compounds screened were not found to cause any toxic effects in HFF, U-2OS, HEK-293, or HC-04 human cells (Table 4). U21 and U30 were found to be highly toxic to macrophage like cells including *ex vivo* murine BMDM at sub 20 µM IC_{50} values (Table 5).

Pre-parasitic treated samples identified that U21, U26, and U28 caused significant decreases in tachyzoite growth, while in pre-treated host cells no compound caused a significant parasite inhibition (Figure 5). These results were surprising due to the drug-like physicochemical properties observed in Table 3. U21, U26, and U28 may not be readily able to pass through the cell membrane of mammalian cells based on Figure 5 data, but the lipophilic character (Table 3) contradicts that conclusion. In addition, these *N,N* di-aryl urea compounds are still significantly effective against *in vitro* acute *T. gondii* cultures suggesting that the pre-treatment assay may indeed not allow for accurate conclusions.

Yet mice that are treated with *N,N* di-aryl urea compounds do not exhibit any signs of toxicity even when treated with high doses (100 mg/kg) for multiple days [52]. This was further confirmed through treating mice with U21 and subsequent H&E analysis of treated versus untreated alveolar macrophages (Figure 4). It could be hypothesized that *N,N* di-aryl urea compounds are metabolized rapidly into metabolites *in vivo* and the respective metabolites are not toxic to macrophages. This is most likely not the case due

to U21 and other *N,N* di-aryl urea compounds exhibiting extended half-lives in mice and low *in vitro* intrinsic clearance ratios [51]. For future analysis, flow cytometry analysis (FACs) would allow for a quantitative approach for the quantification of viable *in vivo* macrophages following *N,N* di-aryl urea compound treatment.

Of the four *N,N* di-aryl urea compounds tested for activity in acute lethal *T. gondii* infection model in mice, 100 mg/kg of U21 was the most effective allowing for pyrimethamine levels of survival (Figure 5). An additional *in vivo* study was conducted to assess if lower doses of U21 could allow for similar levels of survival resulting in a dose dependent response. Only 100 mg/kg of U21 allowed for pyrimethamine levels of survival with 75, 50 and 25 mg/kg allowing for 40%, 20% and 0% survival respectively (Figure 6). Confirming that U21 allows for a dose dependent survival response in mice that are infected with a lethal amount of *T. gondii* tachyzoites. Compared to current therapeutics such as pyrimethamine, U21 exhibited similar levels of activity *in vitro* and *in vivo* against acute *T. gondii* infection. Cell viability analysis against a panel of immortalized human and mouse cell lines confirmed that U21 was not overtly toxic except for *ex vivo* and *in vitro* macrophage cell lines. In conclusion, U21 exhibited clear drug like properties and selectivity for acute toxoplasmosis prompting further investigation in hopes of identifying a novel anti-toxoplasma therapeutic.

I.V Conclusion

In conclusion, U21 exhibited clear drug like properties and selectivity for acute toxoplasmosis prompting further investigation in hopes of identifying a novel anti-Toxoplasma therapeutic. Thus, U21 was selected for further analysis including mechanism of action analysis and activity against the chronic stage of *T. gondii* infection in both *in vitro* and *in vivo* analysis. In the following chapter, Chapter 2, a possible mode

of action of U21 is investigated through genetic manipulation and phenotypic growth assays.

CHAPTER 2: Mechanism of Action Analysis of Top *N,N* Di-aryl Urea Compounds against *Toxoplasma gondii*

2.I Introduction

Investigating and identifying a possible molecular target or effected pathway of a compound of interest is pivotal for drug-development. Due to U21 allowing for pyrimethamine levels of survival, it was selected for mechanism of action analysis (Figure 5, Figure 6). MMV52, the parent compound of U21, was based on the previously hypothesized prokaryote FASII inhibitor triclocarban. Unlike human cells, *T. gondii* has both the cytosolic eukaryotic Fatty Acid Synthesis I (FASI) pathway and the multi-enzyme FASII pathway that functional the apicoplast organelle. *T. gondii* relies on FASII to produce essential fatty acids that are utilized for essential growth processes. When knocked out or inhibited, *T. gondii* tachyzoites are unable to survive and parasitic growth is inhibited [54]. I hypothesized that these *N,N* di-aryl urea compounds targeted FASII in *T. gondii* as well. To assess if *N,N* di-aryl urea compound treatment targets the essential FASII pathway in *T. gondii*, an *in vitro* fatty acid supplementation based assay is utilized.

Disruption of an apicoplast related pathway is known to cause an *in vitro* phenotype known as delayed death [55]. During the division of tachyzoites through endodyogeny to produce daughter tachyzoites within host cells, tachyzoites can sequester essential metabolites that are normally produced by the apicoplast. When these apicoplast pathways are inhibited, tachyzoites within host cells can continue to divide and the subsequent daughter cells egress from the infected host cell. Once these effected daughter tachyzoites are released and subsequently infect other host cells, they are unable to infect or divide within the newly infected host cell effectively due to the effected apicoplast [55]. This phenotype is investigated in this work to identify if *N,N* di-aryl urea treatment causes any perturbations to apicoplast related pathways such as FASII or any other pathways.

Along with fatty acid synthesis, the apicoplast synthesis of isoprenoids is known to be essential in tachyzoites that are not within host cells and existing in extracellular space, similar to the FASII pathway. *De novo* isoprenoid production is complemented by tachyzoites sequestering isoprenoids, lipids, and cholesterol essential from their host cell for division and survival [56]. Once extracellular, tachyzoites are unable to synthesize all needed isoprenoids through the methylerythritol phosphate (MEP) pathway. To assess if *N,N* di-aryl urea compounds have any effect on isoprenoid production, *in vitro* isoprenoid supplementation is utilized here to quantify effects of treatment to *T. gondii* isoprenoid production.

Exploring if *N,N* di-aryl treatment has an effect on the apicoplast of *T. gondii* based on the hypothesized target of the parent compound, MMV52, may not allow for the capture of how these compounds are effecting *T. gondii* on a molecular level. Forward genetic screening through random chemical mutagenesis is a published method for the discovery of molecular targets of anti-Toxoplasma compounds. Through random mutations of *in vitro* tachyzoites and the selection of resistant tachyzoites by compound treatment, resistance can be established [37]. Resistant isolates are then screened for single nucleotide variants (SNVs) and are further investigated to determine possible molecular targets [37].

In this chapter the *N,N* di-aryl urea compound, U21, is further characterized by phenotypic growth assays and random chemical mutagenesis to identify a possible mechanism of action against *T. gondii*. Phenotypic growth analysis did not allow for a clear observation to conclude a possible mode of action. Additionally, random chemical mutagenesis failed to induce resistance in *T. gondii* tachyzoites, thus not allowing for further target analysis. Prompting further investigation and other techniques to be utilized which will be discussed in the following chapter, Chapter 3.

2.II Methods

Host Cell & *Toxoplasma gondii In Vitro* Culture

Host cells (HFF) and *T. gondii* tachyzoites were cultured as explained in Chapter 1: Methods [Section I.II].

Toxoplasma gondii Delayed Death Phenotype Analysis

HFF cells were grown to confluence in sterile T25 flasks. Once confluent, HFF cells were infected with 2000 *T. gondii* RH-dTom tachyzoites isolated from HFF cells. Once ~30% of HFF cells were confirmed to be infected through light microscopy, infected T25 flasks were then treated with U21 (IC_{90} concentration) for 4 days at 37C plus 5% CO_2. After 4 days of treatment, tachyzoites were isolated, centrifuged at 900G for 10 minutes, washed twice with 1X PBS to remove compound, and placed on uninfected HFF cells in T25 flasks at 2e4 tachyzoites/mL. Tachyzoite counts were taken daily through a BioTek LionHeart automated microscope via a red fluorescent protein filter and tachyzoite/mL values were calculated. Three days post-infection, tachyzoites were isolated and passed into uninfected HFF in T25 flasks at 2e4 tachyzoites/mL and tachyzoite counts were taken daily for 3 days. This process was repeated a total of two times. Clindamycin treated tachyzoites were included as a positive control for delayed death. Pyrimethamine and DMSO treated tachyzoites were included as negative controls.

FASII Pathway Target Analysis: Fatty Acid Supplementation

FASII target analysis was quantified through fatty acid supplementation. Confluent HFF cells in sterile tissue grade 96 well plates were infected with 2e4 *T. gondii* RH-dTom tachyzoites/mL. 24 hours after infection, infected cells were treated with increasing concentrations (0 – 100 µM) of U21 in duplicate. For fatty acid supplemented

groups, 1 µM of palmitic and myristic acid dissolved in 10% bovine serum albumin (BSA) were added. Tachyzoite viability was quantified through fluorescent readings by a BioTek Synergy plate reader for 5 days at 530/25 excitation and 590/25 emission. On day 5, IC_{50}s were calculated for each group. Triclosan was included as a positive control for FASII pathway inhibition. DMSO and pyrimethamine were included as negative controls.

MEP Pathway Target Analysis: Isopentyl Pyrophosphate Supplementation

Isoprenoid supplementation was utilized to determine if *N,N* di-aryl urea compounds inhibit the apicoplast dependent MEP pathway. HFF cells grown to confluence in tissue grade sterile 96 well plates were infected with 2e4 *T. gondii* RH-dTom tachyzoites/mL. 24 hours after infection, U21 compound treatment began at increasing concentrations (0 – 100 µM) in duplicate. To analyze if the MEP pathway was disrupted by compound treatment, isoprenoid pyrophosphate (IPP) was supplemented to treated tachyzoites added at 200 µM. Parasite growth was quantified via fluorescent readings through a BioTek Synergy plate reader at 530/25 excitation and 590/25 emission. Pyrimethamine and DMSO treated tachyzoites were included as negative controls.

Mechanism of Resistance Identification: Random Chemical Mutagenesis

Single point polymorphisms (SNPs) in *T. gondii* RH-dTom tachyzoites were induced through exposing a *T. gondii* infected HFF monolayer in a T175 culture flask at 10 µM of ethyl methanesulfonate (EMS) for 4 hours. Following EMS exposure, infected monolayers were gently washed twice with sterile 1X PBS. Mutated tachyzoites were isolated and transferred to a T25 flask of confluent HFF. 24 hours post infection, mutated parasites were isolated and passed to a fresh T25 flask of HFF and compound exposure

began at the respective IC_{25} concentration. Mutated parasites were maintained under compound selection and passed to uninfected T25 flasks once needed. Compound exposure was increased weekly through the following: IC_{30}, IC_{50}, IC_{70}, and then the respective IC_{90} concentration. A control group of *N,N* di-aryl urea compound treated non-mutated tachyzoites was included as a negative control. Once non-mutated tachyzoites were observed to be cleared by compound treatment through both light microscopy and fluorescent microscopy, mutated tachyzoites were labelled as potentially resistant. Resistant tachyzoites were then clonally isolated through serial dilutions in confluent HFF cells in 96 well plates and cultured further in HFF confluent T25 culture flasks. To quantify resistance of mutated tachyzoites, IC_{50}s were measured as described previously and fold resistance was calculated compared to wild type tachyzoite IC_{50} values.

2.III Results

I. *Toxoplasma gondii* Delayed Death Phenotype Analysis

Compound induced delayed death in *T. gondii* through *N,N* di-aryl urea compound treatment was assessed to determine potential apicoplast targeting through consecutive passages of previously treated tachyzoites. U21 was chosen for further analysis and characterization based on the survival rates of treated mice lethally infected with tachyzoites seen in Chapter 1. Over three passages after initial U21 treatment, no delayed death was observed following treatment (Figure 9). Pyrimethamine which is known to target a non-apicoplast target, folate metabolism through targeting *DHFR* [18], was included as a negative control for delayed death. Only clindamycin, a positive control for delayed death, was observed to have decreased parasite survival after the second passage (Figure 9).

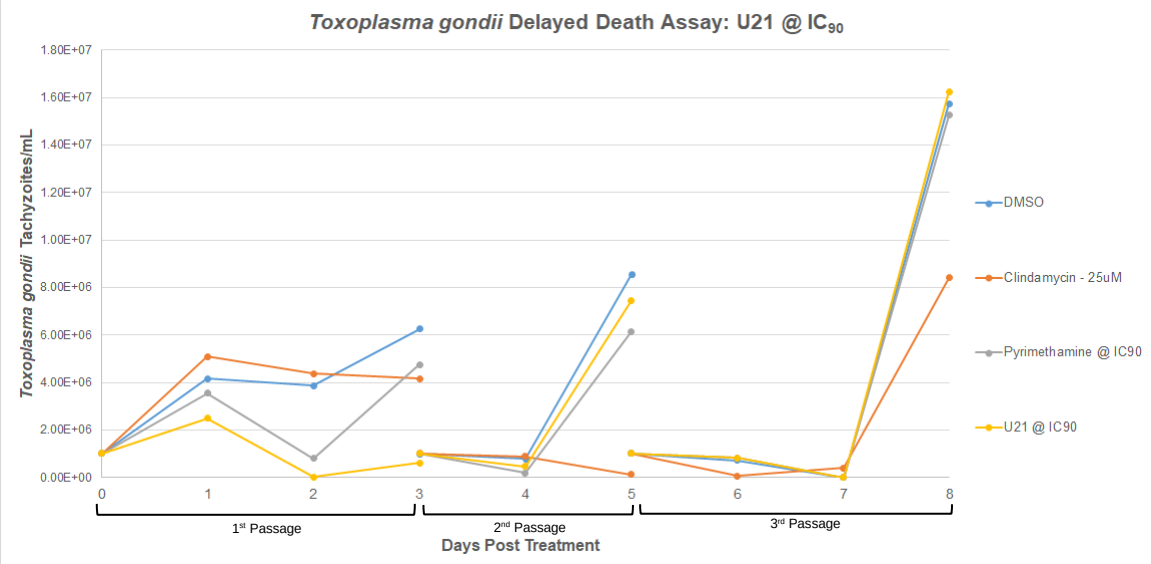

Figure 9: **Delayed death analysis of U21 treated *Toxoplasma gondii* tachyzoites.** HFF cells were allowed to grow to confluency in a T25 tissue culture flasks. Flasks were then infected with 2000 RH-dTom *T. gondii* tachyzoites and were allowed to infect HFF cells until ~30% of host cells were seen to be infected through light microscopy. To assess for any delayed death phenotypes, pyrimethamine (IC90 concentration), U21 (IC90 concentration), clindamycin (25 uM) or DMSO were then added to respective flasks and allowed to incubate with infected monolayers for 3 days. Following treatment, tachyzoites were isolated, spun down at 900G for 10 minutes to remove drug/compound, and 1EX tachyzoites were passed to a flask of uninfected HFF cells. Tachyzoite numbers were quantified through a BioTek LionHeart automated microscope and tachyzoites/mL were calculated. Three days post-infection, tachyzoites were isolated and diluted to 1EX tachyzoites/mL. This process was repeated two times to observe any delayed death phenotypes. Clindamycin was included as a positive control for delayed death in *T. gondii.*

II. FASII Pathway Target Analysis: Fatty Acid Supplementation

Fatty acid synthesis (FASII), a known essential pathway of the apicoplast [54]. Possible FASII inhibition was observed through supplementing U21 treated tachyzoites with palmitic and myristic acid which are known products of FASII in *T. gondii* [57]. U21 treated tachyzoites supplemented with fatty acids only caused an IC_{50} fold increase of 1.26 suggesting FASII is not inhibited by U21 treatment (Figure 10). Triclosan, a known FASII inhibitor in both prokaryotes and *T. gondii* [58], was seen to cause a partial rescue effect with an IC_{50} fold increase of 2.08 (Figure 10). Pyrimethamine, a known non-apicoplast inhibiting anti-toxoplasma drug, was included as a negative control for FASII inhibition with an observed IC_{50} fold increase of 1.08 with fatty acid supplementation (Figure 10).

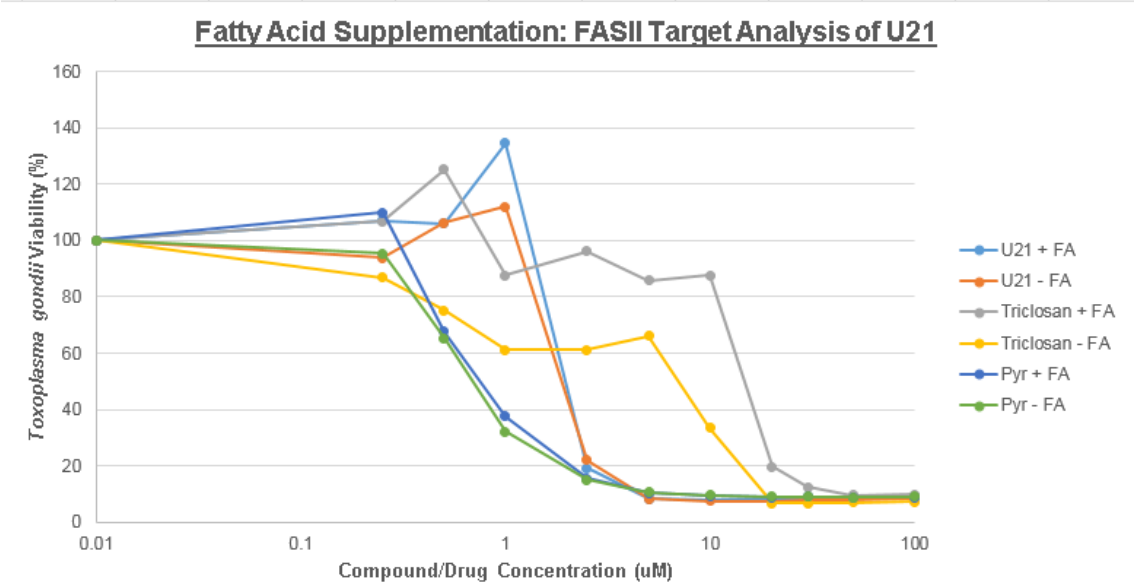

Compound/Drug ID	Fatty Acid Supplementation (+/-)	*Toxoplasma gondii* IC_{50}	IC_{50} Fold Increase
U21	+	2.1	1.26
U21	-	2.03	
Triclosan	+	15.55	2.08
Triclosan	-	7.47	
Pyrimethamine	+	0.79	1.08
Pyrimethamine	-	0.73	

Figure 10: FASII target analysis in *Toxoplasma gondii* utilizing fatty acid supplementation with U21. *T. gondii* RH-dTom tachyzoites were allowed to infect fresh HFF cells in a tissue grade 96 well plate at 2e4 tachyzoites/mL overnight. Once infection was confirmed through microscopy, respective compounds were then added at increasing concentrations in duplicate (0-100 µM). Additionally, fatty acids (myristic and palmitic acid) were added concurrently at 1 µM. A separate group did not receive fatty acid supplementation as a control. Triclosan, known FASII inhibitor in *T. gondii,* served as a positive control and pyrimethamine, *DHFR* inhibitor, served as a negative control. Fluorescent readings were taken daily and respective IC_{50}s calculated**.**

III. MEP Pathway Target Analysis: Isopentyl Pyrophosphate Supplementation

Apicoplast derived isoprenoid production via MEP pathway inhibition was investigated through supplementation of the isoprenoid isopentyl pyrophosphate (IPP). Following U21 treatment at increasing concentration (0 – 100 µM) with and without IPP supplementation, no rescue phenotype was observed when following IPP addition in an IC_{50} growth curve (Figure 11). Pyrimethamine was included as a negative control due to its known non-isoprenoid synthesis target, folate metabolism through inhibiting *DHFR*. Observed IC_{50} values of U21 or pyrimethamine treated tachyzoites were nearly identical

with or without IPP supplementation suggesting no U21 activity against isoprenoid production via the apicoplast (Figure 11).

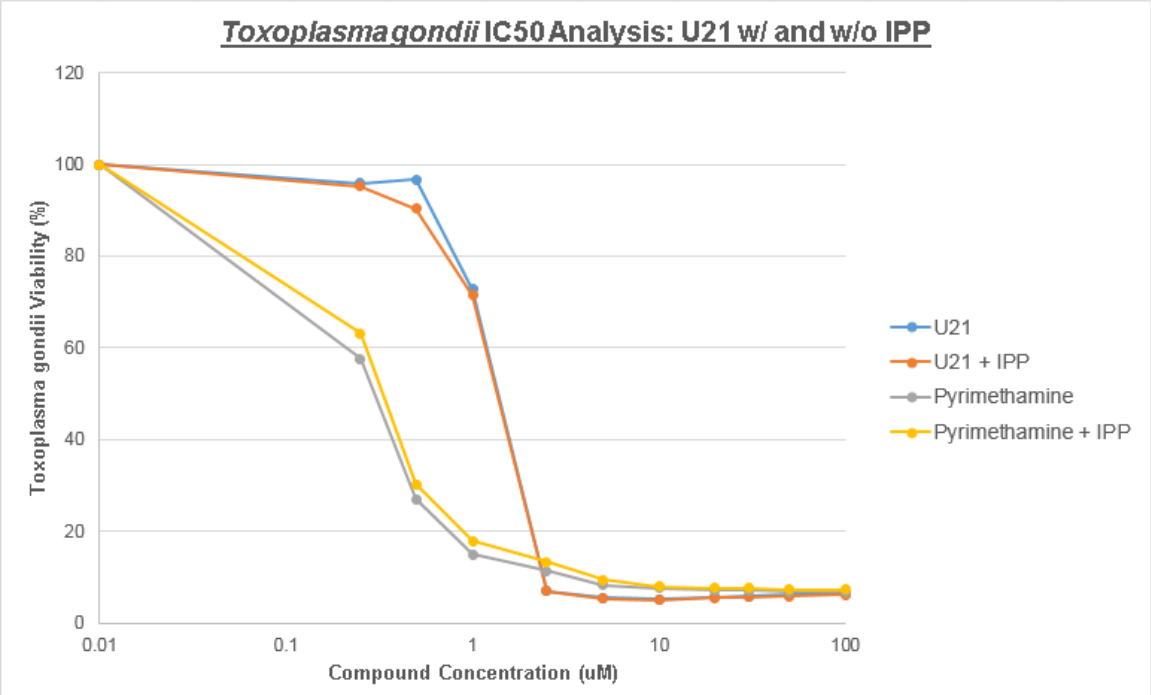

Figure 11: *Toxoplasma gondii* MEP Pathway Analysis Through Isopentyl Pyrophosphate Supplementation. Confluent HFF cells were infected with 2e4 RH-dTom *T. gondii* tachyzoites in a 96 well plate. 24 hours after infection, U21 was then added at increasing concentrations (0 – 100 µM) with and without isopentyl pyrophosphate (IPP) supplementation. Tachyzoite growth was monitored for 5 days through fluorescent readings at 530/25 excitation and 590/25 emission. On day 5, tachyzoite viability was quantified and relative IC_{50}'s calculated. Pyrimethamine treated tachyzoites were included as a control for IPP supplementation. All treatment groups were tested in duplicate.

IV. Mechanism of Resistance Identification: Random Chemical Mutagenesis

In attempts to identify a possible mechanism of resistance of U21 treated tachyzoites, random chemical mutagenesis was utilized. Following induction of random mutations through EMS exposure, mutated tachyzoites were selected for single nucleotide polymorphisms (SNPs) that conferred possible resistance to U21 through prolonged treatment over an extended period. U21 concentrations were increased over several months until an included negative control of U21 treated non-mutated tachyzoites were observed to be completely cleared in cell culture. Once observed, surviving mutated tachyzoites were clonally isolated and screened for resistance through IC_{50} analysis. Multiple separate rounds of mutagenesis were conducted in attempts to

capture resistant tachyzoites. Here, two separate rounds are shown for reference (Figure 12). Compared to wild-type (WT) IC_{50}s, no clonal isolates (A1, B1, C1, etc.) were identified to exhibit resistance to U21 (Figure 12). To conclude that isolates are resistant, at least a twofold increase in IC_{50} values would have to be observed. Further SNP dentification through bioinformatic analysis did not occur due to no measured resistance in any clonal isolates tested.

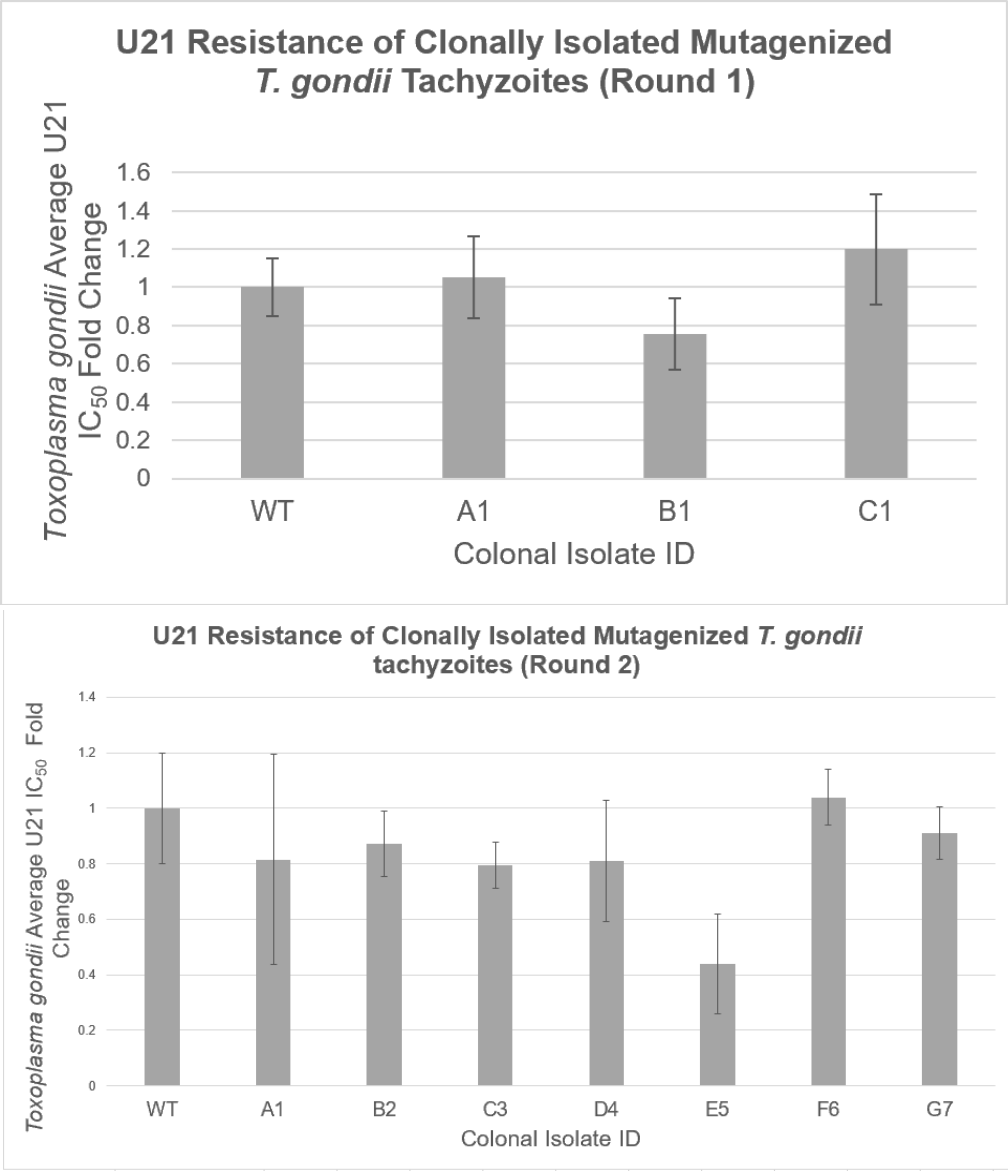

Figure 12: **U21 Resistance of clonally isolated mutagenized *T. gondii* tachyzoites**. Tachyzoites that survived EMS induced mutagenesis and appeared to confer resistance to U21 were clonally isolated. Resistant isolates were selected through serial dilutions and selection of cultures that only had one initial plaque form. Clonally isolated tachyzoites were allowed to grow to confluence and subsequent IC_{50} analysis was performed to calculate the fold change of resistance isolates compared to wild type (WT) tachyzoites. Figure A and Figure B represent two separate mutagenesis runs that subsequently did not produce U21 resistant T. gondii tachyzoites.

2.IV Discussion

Possible targets of U21 treated *T. gondii* tachyzoites were explored through phenotypic growth assays, supplementation assays, and random chemical mutagenesis. To investigate apicoplast targeting of *N,N* di-aryl urea compounds, a delayed death assay was utilized. Compounds and drugs that cause a delayed death phenotype in apicomplexan parasites after multiple passages following treatment is a known phenotype caused by apicoplast disruption [55]. U21 treatment did not cause observable delayed death suggesting that disruption of apicoplast related pathways is not the main mechanism of action of tachyzoite growth inhibition.

Activity against specific apicoplast pathways, fatty acid and isoprenoid production, were then quantified through supplementation-based assays followed by IC_{50} analysis. Fatty acid synthesis via the FASII pathway is a shared pathway of apicomplexan parasites and prokaryotes due to the hypothesized prokaryotic origin of the apicoplast itself [58]. Previous work has shown that fatty acid synthesis via the FASII pathway is essential for parasite growth and survival in both *Plasmodium* and *Toxoplasma*, suggesting a possible targetable pathway for future drug discovery [58]. Known prokaryotic FASII inhibitors, such as triclosan, are known to inhibit the FASII pathway in *T. gondii* proving that it is indeed a viable target for tachyzoite growth inhibition [58]. The di-aryl urea triclocarban, the parent compound of MMV52, has been hypothesized to target FASII in prokaryotes. Because of the potential activity of MMV52 against prokaryotic FASII synthesis, a fatty acid supplementation-based assay was utilized to investigate any effects U21 may have on the FASII pathway in *T. gondii* [58]. Fatty acid supplementation of U21 treated tachyzoites did not cause measurable rescue suggesting that U21 does not inhibit apicoplast derived fatty acid production via FASII pathway targeting.

The importance of isoprenoid production by the apicoplast of *T. gondii* and other apicomplexans is currently a point of debate in the field [59]. In *Plasmodium*, isoprenoid production during the red blood cell asexual stage, known as merozoites, is published to be a core process of the apicoplast [60]. Supplementation of the isoprenoid IPP in merozoites lacking an apicoplast allows for parasite survival, while merozoites lacking an apicoplast are not viable after several consecutive passages [60]. In contrast, in *T. gondii* isoprenoid production is one of many processes of the apicoplast during the tachyzoite life stage. Salvaging of isoprenoids from the host has also been reported, leading to further questions regarding how essential *de novo T. gondii* isoprenoid production is for parasite survival [61]. While it has been shown that intracellular parasites are capable of scavenging isoprenoids from the host, extracellular tachyzoites are known to be dependent on *de novo* synthesis of isoprenoids. To observe any effects that U21 may have on isoprenoid production, an IPP supplementation assay was utilized. U21 treated tachyzoites that were supplemented with IPP did not have an observed rescue phenotype suggesting that isoprenoid production is most likely not affected by treatment. Further analysis is needed to definitively conclude that U21 has no effect on *T*. gondii isoprenoid production.

Lastly, SNPs were induced throughout the entire *T. gondii* genome through random chemical mutagenesis followed by prolonged treatment with U21 to cause resistance in hopes to discover a mechanism of resistance and identification of a possible target through further genetic manipulation. In this study, random chemical mutagenesis failed to induce resistance to U21 treatment. In total, four complete mutagenesis runs were conducted, each not causing any significant resistance. These results may be the result of the random chemical mutagenesis assay design. Compound targets that are directly encoded by the nucleus of *T. gondii* which include enzymes that catalyze multi-step reactions when inhibited cause parasite death can be captured

through random chemical mutagenesis. While targets that would be unable to be identified by random chemical mutagenesis can include genes that are essential for parasite survival that cannot be mutated, metabolites of essential pathways, or targets that cause a phenotypic growth defect such as causing dysregulated invasion, motility, or membrane integrity. In addition, random chemical mutagenesis would be unable to capture if a compound of interest is modulating the infected host cell in a way that causes tachyzoite death.

2.V Conclusion

In conclusion, phenotypic growth and supplementation assays of U21 treated tachyzoites suggest a non-apicoplast target. In addition, random chemical mutagenesis failed to produce a U21 resistant isolate suggesting either multiple targets of U21 or a target that cannot be mutated is causing *T. gondii* growth inhibition. To further pursue how U21 is affecting *T. gondii*, differential expression analysis of treated tachyzoites and electron microscopy imaging is utilized in Chapter 3. Characterization of *N,N* di-aryl urea compounds activity against the chronic stage of *T. gondii* is also investigated in both *in vitro* and *in vivo* based assays.

CHAPTER 3: *In vivo* Chronic Activity and Differential Expression Analysis of Top Di-Aryl Urea Compound in *Toxoplasma gondii*

3.I Introduction

Clearing the quiescent chronic stage of *T. gondii* infection is imperative for the prevention of *Toxoplasma* encephalitis in immunocompromised patients [18]. For compounds to reach *T. gondii* cysts residing in brain tissue, they must first be able to pass through the blood brain barrier (BBB). Lipophilic compounds are more readily able to cross the BBB while hydrophilic compounds often are unable to cross [24]. Physicochemical analysis of *N,N* di-aryl urea compounds discussed in Chapter 1 identified that all were generally lipophilic compared to the parent compound MMV52. Therefore, I hypothesized that *N,N* di-aryl urea compounds would be able to cross the BBB and potentially effect *T. gondii* cysts. To evaluate this possibility, first the activity of *N,N* di-aryl urea compounds against *in vitro T. gondii* bradyzoites within tissue culture cysts can be quantified to determine if compounds have any general inhibitory effects to the chronic stage of *Toxoplasma*.

An assay capable of determining inhibitory effects of compounds against *in vitro* derived *T. gondii* cysts did not exist prior to this effort. The development of an *in vitro* assay allowed for the screening of experimental compounds for activity against chronic *T. gondii* infection prior to moving to an *in vivo* model. Once activity of *N,N* di-aryl urea compounds was established in an *in vitro* model, a murine model could then be utilized to determine efficacy against *T. gondii* cyst formation and *T. gondii* cyst clearance in brain tissue.

Visualizing the effects of treated *T. gondii* allows for the identification of physical phenotypes caused by treatment. Scanning electron microscopy (SEM) captures surface phenotypes of *in vitro* treated tachyzoites [62] while transmission electron microscopy (TEM) images ultrastructure phenotypes such as organelle structure, intracellular

processes, formation of the parasitophorous vacuole, and tachyzoite division within host cells [63]. Electron microscopy analysis only allows for qualitative analysis and should not be utilized for the conclusion of how compounds are affecting *T. gondii*. Previous experiments in Chapter 1 and Chapter 2 did not give any indication on how *N,N* di-aryl urea compounds are inhibiting *T. gondii*. Hypothesizing what effects would be visualized by electron microscopy analysis was therefore difficult. I hypothesized that *N,N* di-aryl urea compound treatment would cause a phenotype, or multiple phenotypes, but hypothesizing what those phenotypes may be was not possible with the available data. In this chapter, SEM analysis allowed for the visualization of the perturbation of the cell membrane of tachyzoites when under *N,N* di-aryl urea treatment.

Quantifying activity against the chronic stage of *T. gondii* is equally as important for characterization of *N,N* di-aryl urea compounds and the identification of a mechanism of action of *N,N* di-aryl urea compounds is pivotal for future drug development. Understanding how compounds are affecting *T. gondii* on a molecular level would allow for further derivatization to optimize activity against that target. In Chapter 2, U21 was concluded to not affect the apicoplast of *T. gondii*. Random chemical mutagenesis also failed to identify a mechanism of action due to the inability to force U21 resistance in *in vitro* tachyzoites. Knowing that random chemical mutagenesis failed allowed for the conclusion that U21 may be targeting a target or pathway that cannot be mutated such as an essential gene or effecting the structural integrity of *T. gondii*. Based on the knowledge that U21 does not affect the apicoplast of *T. gondii* and random chemical mutagenesis failed, I hypothesized that U21 is affecting a pathway or target that is not related to the apicoplast and is targeting a process in *T. gondii* that random chemical mutagenesis is unable to identify.

To then further investigate how *N,N* di-aryl urea compound treatment are inhibiting *T. gondii*, differential expression was utilized. Quantifying both up and down regulated transcripts by RNA-seq analysis allows for the identification of pathways that are directly affected by treatment [41]. Based on SEM analysis identifying that treatment caused cell membrane disruption, I hypothesized that treatment disrupts the synthesis or structural integrity of the cell membrane of tachyzoites. Surprisingly, this effect was confirmed by RNA-seq analysis suggesting that *N,N* di-aryl urea compounds do indeed cause cell membrane disruption in tachyzoites.

3.II Methods

Host Cell and *T. gondii In vitro Cell Culture*

HFF cells and *T. gondii* tachyzoites were cultured as described in Chapter 1 [Section II].

Activity Analysis of Compounds against *In vitro* Chronic *Toxoplasma gondii* – Fluorescent Imaging

To assess activity of di-aryl urea compounds against *in vitro* chronic *T. gondii* infection, HFF cells were cultured in optically correct 96 well cell culture grade plates. Once confluent, HFF cells were infected with 2e5 *T. gondii* PRUku80 tachyzoites and cultured at 37C at 5% CO2. Tachyzoites were given at least 48 hours to infect host cells, or until ~40% of host cells were infected. Stage conversion from tachyzoites to bradyzoites within *in vitro* cysts was induced by either exposure to Compound 1 or alkaline D10 media (pH 8.5).

For Compound 1 exposure, infected HFF monolayers were exposed to 1uM of Compound 1 for 72 hours. For the differentiation of tachyzoites in alkaline media, infected monolayers were exposed to alkaline media at 37C with no CO_2 for 7 days.

Stage differentiation was confirmed through fluorescent microscopy. *T. gondii* PRUku80 tachyzoites constitutively express green fluorescent protein (GFP) under the *T. gondii* lactate dehydrogenase 2 (LDH2) promotor [64]. Alkaline induction of bradyzoite differentiation through culturing infected HFF monolayers with alkaline media at 37C with no CO_2.

Following differentiation of tachyzoites to bradyzoites through *in vitro* culture and confirmation by fluorescent microscopy, compounds were added in duplicate at increasing concentrations (0 – 100 µM). Cyst burdens in treated and untreated samples were determined by automated counts of GFP positive cysts using a BioTek LionHeart automated microscope. IC_{50} values were calculated from respective cyst counts day 5 post-treatment.

Activity Analysis of Compounds against *In vitro* Chronic *Toxoplasma gondii* –Plaque Assay

Di-aryl urea compound activity against *in vitro* chronic *T. gondii* infection was also explored by a modified plaque assay. Briefly, HFF cells were cultured in T25 culture flasks until confluent and infected with 2e5 *T. gondii* PRUku80 tachyzoites. Tachyzoites were given at least 72 hours to infect HFF cells. Following infection, 1 µM of Compound was then added to differentiate tachyzoites to bradyzoites within *in vitro* cysts. Compound 1 exposure lasted 72 hours and stage conversion was confirmed by fluorescence microscopy. Compound treatment then began at increasing concentrations, up to 10 µM, and lasted 5 days. Pyrimethamine was included as a negative control for targeting bradyzoites and atovaquone as a positive control for activity against bradyzoites.

To quantify surviving bradyzoites, cysts were isolated with a modified pepsin digestion method. Treated infected monolayers were lightly scrapped with a rubber

spatula, transferred to conical tubes, spun down at 900G for 10 minutes, and resuspended in 1mL of 1X PBS. 1mL of pepsin digestion solution (0.26g pepsin, 5g NaCl, 7 g HCL, and 500mL distilled water) was then added and allowed to incubate at room temperature for 10 minutes. Digestion was quenched with 1mL of 350 mM sodium carbonate and spun down at 400G for 10 minutes. Supernatant was aspirated off, isolated bradyzoites were resuspended in 5mL of D10 media, and then placed in a confluent HFF 12 well plate. Bradyzoites were allowed to reconvert back to tachyzoites and infect HFF cells for a minimum of 7 days. Once individual plaques were formed by tachyzoites infecting and lysing HFF cells, monolayers were fixed with ice-cold methanol for 2 minutes and stained with 2% crystal violet solution containing 0.8% ammonium oxalate and 20% ethanol for 10 minutes. Crystal violet was then removed by washing with distilled water until plaques could clearly be seen and counted under light microscopy.

In vivo Toxoplasma gondii Cyst Prevention

Mice that received a lethal infection of *T. gondii* tachyzoites and were treated with U21 at 100 mg/kg through oral gavage administration on day 3, 5, and 7 post-infection. 28 days post-infection, mice were sacrificed by CO_2 induction and brain tissue was isolated through necroscopy. Brain tissue was homogenized by a Tissue Tearer in 1mL of DNA extraction buffer (60 mM Tris pH 8.0, 100 mM EDTA, 0.5% SDS) until a homogenous solution was obtained. Samples were spun down at 400G for 4 minutes at 4C. Supernatant was removed and 1 volume of phenol/chloroform/isoamyl alcohol (25:24:1) was added and vortexed for 20 seconds and centrifuged at max speed for 5 minutes. This process of added phenol/chloroform/isoamyl alcohol was repeated twice to allow for clean extraction of genomic DNA. Isolated genomic DNA was then ethanol precipitated through adding 1/10 volume of 3 M sodium acetate (pH 5.2) and 2 volumes

of 100% ethanol. Samples were placed at -20C for 25 minutes, spun at max speed for 5 minutes, supernatant removed, pellet washed with ice cold 70% ethanol, pellet resuspended, spun again at max speed for 5 minutes, supernatant removed, and the pellet was then allowed to dry for 15 minutes at room temperature. Once dry, pellets were resuspended in 100 µL of nuclease free H_2O and stored at -20C. Genomic DNA values were obtained by a NanoDrop (ThermoFischer).

T. gondii genomic DNA was quantified through quantitative polymerase chain reaction (qPCR) analysis. Primers used are described in Table 6. Delta delta Ct values were calculated by normalizing samples to brain derived neuroeffector (BDNF) and fold expression of *T. gondii* REP529 was determined by comparing treated infected mice to an untreated mouse that received a lethal infection of *T. gondii* tachyzoites.

Toxoplasma gondii In vivo Cyst Clearance

Six-week-old female CBA/J mice from Jackson Laboratories were infected with 2000 *T. gondii* PRUku80 tachyzoites. Four days post-infection, mice were administered 5 mg/kg sulfadiazine in drinking water supplemented with 2% w/v sugar. On day 13 and day 14 post-infection, mice were given 5 mg/kg pyrimethamine through intraperitoneal injection to allow mouse survival and the subsequent formation of *T. gondii* cysts. Experimental compound administration began on day 25 post-infection and lasted 14 days. U2 was administered every three days through oral gavage (n=15). Mice administered only solvent through oral gavage were included as a negative control.

Once treatment ended, brain tissue was extracted through necropsy and homogenized with a TissueTearor in 2 mL DNA extraction buffer until a homogenous mixture was obtained. DNA was extracted using Phenol-Chloroform based isolation described above. *T. gondii* genomic DNA was quantified through absolute quantification-based qPCR. Primers utilized are described in Table 6. Briefly, a standard curve was

determined by performing qPCR on genomic DNA from a known number of tachyzoites cultured *in vitro*. The number of tachyzoites were serially diluted, DNA isolated, and Ct values determined by qPCR using three *T. gondii* genes: REP529, ITS1, and B1. All samples were normalized to mouse brain neuro derived neuro factor (BDNF). This process was replicated until a consistent standard curve that had a respective R^2 value of at least 0.9 was obtained. Parasite burden in mouse brain tissue was determined through qPCR analysis primers specific for *T.* gondii including REP529, ITS1, and B1 (Table 6) and plotting Ct values on the previously mentioned standard curve. A control of genomic DNA isolated from *in vitro* 1E4 *T. gondii* PRUku80 tachyzoites was included to verify the accuracy of the derived standard curve in each qPCR experiment.

Scanning Electron Microscopy

HFF cells were cultured T25 cell culture flasks at 37C plus 5% CO2 until confluent. Once confluent, 2e5 *T. gondii* RH-dTom tachyzoites/mL were added and allowed to infect until at least 50% of cells were confirmed to be infected through light microscopy. Infected cell cultures were then treated at the IC_{50} concentration of U21 for 24 hours of dimethyl sulfoxide (DMSO) as a negative control. After treatment, tachyzoites were isolated through Dounce homogenization and filtered through a 5 µm and then a 3 µm filter. Isolated tachyzoites were spun down at 900G for 10 minutes and then subsequently fixed in 2% glutaraldehyde, 2% paraformaldehyde, and 0.1 M Sorensen's phosphate buffer. Tachyzoites were submitted to the Electron Microscopy Core Facility at the University of Nebraska Medical Center for scanning electron microscopy imaging of both U21 and DMSO treated samples.

Transmission Electron Microscopy

HFF cells were cultured in tissue grade 6 well plates on coverslips until confluent. Once confluent, HFF monolayers were then infected with 2e5 *T. gondii* RH-dtom tachyzoites/mL and allowed to infect until at least 50% of HFF cells were confirmed to be infected through light microscopy analysis. Infected monolayers were then treated with U21 at the IC_{50} or IC_{90} concentration for 24 hours. DMSO treated tachyzoites were included as a negative control. After treatment, media was removed and fixed with 2% glutaraldehyde, 2% paraformaldehyde, and 0.1 M Sorensen's phosphate buffer. Fixed samples were submitted for transmission electron microscopy at the Electron Microscopy Core Facility - University of Nebraska Medical Center.

Gene Name	**Primer ID**	**Forward Primer**	**Reverse Primer**
Murine BDNF	BDNF	CTCTTTCTGCTGGAGGAATACA	ACATGTCCACTGCAGTCTTT
T. gondii REP529	REP529	AGAGACACCGGAATGCGATCT	TCGTCCAAGCCTCCGACT
T. gondii B1	B1	CAAGCAGCGTATTGTCGAGTA GAT	GCGTCTCTTTCATTCCCACAT TTT
T. gondii ITS1	ITS1	GATTTGCATTCAAGAAGCGTGA TAGTAT	AGTTTAGGAAGCAATCTGAA AGCACATC
T. gondii phosphatidylserine synthase	TgPSS	GAAACCTGGCGATGTTGCTG	CCCCAGTGTCGGAGAATGAC
T. gondii phosphatidylinositol synthase	TgPIS	GGAGGCAAAAGTGTCCAAGC	CGATCGCCGAAAACATGACC

Table 6: Primers were designed for qPCR analysis of target genes. Amplification of genes was confirmed through PCR amplification and visualized on a 2% agarose gel (data not shown).

RNA-seq Differential Expression Analysis

HFF cells were cultured in T25 tissue culture flasks until confluency was reached. 2e4 *T. gondii* RH-dTom tachyzoites/mL were then added and allowed to infect cells until

~50% of host cells were observed to be infected by light microscopy. U21 treatment then began at the IC_{25} and IC_{50} concentration for 24 hours. DMSO treated tachyzoites were included as a negative control for differential expression analysis. After treatment, infected monolayers were rinsed twice with sterile 1X PBS. The infected monolayer was then scraped gently with a rubber policeman and spun down at 400G for 10 minutes. PBS was aspirated off and 600uL of lysis solution, containing 10 µL 2-mercaptoethanol, was added and pipetted up and down until homogenous. Lysate was transferred to a QiaShredder tube and spun at max speed for 2 minutes. Isolation of RNA was completed through the use of a RNAeasy mini kit (Qiagen). RNA values were measured on a NanoDrop and 260/280 values were measured to ensure RNA quality. RNA was submitted to The University of Nebraska Medical Center NGS Core for Next Generation Sequencing analysis with a NextSeq under the following parameters: 200 basepair length, paired end reads and high output.

Raw NGS reads (NCBI Accession ID: PRJNA725840) were aligned to the TgGT1 transcriptome for non-host reads and HG38 for host reads by BowTie2. Quantification of *T. gondii* transcripts was performed with Salmon and differential expression (Log2 fold change) was calculated with DESeq2. Fold change was gated to a Log2 fold change of 1.5 with a p value less than 0.05. Both upregulated and downregulated transcripts were then inputted into ToxoDB for gene ontology analysis for affected biological processes.

Differential Expression Analysis - qPCR Verification

To verify differential expression analysis, qPCR analysis was utilized. The following significantly upregulated transcripts that were identified through gene ontology analysis of affected biological processes were chosen: *T. gondii* phosphatidylserine synthase (TgPSS) and *T. gondii* phosphatidylinositol synthase (TgPIS). Primers utilized are described in Table 6. In addition to the RNA isolated from U21 and DMSO treated

tachyzoites, RNA was also isolated from tachyzoites treated with 10 µM of Elacridar as a positive control for dysregulated lipid metabolism in *T. gondii*. cDNA was synthesized from isolated RNA using a Maxima First Strand cDNA Synthesis Kit (Fisher Scientific). All treatment groups were tested in triplicate and compared to the *T. gondii* house-keeping genes REP529, RibosomeL33, and Histone2B. Delta delta Ct values were calculated by comparing treated values to untreated (DMSO) samples and Log2 fold increases or decreases were plotted through Microsoft Excel. Statistical analysis on log2 fold change was performed through a single tailed Student's T-test on Microsoft Excel.

3.III Results

Activity Analysis of Compounds against *In vitro* Chronic *Toxoplasma gondii* – Fluorescent Imaging

To assess U21 activity against *in vitro T. gondii* cysts, a fluorescent based counting assay was initially utilized by quantifying green fluorescent protein (GFP) expressing bradyzoites in tissue grade 96 well plates. Acutely infected HFF monolayers were differentiated to bradyzoites within cysts by both the cyclic GMP dependent protein kinase inhibitor Compound 1 [65] and through culturing infected monolayers in alkaline media [66]. Following Compound 1 differentiation, U21 compound was administered in duplicate at increasing concentrations. Atovaquone, published to exhibit activity against *in vivo T. gondii* cysts *in vivo* [67], was included as a positive control. Doxycycline, a known antibiotic that is effective against both *in vitro* and *in vivo* acute *T. gondii* infection [15] was included as well. Five days after treatment began, cysts were quantified by an automated fluorescent scope and respective IC_{50}s determined. Both doxycycline and atovaquone were observed to be effective at IC_{50}s of 19.28 and 12.69 µM respectively (Figure 13). U21's IC_{50} value impressively was measured at 3.52 µM (Figure 13).

To confirm that U21 activity was not dependent on Compound 1 differentiation of acutely infected HFF monolayers, activity was also measured against chronically infected monolayers differentiated by alkaline media. Similar to IC_{50} values against Compound 1 differentiated *T. gondii* cysts, alkaline induced cysts exhibited an IC_{50} value of 6.62 µM (data not shown).

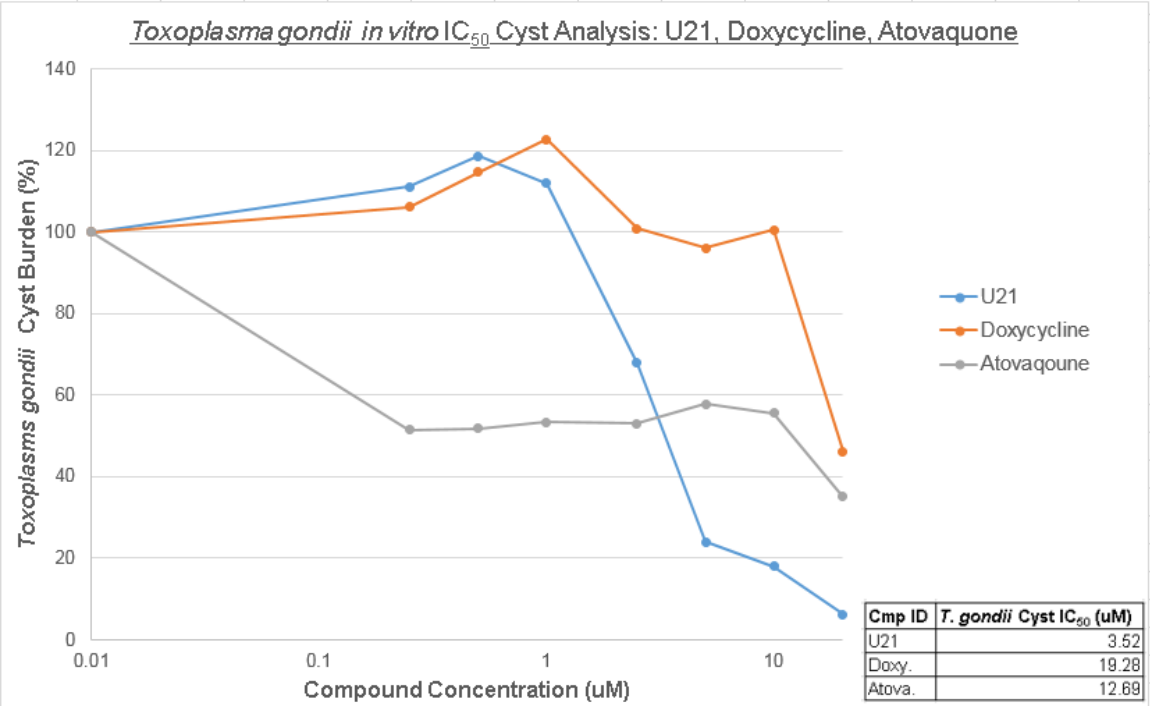

Figure 13: *Toxoplasma gondii in vitro* Cyst Inhibition Analysis: Fluorescent Imaging. HFF monolayers in tissue grade 96 well plates were infected with 2e5 *T. gondii* PRU tachyzoites and allowed to infect for 2 days. Intracellular tachyzoites were then differentiated to bradyzoites within *in vitro* cysts through Compound 1 exposure at 3 µM for an additional 2 days. Stage differentiation was confirmed by fluorescent microscopy and the identification of GFP expressing *T. gondii cysts.* Once confirmed U21, doxycycline, and atovaquone were added at increasing concentrations (0 – 50 µM) in duplicate while keeping Compound 1 exposure on cysts. GFP expressing cysts were quantified by a BioTek LionHeart over the course of 5 days. On day 5, cyst burdens were quantified and IC_{50}s were calculated.

Activity Analysis of Compounds against *In vitro* Chronic *Toxoplasma gondii* –Plaque Assay

Following IC_{50} analysis of *in vitro T. gondii* cysts through IC_{50}s derived from fluorescent counts of GFP expressing cysts, plaque assays were then utilized to further

characterize activity of *N,N* di-aryl urea compounds against the chronic stage of *T. gondii in vitro*. Following *in vitro* Compound 1 cyst differentiation of acutely infected HFF monolayers, *N,N* di-aryl urea compound administration began at 1, 5 and 10 µM. Atovaquone treated *in vitro* cysts were included a positive control for cyst activity while pyrimethamine was included as a negative control due to the known lack of activity against chronic *T. gondii* infection. Triclocarban, a parent to MMV52, was also included and exhibited activity against *in vitro* cysts beginning at 5 µM (Table 7). AR33, the parent compound of all tested U compounds, was observed to only have moderate activity at 10 µM. Both U21 and U26 exhibited similar activity profiles with U21 being the most effective with no visual plaques present at 10 µM. While U28 was the least effective of the three tested di-aryl urea compounds with no measurable activity up to 10 µM (Table 7). As expected, no activity was measured for either DMSO, solvent, or pyrimethamine treated. Moderate activity was measured for the positive control Atovaquone at 10 µM (Table 7).

	DMSO	Pyr	TCC			AR33			U21			U26			U28			Atov
Concentration (μM)	-	10	1	5	10	1	5	10	1	5	10	1	5	10	1	5	10	10
Number of Plaques	>60	>60	>60	2	0	>60	>60	33	>60	11	0	>60	20	3	>60	>60	>60	30

Table 7: *Toxoplasma gondii* Bradyzoite Inhibition by U21. *T. gondii* PRUku80 tachyzoites were differentiated to bradyzoites via exposure to 3uM of Compound 1 for 4 days. Following differentiation, compound was added at increasing concentrations. Pyrimethamine was tested as a negative control. Compound exposure lasted for 4 days. Remaining bradyzoites were then isolated through pepsin digestion. To determine amount of isolated bradyzoites, a plaque assay was utilized via crystal violet staining and light microscopy.

In vivo Toxoplasma gondii Cyst Prevention

Activity of U21 against the prevention of cyst formation *in vivo* cysts of mice infected with a lethal amount of tachyzoites and subsequently treated for 10 days with compound (Figure 5) 24 hours after infection was determined through qPCR analysis of isolated brain tissue (n=4). Pyrimethamine treated mice (n=4) were included as a control because of the published lack of significant activity *in vivo* against chronic *T. gondii* infection. Levels of *T. gondii* activity in both groups were normalized to an acutely infected mouse that received no treatment. Accordingly, pyrimethamine treated mice exhibited a very slight decrease in bradyzoite burden, with U21 also having little to no effect (Figure 14). It is important to note that neither values were statistically significant. Due to these inconclusive results, a standardized method of measuring cyst burdens in mice with already formed chronic infections was utilized in the next assay.

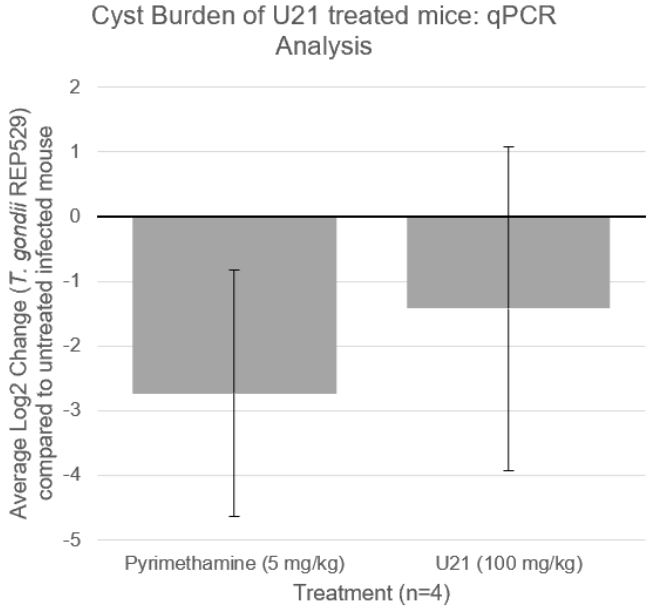

Figure 14: Cyst Burden Values of Acutely Infected Mice Treated with U21. CFW mice that were infected with 2e4 *T. gondii* ME49 tachyzoites and treated with either U21 (100mg/kg, n=4), pyrimethamine (5 mg/kg, n=4) or solvent (n=1) were sacrificed for the collection of brain tissue. Brain tissue was homogenized by a TissueTearor and DNA isolated using phenol & chloroform. Cyst burdens were quantified by qPCR through delta delta ct calculations of *T. gondii* REP529 compared to an untreated infected mouse and Log2 fold changes were plotted.

Toxoplasma gondii In vivo Cyst Clearance

To assess U21's ability to clear *T. gondii* cysts in chronically infected CBA/J mice, mice were infected with a sub-lethal amount of *T. gondii* PRUku80 tachyzoites. Once chronic infection was established, 25 days post infection, U21 treatment began at 100 mg/kg through oral gavage administered every three days for 2 weeks (n=11). After treatment, mice were sacrificed, and brain tissue harvested. Parasite burden was quantified through absolute quantification qPCR analysis on isolated DNA. Compared to solvent treated mice (n=11), U21 did not allow for a significant decrease in *T. gondii* counts in brain tissue of chronically infected mice (Figure 15, p value > 0.05).

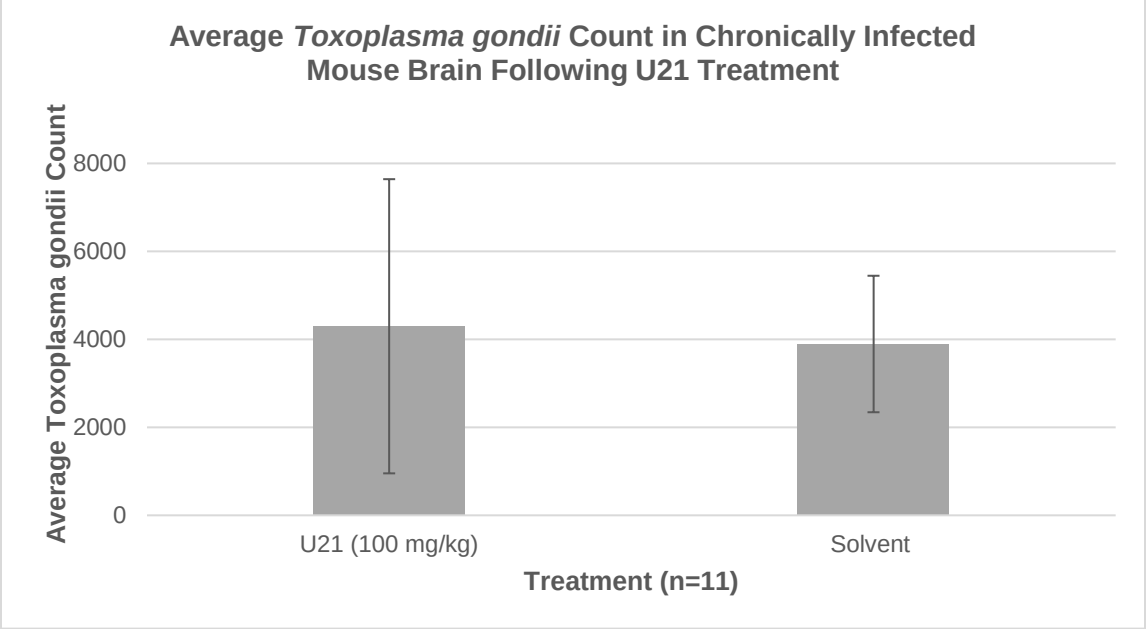

Figure 15: Average *Toxoplasma gondii* Count in Chronically Infected Mouse Brain Following U21 Treatment. CBA/J mice (n=30) were infected with a sub-lethal amount of *T. gondii* PRUku80 tachyzoites (1000) and allowed to form chronic infection. Mice were administered sulfadiazine at 5 mg/kg in their water supply on day 5 post infection for two weeks and pyrimethamine through intraperitoneal injection on days 14 and 15 post infection to allow for survival of acute infection. 25 days post infection, mice were administered 100 mg/kg of U21 through oral gavage every 3 days for two weeks (n=11). After treatment mice were sacrificed, brain tissue harvested, DNA isolated, and parasite counts then determined through absolute quantification qPCR. Mice treated with solvent were included as a control. U21 did not allow for a significant decrease in parasite load compared to solvent treated in chronically infected mice (p value > 0.05).

Scanning Electron Microscopy Imaging

Surface effects of U21 treated *in vitro* tachyzoites isolated from an infected HFF cells were visualized through Scanning Electron Microscopy (SEM). Solvent treated, DMSO, tachyzoites were included as a negative control to serve as a point of reference. U21 treated tachyzoites were isolated 24 hours after treatment and submitted for SEM imaging. Interestingly, a subset of tachyzoites were seen to have altered cell membranes that were potentially partially collapsed (Figure 15B & 15C). DMSO treated tachyzoites (Figure 15A) did not exhibit this phenotype of altered cell membranes.

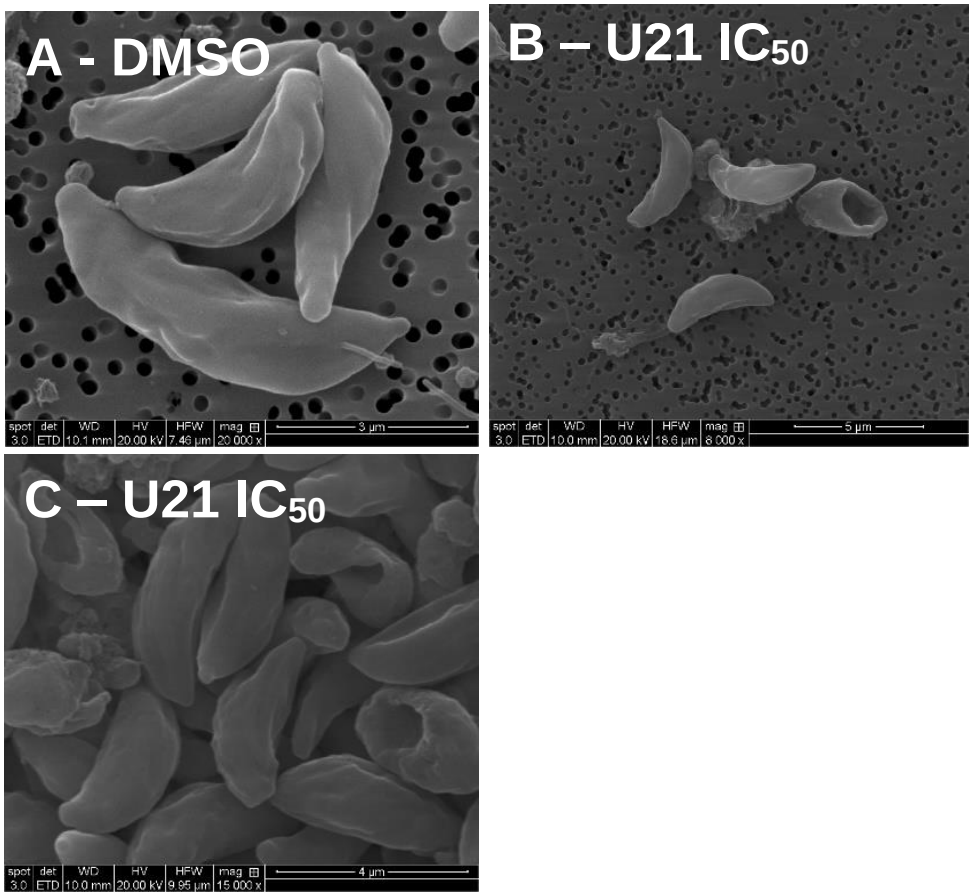

Figure 16: Scanning Electron Microscopy Analysis of U21 treated *Toxoplasma gondii* tachyzoites. HFF cells were infected with RH-dTom *T. gondii* tachyzoites and allowed to infect until ~50% confluency was observed. Treatment with DMSO [Image A -Negative Control] or U21 at IC_{50} [Image B & C] then began and lasted for 24hrs. Parasites were then isolated from HFF cells, filtered, and submitted for SEM scanning.

Transmission Electron Microscopy Imaging

Ultrastructure phenotypes of *in vitro* intracellular tachyzoites caused by U21 treatment were visualized through Transmission Electron Microscopy (TEM). DMSO treated tachyzoites were included as a negative control for no treatment to serve as a point of reference for treated tachyzoites (Figure 16A). Compared to DMSO treated tachyzoites, no observable phenotypes were observed when tachyzoites were treated with U21 at the IC_{50} or IC_{90} concentration (Figure 16B & 16C). This was confirmed by a well-established *T. gondii* TEM research group at Washington University.

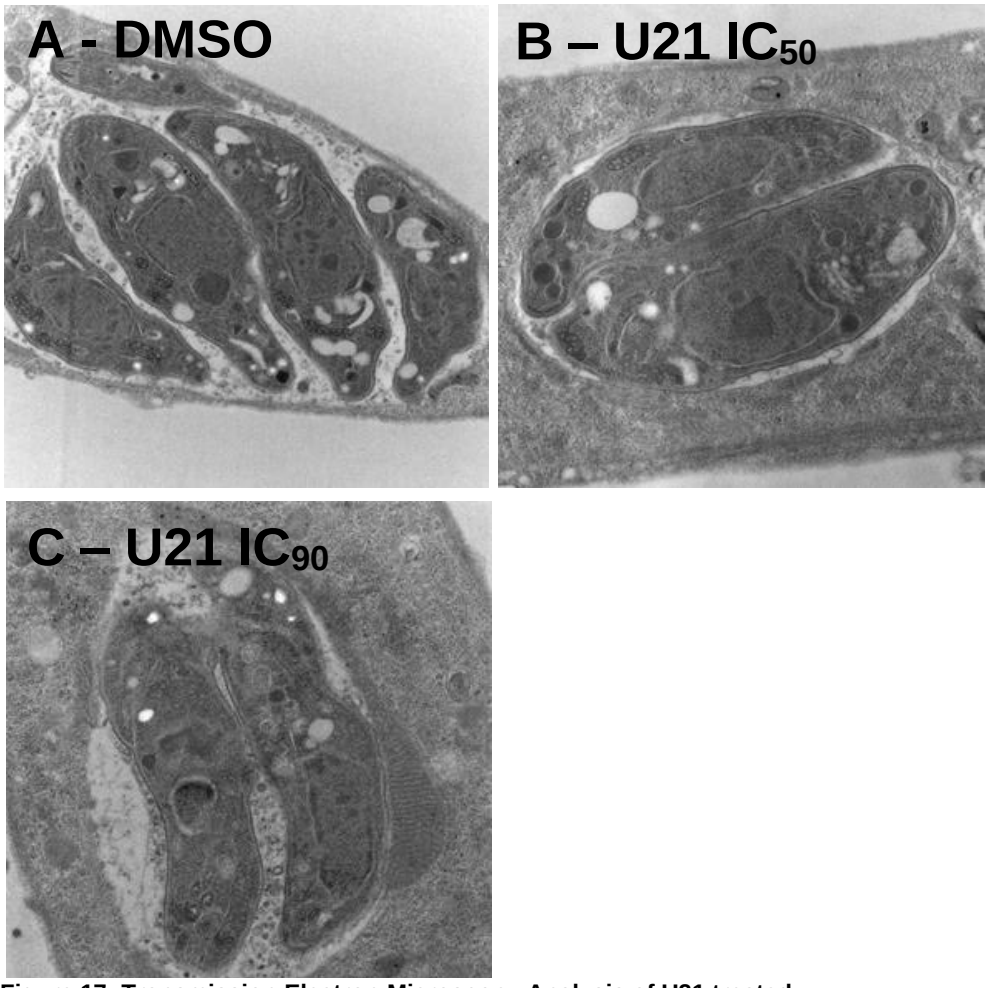

Figure 17: Transmission Electron Microscopy Analysis of U21 treated *Toxoplasma gondii* tachyzoites. HFF cells were infected with RH-dTom *T. gondii* tachyzoites and allowed to infect until ~50% confluency was observed. Treatment with DMSO [Image A - Negative Control] or U21 at IC_{50} [Image B] or IC_{90} [Image C] then began and lasted for 24hrs. Infected host cells were then fixed and submitted for TEM scanning.

RNA-seq Differential Expression Analysis

Following unsuccessful attempts to identify a potential mechanism of action of U21 in Chapter 2, differential expression analysis by RNA-seq technology was utilized. Differential expression analysis was completed through the comparison of treated versus untreated tachyzoite transcriptomes (NCBI Accession ID: PRJNA725840). Significantly upregulated (358 transcripts, p value < 0.05) and downregulated (171 transcripts, p value < 0.05) transcripts were selected to identify biological processes via gene ontology analysis that were directly affected by U21 treatment. Gene ontology (GO) analysis of significantly upregulated genes identified that transcripts responsible for *T. gondii* lipid metabolism were significantly upregulated (Table 8). A subset of these transcripts from a singular gene ontology ID are presented in Table 8. No biological processes were identified from significantly down regulated transcripts. In addition, both upregulated and downregulated pathways were included in gene ontology analysis for affected biological processes and no other processes were identified through GO analysis.

REF Seq ID	log2FoldChange	Gene Description	pvalue
TGGT1_202390	1.62	S15 sporozoite-expressed protein	5.99E-21
TGGT1_202750	2.68	3' exoribonuclease family, domain 1 domain-containing protein	3.30E-03
TGGT1_203390	1.82	CRAL/TRIO domain-containing protein	5.59E-10
TGGT1_203470	1.68	hypothetical protein	1.06E-03
TGGT1_204090	1.99	eIF2 kinase IF2K-C	1.89E-04
TGGT1_206610	1.76	pyruvate dehydrogenase complex subunit PDH-E2	7.00E-07
TGGT1_207450	1.58	DNA segment, Chr 10, Wayne State University 52, expressed family protein	7.26E-07
TGGT1_207710	2.10	putative phosphatidylinositol synthase	5.18E-04
TGGT1_209080	2.65	transport protein particle (trapp) component, bet3 protein	6.77E-04
TGGT1_211040	2.67	Sec61beta family protein	6.01E-04
TGGT1_213690	3.43	ring box protein 1 family protein	1.69E-03
TGGT1_213752	1.64	herpesviridae ul52/ul70 dna primase	9.26E-04
TGGT1_214290	1.51	DJ-1 family protein	6.19E-19
TGGT1_214480	1.80	replication factor a protein 3 protein	4.46E-05
TGGT1_216000	1.57	alveolin domain containing intermediate filament IMC3	3.19E-46
TGGT1_217700	1.61	AP2 domain transcription factor AP2XII-2	8.84E-06
TGGT1_218540	1.63	putative peptidase S15	9.58E-10
TGGT1_219682	2.41	putative pyruvate dehydrogenase kinase	1.13E-04
TGGT1_220160	1.77	WD domain-containing protein	2.73E-03
TGGT1_220270	2.08	alveolin domain containing intermediate filament IMC6	3.77E-26
TGGT1_221410	2.43	actin-like protein ALP4	1.40E-05
TGGT1_223920	1.63	rhoptry neck protein RON3	1.38E-117
TGGT1_226370	1.99	dgat2l1-prov protein	7.25E-08
TGGT1_228990	1.65	zinc finger (CCCH type) motif-containing protein	2.57E-09
TGGT1_229200	1.54	hypothetical protein	5.95E-04
TGGT1_229330	3.41	Cof family hydrolase subfamily protein	3.16E-03
TGGT1_230380	1.58	protein translocation complex, SEC61 gamma subunit	3.78E-22
TGGT1_231400A	4.34	tubulin/FtsZ family, GTPase domain-containing protein	1.42E-04
TGGT1_231630	1.57	alveolin domain containing intermediate filament IMC4	2.37E-188
TGGT1_231640	1.79	alveolin domain containing intermediate filament IMC1	3.68E-216
TGGT1_234670	3.61	actin-like family protein	1.14E-03
TGGT1_236960	1.56	transporter, major facilitator family protein	2.91E-05
TGGT1_237090	1.87	AP2 domain transcription factor AP2X-5	1.43E-21
TGGT1_237210	2.65	Tyrosine kinase-like (TKL) protein	1.34E-12
TGGT1_239490	1.79	dehydrogenase E1 component family protein	2.20E-38
TGGT1_239830	1.56	TBC domain-containing protein	1.08E-41
TGGT1_240240	3.85	subtilisin SUB5	6.29E-04
TGGT1_240860	1.73	acyltransferase domain-containing protein	9.81E-09
TGGT1_241010	1.94	K+ channel tetramerisation domain-containing protein	1.42E-11
TGGT1_241820	1.62	putative membrane protein	2.15E-04
TGGT1_244080	1.67	hypothetical protein	7.01E-10
TGGT1_244500	1.96	Tubulin-tyrosine ligase family protein	1.15E-42
TGGT1_244590	3.53	katanin-like family protein	4.01E-03
TGGT1_246910	1.78	putative histone lysine methyltransferase, SET	1.43E-03
TGGT1_249380	1.77	DHHC zinc finger domain-containing protein	5.35E-04
TGGT1_249850	2.10	GAP40 protein	1.39E-68
TGGT1_251740	1.71	AP2 domain transcription factor AP2XII-9	2.10E-07
TGGT1_251930	1.51	enoyl-acyl carrier reductase ENR	2.38E-04
TGGT1_252200	3.44	cell cycle regulator with zn-finger domain-containing protein	2.99E-07
TGGT1_254380	3.53	putative ribosomal protein L11	2.51E-03
TGGT1_254600	2.19	ubiquitin family protein	3.20E-06
TGGT1_254880	2.86	Alpha-galactosidase	5.59E-24
TGGT1_255200	3.50	putative Radial spoke head protein 9	1.26E-03
TGGT1_255670	1.72	methyltransferase domain-containing protein	2.93E-07
TGGT1_255900	2.07	putative Bax inhibitor-1	2.34E-07
TGGT1_256020	4.00	putative EFHC1	8.46E-04
TGGT1_257470	1.63	myosin J	2.22E-27

TGGT1_258110	1.93	N-acetylglucosaminylphosphatidylinositol deacetylase	1.97E-03
TGGT1_258660	1.56	rhoptry protein ROP6	1.80E-61
TGGT1_258700	3.49	transporter, major facilitator family protein	1.17E-08
TGGT1_260500	1.52	putative COPI associated protein	3.93E-39
TGGT1_261070	1.97	apicoplast triosephosphate translocator APT1	4.41E-04
TGGT1_261530	3.56	eukaryotic aspartyl protease superfamily protein	2.43E-03
TGGT1_262650	1.90	WD domain, G-beta repeat-containing protein	2.80E-04
TGGT1_263500	1.55	putative vacuolar protein sorting-associated protein 26	2.45E-05
TGGT1_263520	2.52	microtubule associated protein SPM1	1.66E-38
TGGT1_265080	1.83	Tubulin-tyrosine ligase family protein	5.56E-23
TGGT1_266310	3.41	Alpha-1,3-mannosyl-glycoprotein 2-beta-N-acetylglucosaminyltransferase	2.30E-03
TGGT1_267070	2.03	aquaporin 2	3.18E-07
TGGT1_268870	1.91	tetratricopeptide repeat-containing protein	1.79E-09
TGGT1_269460	1.54	Ser/Thr phosphatase family protein	7.65E-06
TGGT1_270540	3.53	Trm112p family domain-containing protein	1.63E-03
TGGT1_271060	1.89	Sec1 family protein	2.04E-03
TGGT1_271970	1.90	glideosome-associated protein with multiple-membrane spans GAPM3	2.24E-48
TGGT1_272490	1.63	protoporphyrinogen oxidase	2.48E-03
TGGT1_272640	2.08	putative eukaryotic initiation factor-2B, epsilon subunit	2.49E-14
TGGT1_272650	1.87	3'5'-cyclic nucleotide phosphodiesterase domain-containing protein	1.11E-07
TGGT1_273540	1.81	putative phosphatidylserine synthase	5.19E-08
TGGT1_275670	1.83	alveolin domain containing intermediate filament IMC15	1.60E-40
TGGT1_278270	1.83	putative nucleolar protein, structural component of H/ACA snoRNP	3.03E-04
TGGT1_278365	3.08	Toxoplasma gondii family A protein	4.21E-03
TGGT1_278370	2.03	Toxoplasma gondii family A protein	2.72E-06
TGGT1_278878	1.60	GDA1/CD39 (nucleoside phosphatase) family protein	6.32E-04
TGGT1_281490	2.01	putative glutamine amidotransferase subunit pdxt	2.47E-03
TGGT1_283730	1.68	endomembrane protein 70 subfamily protein	3.99E-03
TGGT1_285870	1.55	SAG-related sequence SRS20A	5.77E-17
TGGT1_286590	1.79	microtubule associated protein SPM2	2.38E-20
TGGT1_290160	1.51	putative sortilin	2.75E-20
TGGT1_291050	1.56	putative histone kinase SNF1	4.17E-25
TGGT1_291350	1.61	hypothetical protein	1.36E-04
TGGT1_291800	2.19	ADP-ribosylation factor family protein	1.06E-04
TGGT1_292010	1.78	transcription initiation factor IIB	3.99E-08
TGGT1_294330	1.67	EGF family domain-containing protein	7.53E-16
TGGT1_294610	1.80	putative histone lysine methyltransferase, SET	1.29E-108
TGGT1_295105	1.59	putative rhoptry protein	1.99E-03
TGGT1_295110	1.87	rhoptry protein ROP7	5.20E-87
TGGT1_295125	2.04	rhoptry protein ROP4	3.71E-28
TGGT1_297925	1.54	HesB-like domain-containing protein	3.82E-04
TGGT1_297960B	1.69	rhoptry neck protein RON6	4.47E-23
TGGT1_300100	1.58	rhoptry neck protein RON2	1.83E-93
TGGT1_300240	3.63	putative syntaxin 6 protein	1.12E-03
TGGT1_300360	2.11	ADP/ATP translocase	3.41E-03
TGGT1_305590	1.51	ABC transporter transmembrane region domain-containing protein	3.60E-10
TGGT1_305870	1.89	DAD family protein	4.24E-04
TGGT1_306030	1.51	glutathione s-transferase, n-terminal domain containing protein	2.42E-09
TGGT1_308000	2.46	Gpi16 subunit, GPI transamidase component protein	4.61E-04
TGGT1_309560	1.60	nmda receptor glutamate-binding chain	2.47E-30
TGGT1_310100	1.84	mannosyltransferase (pig-m) protein	9.60E-05
TGGT1_311470	1.51	rhoptry neck protein RON5	1.55E-121
TGGT1_312100	1.83	plasma membrane-type Ca(2+)-ATPase A1 PMCAA1	2.30E-19
TGGT1_312270	1.96	rhoptry protein ROP13	4.97E-41
TGGT1_313190	2.35	Rab18/RabC-family small GTPase	9.72E-04
TGGT1_313560	1.66	putative 60S ribosomal protein L7a	1.12E-05
TGGT1_314090	1.82	proteasome beta subunit	1.82E-06
TGGT1_315620	1.60	putative vacuolar ATP synthase subunit C	8.29E-07

TGGT1_315680	1.64	putative vacuolar protein sorting-associated protein vps4	8.34E-04
TGGT1_315980	1.69	EREBP-4 family protein	2.07E-05
TGGT1_322000	2.61	myosin-light-chain kinase	1.77E-06
TGGT1_356400	3.84	cAMP-dependent protein kinase	2.76E-04
TGGT1_361650	1.64	proteasome/cyclosome repeat protein	4.07E-03
TGGT1_411090	1.77	TPRX1 protein	2.27E-03
TGGT1_411430	1.62	rhoptry protein ROP5	1.09E-153

Table 8: Significantly upregulated *T. gondii* transcripts caused by U21 treatment identified by RNA-seq analysis. Following U21 treatment (or DMSO treatment), RNA from treated *T. gondii* tachyzoites was submitted for RNA-seq analysis. Raw transcriptomic data was aligned to the GT1 transcriptome of *T. gondii*, transcripts quantified through Salmon, and differential expression determined by DESeq2. Significance was gated to a p value less than 0.05 and a log2 fold increase of at least 1.5. Transcripts that encoded for hypothetical proteins were sorted out to allow for subsequent gene ontology analysis.

REF Seq ID	log2FoldChange	Gene Description	pvalue
TGGT1_202360	-2.31	putative methylase	9.17E-09
TGGT1_203340	-4.29	metallo-beta-lactamase domain-containing protein	4.14E-03
TGGT1_205110	-1.64	hypothetical protein	1.05E-15
TGGT1_205600	-1.87	zinc finger, C3HC4 type (RING finger) domain-containing protein	5.60E-179
TGGT1_213850	-2.36	MORN repeat-containing protein	4.09E-03
TGGT1_215670	-4.97	cAMP-dependent protein kinase	8.77E-05
TGGT1_219300	-1.68	ran binding protein	4.36E-04
TGGT1_219430	-1.54	tRNA ligase class II core domain (G, H, P, S and T) domain-containing protein	3.42E-14
TGGT1_219790A	-1.72	pre-mRNA processing factor PRP3	2.41E-33
TGGT1_221200B	-1.61	CW-type Zinc Finger protein	2.20E-117
TGGT1_223120	-3.86	cyclin-dependent kinase regulatory subunit protein	4.54E-03
TGGT1_224200	-1.62	tRNA pseudouridine synthase	4.07E-52
TGGT1_225028	-1.60	putative myosin heavy chain	1.67E-03
TGGT1_227430	-1.61	transmembrane amino acid transporter protein	7.96E-09
TGGT1_230555	-2.11	adenylate and guanylate cyclase catalytic domain-containing protein	1.26E-07
TGGT1_230890	-2.40	PHD-finger domain-containing protein	1.53E-100
TGGT1_232760	-1.85	protein phosphatase inhibitor IPP2	6.04E-267
TGGT1_235890	-2.49	dual-specificity protein phosphatase	1.37E-18
TGGT1_236840	-1.59	putative zinc finger (C-x8-C-x5-C-x3-H)-2	1.33E-190
TGGT1_243240	-1.72	WD domain, G-beta repeat-containing protein	5.63E-15
TGGT1_243280A	-1.66	Met-10+ like-protein	4.39E-57
TGGT1_243680	-1.54	dihydrodipicolinate reductase	1.13E-20
TGGT1_243740	-1.85	WD domain, G-beta repeat-containing protein	5.26E-12
TGGT1_248960	-1.56	methyltransferase domain-containing protein	1.40E-99
TGGT1_253040	-1.58	actin-related protein ARP4A	3.30E-41
TGGT1_260270	-1.78	HEAT repeat-containing protein	3.87E-13
TGGT1_263595	-1.66	RNA-binding protein	1.27E-234
TGGT1_264420	-1.91	putative lipoprotein	4.55E-27
TGGT1_268210	-1.65	AGC kinase	8.17E-34
TGGT1_269400	-3.82	oxidoreductase, short chain dehydrogenase/reductase family protein	4.37E-03
TGGT1_269910	-2.28	putative transcription factor C2H2	4.45E-04
TGGT1_271100	-1.62	NUC153 domain-containing protein	0.00E+00
TGGT1_271810	-1.53	putative lanp	1.10E-214
TGGT1_273150	-2.03	zinc finger, C3HC4 type (RING finger) domain-containing protein	8.78E-08
TGGT1_278900	-1.72	putative protein kinase	2.92E-17
TGGT1_285490	-1.52	helix-hairpin-helix motif domain-containing protein	2.23E-30
TGGT1_286920	-1.84	SWIRM domain-containing protein	1.13E-86
TGGT1_288390	-1.89	B3GNTL1 protein	1.76E-27
TGGT1_289560	-1.90	RNA recognition motif-containing protein	1.37E-04
TGGT1_293300	-1.71	Yip1 domain-containing protein	1.81E-162
TGGT1_294930	-1.76	leucine rich repeat-containing protein	1.08E-136
TGGT1_295010	-1.62	DEAD/DEAH box helicase domain-containing protein	9.98E-53
TGGT1_300621A	-2.39	ribosomal protein L2	1.30E-304
TGGT1_300621B	-3.86	ribosomal protein L2	0.00E+00
TGGT1_300631	-1.92	ribosomal protein L4	8.76E-105
TGGT1_300641B	-2.28	ribosomal protein S4	2.84E-07
TGGT1_301222	-1.75	DNA repair protein Rad4 domain-containing protein	1.36E-64
TGGT1_305310	-1.75	ERCC4 domain-containing protein	2.39E-268
TGGT1_315845	-3.61	kinesin motor domain-containing protein	1.56E-03

TGGT1_316110	-1.83	ribosomal protein RPS15	9.22E-30
TGGT1_365980	-2.09	putative transmembrane protein	1.03E-03
TGGT1_409540	-1.51	protamine protein P1	1.78E-12
TGGT1_409790	-2.00	putative transmembrane protein	8.96E-27

Table 9: Significantly downregulated *T. gondii* transcripts caused by U21 treatment identified by RNA-seq analysis. Following U21 treatment (or DMSO treatment), RNA from treated *T. gondii* tachyzoites was submitted for RNA-seq analysis. Raw transcriptomic data was aligned to the GT1 transcriptome of *T. gondii*, transcripts quantified through Salmon, and differential expression determined by DESeq2. Significance was gated to a p value less than 0.005 and a log2 fold decrease of at least 1.5. Transcripts that encoded for hypothetical proteins were sorted out to allow for subsequent gene ontology analysis.

***Toxoplasma gondii* Gene Ontology Analysis: U21 Treated Tachyzoites (GO ID:0008654)**				
Gene ID	**Gene Function**	**Gene Type**	**log2 Fold Change**	**p value**
TGGT1_207710	CDP-diacylglycerol--inositol 3-phosphatidyltransferase	Protein Coding Gene	2.0998	0.0005
TGGT1_224920	hypothetical protein	Protein Coding Gene	1.5575	0.0002
TGGT1_258110	N-acetylglucosaminylphosphatidylinositol deacetylase	Protein Coding Gene	1.9344	0.0020
TGGT1_273540	Putative phosphatidylserine synthase	Protein Coding Gene	1.8100	5.19E-08
TGGT1_308000	Gpi16 subunit, GPI transamidase component protein	Protein Coding Gene	2.4643	0.0005
TGGT1_310100	GPI mannosyltransferase 1	Protein Coding Gene	1.8362	9.60E-05

Table 10: Gene Ontology Analysis from Differential Expression Analysis: U21 Treated *Toxoplasma gondii* Tachyzoites.

Differential Expression Analysis qPCR Verification

RNA-seq observations were then verified by qPCR analysis. *T. gondii* phosphatidylserine synthase (TgPSS), log2 fold change of 1.8100, was investigated for upregulation following U21 treatment of *T. gondii* tachyzoites. Elacridar was included as a positive control due to being published to cause dysregulated lipid metabolism in *T. gondii* [69]. *In vitro* tachyzoite infected HFF monolayers were treated with either U21 at the IC_{25} or IC_{50} concentration for 24 hours. DMSO treated tachyzoites served as a negative control for no treatment. RNA was isolated, converted to cDNA, and relative levels of TgPSS and *T. gondii* phosphatidylinositol synthase (TgPIS) were determined by qPCR analysis. At the IC_{25} concentration, a significant log2 fold decrease of TgPSS was observed (Figure 18, p value < 0.05) while at the IC_{50} concentration nearly a log2 fold increase of 7 was seen. (Figure 18, p value < 0.005). Interestingly, Elacridar had no effect on TgPSS transcript levels.

Expression of TgPIS was also investigated by qPCR analysis. Unlike PSS, both U21 at the IC_{25} and IC_{50} caused significant upregulated expression of PIS with the IC_{50} concentration causing higher expression values (Figure 19, p value < 0.005). Elacridar caused a log2 fold increase of 1.1 (Figure 19, p value < 0.05).

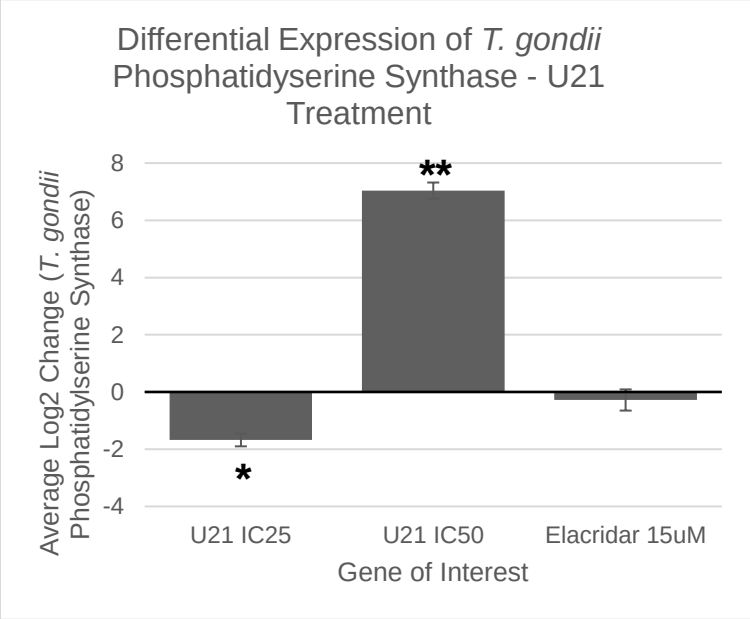

Figure 18: Differential Expression of *T. gondii* Phosphatidylserine Synthase – qPCR Verification. HFF cells infected with 2e5 *T. gondii* RH-dTom tachyzoites/mL were treated with U21 at the IC_{25} and IC_{50} concentrations 24 hours after infection. DMSO, untreated, tachyzoites were included as a negative control and elacridar as positive control for dysregulated lipid metabolism. After 24 hours of treatment, RNA was isolated from infected and treated monolayers and converted to cDNA for qPCR analysis. Expression of *T. gondii* phosphatidylserine synthase (TgPSS) was quantified for all samples and log2 fold changes were calculated through delta delta ct calculations by comparing treated samples to untreated, DMSO, samples. All samples were in triplicate and normalized to the following *T. gondii* house-keeping genes: TgHis2B, TgRiboL33, and TgHelic.(p value < 0.05*, 0.005**)

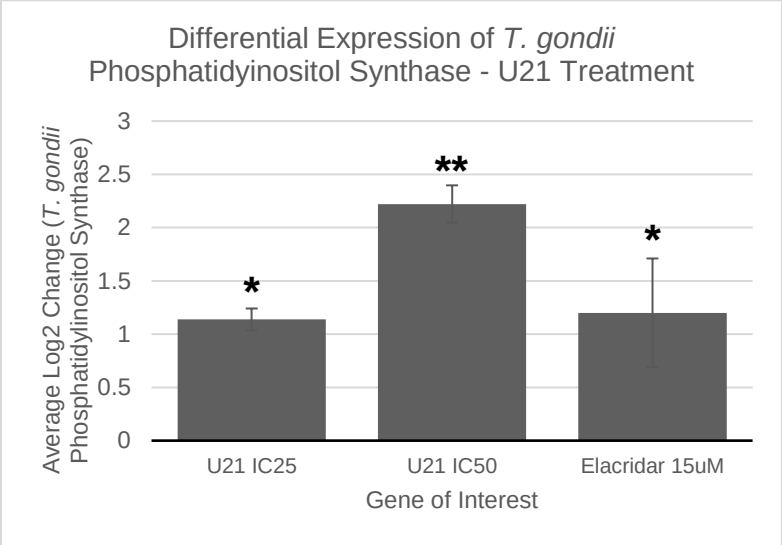

Figure 19: Differential Expression of *T. gondii* Phosphatidylinositol Synthase – qPCR Verification. HFF cells infected with 2e5 *T. gondii* RH-dTom tachyzoites/mL were treated with U21 at the IC_{25} and IC_{50} concentrations 24 hours after infection. DMSO, untreated, tachyzoites were included as a negative control and elacridar as positive control for dysregulated lipid metabolism. After 24 hours of treatment, RNA was isolated from infected and treated monolayers and converted to cDNA for qPCR analysis. Expression of *T. gondii* phosphatidylinositol synthase (TgPIS) was quantified for all samples and log2 fold changes were calculated through delta delta ct calculations by comparing treated samples to untreated, DMSO, samples. All samples were tested in triplicate and normalized to the following *T. gondii* house-keeping genes: TgHis2B, TgRiboL33, and TgHelic. (p value < 0.05*, 0.005**)

3.IV Discussion

Activity of *N,N* di-aryl urea compounds against the chronic stage of *T. gondii* infection was quantified through *in vitro* models for decreases in *T. gondii* cysts in an *in vitro* culture. In both *in vitro* models, GFP counts of cysts (Figure 13) and bradyzoite inhibition (Table 7), compounds were observed to be effective in clearing *T. gondii* cysts from *in vitro* cultures, suggesting that these compounds are effective *in vitro* in both acute, as seen in Chapter 1, and chronic *T. gondii* infection. Through *in vivo* analysis described in Chapter 1 (Figure 6, 7, and 8), *N,N* di-aryl urea compounds were concluded to be orally bioavailable and effective against acute *T. gondii* infection. Knowing that *N,N* di-aryl urea compounds were effective against *in vitro T. gondii* cysts and allowed for significant survival in acutely mice infected cell cultures, activity of compounds against chronic infection were explored through *in vivo* analysis.

Prior to investigating the activity of *N,N* di-aryl urea compounds against chronic infection in an *in vivo* model, the ability of compounds to pass the blood brain barrier (BBB) was assessed. To effectively clear *T. gondii* cysts residing in brain tissue, compounds must be able to cross the BBB to reach *T. gondii* tissue residing cysts. Lipophilic compounds have been proven to diffuse through the BBB by passive diffusion [24]. Through physicochemical analysis in Chapter 1, *N,N* di-aryl urea compounds were identified to be generally lipophilic and therefore were hypothesized to be able to cross the BBB.

First, activity of compound U21 against the formation of cysts was determined in mice that received a lethal infection of tachyzoites and were then treated with U21 to allow for mouse survival. No significant decrease in parasite burden in brain tissue was measured in U21 treated mice, suggesting that U21 does not have an effect of the formation of *T. gondii* cysts in an *in vivo* model (Figure 14). To assess U21's ability to clear *T. gondii* cysts from chronically infected mice, a sub-lethal infection model was utilized to allow for the formation of *T. gondii* cysts in brain tissue. Following two weeks of U21 treatment, no significant decrease was seen in U21 treated mice when compared to mice that received no treatment (Figure 15). This suggests that U21 has no effect on the formation of *T. gondii* cysts and does not clear *T. gondii* cysts from mice.

Following the characterization of *N,N* di-aryl urea compound activity against the chronic stage of *T. gondii* infection, differential expression analysis was utilized in an attempt to identify a possible mechanism of action. Due to random chemical mutagenesis failing in Chapter 2, differential expression analysis by RNA-seq was utilized to determine what *T. gondii* transcripts were being significantly affected by U21 treatment. RNA was isolated from infected cell cultures and submitted for RNA-seq for differential expression analysis. Our initial results from differential expression analysis did not allow for a clear understanding of what pathways in *T. gondii* tachyzoites were

being affected by U21 treatment. To address this, biological processes of *T. gondii* that were directly affected by U21 treatment were determined by gene ontology analysis. Interestingly, lipid metabolism processes of tachyzoites were significantly affected with transcripts measured by differential expression analysis being significantly up regulated when compared to untreated tachyzoites (Table 8). Gene ontology analysis did not identify any biological processes that were affected by down regulated transcripts.

Lipid metabolism in *T. gondii* tachyzoites is a known essential process that allows for proper phospholipid bi-layer formation including cell membrane and parasitophorous vacuole construction as well as tachyzoite mobility, invasion, and aid in essential signaling pathways [68]. The entire lipid synthesis pathway has yet to be fully characterized in *T. gondii* and warrants further research. Elacridar, a previous anti-cancer drug that has since been discontinued that targets a membrane-bound efflux pump known as P-glycoprotein (P-gp), was previously tested for activity against *T. gondii* tachyzoites. The upregulation of P-gp in protozoans and cancer cells is a known multi-drug resistant marker [68]. In *T. gondii*, P-gp is known to be responsible for the uptake of host cholesterol which is an essential process for the growth and division of tachyzoites due to the inability of the parasite to synthesize *de novo* cholesterol [68]. When treated with elacridar, tachyzoites were observed to have a significant decrease in replication and invasion. Additionally, treatment of elacridar caused a reduction in lipid synthesis which may have been due to the downregulation of *T. gondii* P-gp [68]. Other than Elacridar, no other drug or compound has been identified to date to cause disrupted lipid metabolism in *T. gondii*.

To further verify that differential expression analysis was correctly identifying transcripts involved in lipid metabolism in tachyzoites was significantly affected by U21 treatment, qPCR was then utilized to directly measure two separate identified upregulated transcripts: *T. gondii* phosphatidylserine synthase (TgPSS) and *T. gondii*

phosphatidylinositol synthase (TgPIS). Tachyzoites treated with both the IC_{25} and IC_{50} concentration of U21 were investigated for the affects in the expression of TgPSS and TgPIS. qPCR analysis verified that both TgPSS and TgPIS were both significantly upregulated when *in vitro* tachyzoites were treated at the IC_{50} concentration of U21. At the IC_{25} concentration, TgPSS was significantly decreased. It is important to note that RNA-seq and differential expression analysis was done on tachyzoites treated at the IC_{50} concentration of U21. Altogether, transcriptional analysis suggests that U21 does indeed incur dysregulation in *T. gondii* lipid metabolism.

3.V Conclusion

In conclusion, di-aryl urea compounds were determined to be effective against the chronic stage of *T. gondii* via *in vitro* analysis including fluorescent based and plaque assays. Further investigation of U21 activity in a murine model for activity against the chronic stage identified that U21 did not have any significant effect on cyst formation in mice. When mice were infected with a sublethal amount of tachyzoites and allowed to form chronic infection, U21 was unable to cause a significant decrease in parasite burden. Due to the lipophilic physical profile of U21, it would be hypothesized to allow for BBB penetration. Differential expression analysis of U21 treated tachyzoites identified that parasite lipid metabolism dysregulation may be a biological process that is directly affected by treatment. qPCR analysis of TgPSS and TgPIS verified these *in silico* results with a significant upregulation in transcripts of U21 treated tachyzoites. To further investigate if lipid metabolism is a viable target of U21, lipidomic analysis of treated tachyzoites would allow for a deeper assessment of how U21 is affecting *T. gondii* lipid metabolism.

Compared to current anti-*Toxoplasma* therapeutics and novel compounds that exhibit activity against the chronic stage of *T. gondii*, U21 allowed for bradyzoite

inhibition and decreases in cyst counts through *in vitro* analysis along with exhibiting significant acute activity in both *in vitro* and *in vivo* models. Dysregulation of lipid metabolism in *T. gondii* is not fully characterized yet and warrants further investigation as a potential compound target. Through this study, U21 was identified to have at least some effect on lipid metabolism. To conclude that this is a potential mechanism of action of U21 further analysis is clearly warranted.

DISCUSSION CHAPTER

Discovering novel compounds that may act as future anti-*Toxoplasma* therapeutics are crucial for the treatment of *T. gondii* infection in both immunocompromised individuals suffering from Toxoplasma encephalitis as well as fetuses that acquire congenital toxoplasmosis which can cause severe birth defects. Current treatment options for acute toxoplasmosis are clearly limited due to prolonged treatments causing bone marrow suppression and the propensity of severe allergic reactions in patients. Current research has identified a handful of very promising compounds that exhibit activity against acute toxoplasmosis, but the only compounds currently in clinical trials are derivatives of pyrimethamine. Which is known to cause bone marrow suppression due to folic acid metabolism inhibition in both *T. gondii* and in humans. While clearing lifelong chronic *T. gondii* infection by compound administration has yet to be accomplished in mice let alone humans.

Section I: Low Toxicity

In this dissertation, *N,N* di-aryl urea compounds were screened for activity against both the acute and chronic stage of *T. gondii* in *in vitro* and *in vivo* models. Through *in vitro* screening for activity against the acute stage of *T. gondii* infection, it was discovered that nearly all tested compounds exhibited activity against tachyzoites (Table 4). Initial safety profiling identified that all compounds tested did not cause cytotoxic effects in the following human immortalized cell lines: HFF (fibroblast), U-2OS (osteosarcoma), HEK-293 (embryonic kidney), and HC-04 (hepatic carcinoma). Safety screening was then expanded to macrophages based on data provided by collaborators [52] including: J774, RAW264.7, THP-1, and isolated murine monocytes that were differentiated to bone marrow derived macrophages (BMDMs). Interestingly, U21 and

U30 both exhibited acute activity against THP-1 and (BMDMs) suggesting that these di-aryl urea compounds are indeed toxic to macrophages (Table 5).

Section II: Partial Macrophage Toxicity

To then assess if this effect of toxicity to macrophages could be seen in an *in vivo* model, mice were administered U21 at 100 mg/kg once through oral gavage and lungs were then extracted 48 hours after treatment. Lung tissue was fixed and stained for H&E analysis to visualize any abnormal phenotypes caused by U21 treatment to alveolar macrophages. No abnormal alveolar macrophage phenotypes were present when untreated and U21 treated lung tissue were compared to one another suggesting that U21 treatment does not cause toxicity to *in vivo* alveolar macrophages (Figure 4). Further analysis to quantify effects to *in vivo* macrophages in a quantitative manner is warranted. Of important note, mice have been administered up to 200 mg/kg of di-aryl urea compounds with no reported side effects or toxicity. Overall, it is unclear if di-aryl urea compounds are truly toxic to macrophages *in vivo* with the current data available.

Section III: Effective Against *in vitro T. gondii* Cysts

The activity of di-aryl urea compounds was also assessed for activity against the chronic stage of *T. gondii* through *in vitro* analysis. Currently in the field, there is no set method for determining the activity of compounds or drugs against chronic *T. gondii* in an *in vitro* model. The development of an *in vitro* protocol is critical for the screening of compounds for activity against *in vitro T. gondii* cysts to allow for the quantification of activity prior to *in vivo* chronic studies. Through counts of GFP expressing *in vitro T. gondii* cysts treated with *N,N* di-aryl urea compounds (Figure 13) and a quantitative plaque assay of treated differentiated *in vitro T. gondii* cysts (Table 7), it was concluded that both U21 and U26 exhibited significant activity against *in vitro T. gondii* cysts.

Section IV: Effective Against Acute Infection

Through *in vivo* screenings for activity of di-aryl urea compounds against a lethal acute *T. gondii* infection in mice, it was concluded that U21 allowed for pyrimethamine levels of survival at 100 mg/kg (Figure 6(. Following this study, the concentration of U21 administered was then lowered to 75, 50, and 25 mg/kg to assess if lower dosages would allow for similar levels of survival. At these dosages it was concluded that there was a dose-dependent response with survival at 40, 20, and 0% respectively (Figure 7). Therefore, concluding that at 100 mg/kg, U21 is effective at combatting lethal acute infection in mice to allow for survival. Additionally, the lipophilic nature of these di-aryl urea compounds may be causing a low absorption rate due to their hydrophobic nature (Table 3). This may explain why 100 mg/kg of U21 is needed for pyrimethamine levels of survival in murine *in vivo* models.

Section V: No Effect on *in vivo* Cyst Formation of Cyst Clearance

Activity of U21 against the chronic stage of *T. gondii* in a murine *in vivo* model determined that U21 administration had no effect on the formation of cysts in brain tissue (Figure 14). In addition, mice that had chronic infection established and were then treated with U21 had no significant decreases in parasite burden (Figure 15). Therefore, suggesting that U21 administered through oral gavage at 100 mg/kg has no effect on the chronic stage of *T. gondii in vivo. N,N* di-aryl urea compounds were effective *in vitro* against the chronic stage of *T. gondii* infection, while no activity was observed in *in vivo* models prompting the need for further investigation.

Section VI: No Apicoplast Activity

Target identification of U21 through growth supplementation assays did not allow for the identification of an affected pathway. Both FASII and isoprenoid synthesis are located in the apicoplast of *T. gondii* and serve as very attractive drug targets due to human cells lacking the apicoplast organelle. Since the chemical structure of U21 is based on triclocarban, a hypothesized fatty acid synthesis II (FASII) inhibitor in prokaryotes, a fatty acid supplementation assay was utilized to assess if U21 had any effect on fatty acid synthesis in *T. gondii* tachyzoites. No rescue effects were observed following fatty acid supplementation of U21 treated *in vitro* tachyzoites suggesting that FASII was not a direct target of U21 (Figure 10). Additionally, isoprenoid supplementation of U21 treated tachyzoites failed to rescue treated tachyzoites (Figure 11). Concluding that U21 does not cause any effect on the synthesis of apicoplast derived isoprenoids. Any broad affects to the apicoplast of *T. gondii* caused by U21 treatment through delayed death analysis concluded that U21 treatment most likely does not target the apicoplast of *T. gondii* (Figure 9). Through these assays, it was concluded that U21 does not affect the apicoplast or apicoplast related pathways.

Section VIII: Random Chemical Mutagenesis Did Not Form Viable Mutants

Induced mutations to wild-type *T. gondii* tachyzoites through random chemical mutagenesis to cause resistance to U21 treatment failed after multiple attempts (Figure 12). Target identification of compounds through random chemical mutagenesis does have clear disadvantages. For example, if the compound of interest is targeting an essential gene that when mutated causes tachyzoite death, random chemical mutagenesis would be unable to identify that target. In addition, if the compound of interest causes membrane disruption, motility perturbation, or causes invasion inhibition; random chemical mutagenesis would be unable to identify the respective target.

Additionally, random chemical mutagenesis would be unable to determine a molecular target if the compound of interest is affecting a pathway in the host cell that causes tachyzoite death.

Section IX: Electron Microscopy Data Not Telling

To answer how U21 may be affecting tachyzoites, electron microscopy was then utilized to visualize any phenotypes caused by treatment. Scanning electron microscopy (SEM) concluded that U21 treatment may cause cell membrane disruptions in tachyzoites due to the visual phenotype of the cell membrane having a partial collapse (Figure 16). Transmission microscopy (TEM) failed to capture any phenotypes to tachyzoite ultrastructure (Figure 17). Overall, electron microscopy allowed for the visualization of a surface phenotype that was caused by U21 treatment. While this visual observation is not enough to conclude anything definite on how U21 is affecting tachyzoites, it was an important finding that would be complemented with differential expression analysis.

Section X: Transcriptional Changes Following Treatment

Differential expression analysis allowed for the quantification of U21 treated *T. gondii* transcripts that were both significantly up and down regulated. Gene ontology analysis of differentially expressed transcripts for affected biological processes found that lipid metabolism transcripts were significantly upregulated when tachyzoites were treated with U21 (Table 8). This finding was confirmed with qPCR analysis by quantification of *T. gondii* phosphatidylserine synthase and phosphatidylinositol synthase expression (Figure 18 & 19). Both were significantly upregulated when treated at the IC_{50} concentration of U21.Importantly, this finding that lipid metabolism was dysregulated was complemented by SEM analysis. In SEM imaging, the cell membrane of U21

treated tachyzoites seemed to have a partial collapse (Figure 16). If lipid metabolism is truly dysregulated, the cell membrane of tachyzoites may not have the structural integrity needed for survival. Lipid metabolism in *T. gondii* is known to be essential for parasite survival. Host lipids can be scavenged by *T. gondii* when inside a parasitophorous vacuole, but tachyzoites are unable to scavenge all needed lipids and rely on the *de novo* synthesis of some lipids. Previous work has identified that a previous anti-cancer drug, elacridar, caused dysregulated lipid metabolism in *T. gondii* and inhibited tachyzoite growth. Suggesting that causing dysregulated lipid metabolism in *T. gondii* may serve as an attractive therapeutic target. Future studies such as lipidomic analysis of U21 treated tachyzoites would allow for the direct quantification and characterization of lipid profiles compared to untreated tachyzoites. Conversely, U21 may also be causing dysregulated lipid metabolism in host cells. It is known that *T. gondii* relies on the scavenging of lipids and cholesterols from lipid droplets derived from host cells to efficiently divide and persist within the parasitized host cell [70]. Previous work has shown that supplementing *in vitro* tachyzoites with abnormal concentrations of fatty acids, lipids, and cholesterols causes tachyzoite death [71]. From these studies, it was concluded that tachyzoites may uptake host cell lipid droplets at unregulated rates which causes subsequent tachyzoite death. It is important to note that U21 pre-treated *in vitro* host cells did not have any significant effect on tachyzoites. This alone is not enough to disregard that U21 may be causing parasite death through modulation of the infected host cell. Determining if U21 is causing any effect to host cell lipid metabolism through qPCR analysis of lipid synthesis transcripts or differential expression analysis of host cells is needed to conclude if U21 is affecting only *T. gondii* lipid metabolism or also host cell lipid metabolism.

Section XI: Future Work

Current data of *N,N* di-aryl urea compounds has proven that they are effective against helminths, kinetoplasts, and apicomplexan protozoa. Further screening of *N,N* di-aryl urea compounds in an expanded panel of pathogens would be beneficial for the assessment of expanded of activity profiles. Gram-negative and gram-positive pathogenic bacteria have yet to be treated with these compounds. Since the parent compound MMV52 is based on the antibacterial triclocarban, it would be interesting to investigate any antimicrobial effects of these *N,N* di-aryl urea compounds. Additional screening of compounds against pathogenic amoeba would also be interesting to investigate due to the work shown in this dissertation showing acute toxicity to macrophages. Amoeba and macrophages are remarkably similar due to shared molecular functions, physical structure, motility, and both utilize active phagocytosis [71].

Before U21 could move to human Phase I clinical trials for combatting *T. gondii* infection, the potential toxicity of these di-aryl urea compounds to macrophages needs to be fully characterized in other *in vivo* experiments. Flow cytometry analysis could be utilized to directly quantify the number of monocytes or macrophages in untreated and treated mice in the future.

Discovering how U21 is affecting *T. gondii* on a molecular level is essential for the future development of these *N,N* di-aryl urea chemotypes. To assess why 100 mg/kg of U21 is required for pyrimethamine levels of survival in acutely infected mice, mice administered with decreasing concentrations of U21 and levels of compound measured in peripheral blood through LC-MS analysis would allow for the analysis of dose-dependent absorption rates of *N,N* di-aryl urea compounds. If at lower dosages U21 is observed at similar levels compared to higher dosages, it could then be concluded that

the lower absorption rate of U21 may be causing the high dosage needed for survival in acutely infected mice.

Interestingly, U21 had no effect on the chronic stage of *T. gondii* in *in vivo* mouse models. Low absorption rates of *N,N* di-aryl urea compounds may be responsible for lower concentrations of compound reaching the BBB. For future studies, the measurement of how much U21 can penetrate the blood brain barrier (BBB) would answer if compound is even able to reach *T. gondii* cysts residing in brain tissue. If it is found that U21 is not able to penetrate the BBB, further modifications to the chemical structure could allow for penetration of the BBB or U21 could be encapsulated in specialized liposomes that allow for the directed penetration of the BBB.

Lastly, lipidomic analysis of U21 treated tachyzoites would allow for a deeper understanding regarding how U21 is affecting *T. gondii* lipid metabolism. Transcriptome analysis followed by qPCR verification of upregulated transcripts associated with *T. gondii* lipid metabolism identified that *N,N* di-aryl urea compounds may cause dysregulated lipid metabolism. Quantifying and investigating the composition of lipids derived from treated tachyzoites by lipidomic analysis would answer if *N,N* di-aryl urea compounds do indeed cause dysregulated lipid metabolism and subsequent inhibition of *T. gondii* growth.

In conclusion, these di-aryl urea compounds were characterized for activity in both *in vitro* and *in vivo* models for safety and activity against both acute and chronic *T. gondii* infection. Compound U21 was found to be the most effective *in vivo* and through differential expression analysis it was found that treatment may cause dysregulated *T. gondii* lipid metabolism. Compared to other experimental compounds that have been shown to be effective against *T. gondii*, U21 is one of few compounds that have been shown to exhibit activity against the acute stage, and some chronic stage *T. gondii*

infection in a selective manner. This may warrant further investigation as a potential future anti-*Toxoplasma* therapeutic.

BIBLIOGRAPHY

1. Halonen, S. K., & Weiss, L. M. (2013). Toxoplasmosis. *Handbook of clinical neurology*, *114*, 125–145. https://doi.org/10.1016/B978-0-444-53490-3.00008-X
2. Dubey, J. P., Lindsay, D. S., & Speer, C. A. (1998). Structures of Toxoplasma gondii tachyzoites, bradyzoites, and sporozoites and biology and development of tissue cysts. *Clinical microbiology reviews*, *11*(2), 267–299.
3. Salant, H., Spira, D. T., & Hamburger, J. (2010). A comparative analysis of coprologic diagnostic methods for detection of Toxoplama gondii in cats. *The American journal of tropical medicine and hygiene*, *82*(5), 865–870. https://doi.org/10.4269/ajtmh.2010.09-0635
4. Gandhi, R. T. (2019, May). Toxoplasmosis in patients with HIV. Retrieved January 15, 2021, from https://www.uptodate.com/contents/toxoplasmosis-in-patients-with-hiv#H1
5. Fung, H. B., & Kirschenbaum, H. L. (1996). Treatment regimens for patients with toxoplasmic encephalitis. Clinical therapeutics, 18(6), 1037–1036. https://doi.org/10.1016/s0149-2918(96)80059-2
6. Vidal J. E. (2019). HIV-Related Cerebral Toxoplasmosis Revisited: Current Concepts and Controversies of an Old Disease. Journal of the International Association of Providers of AIDS Care, 18, 2325958219867315. https://doi.org/10.1177/2325958219867315
7. Mboera, L., Kishamawe, C., Kimario, E., & Rumisha, S. F. (2019). Mortality Patterns of Toxoplasmosis and Its Comorbidities in Tanzania: A 10-Year Retrospective Hospital-Based Survey. Frontiers in public health, 7, 25. https://doi.org/10.3389/fpubh.2019.00025

8. Kheirandish, F., Ezatpour, B., Fallahi, S. H., Tarahi, M. J., Hosseini, P., Karimi Rouzbahani, A., Seyyed Tabaei, S. J., & Akbari, S. (2019). Toxoplasma Serology Status and Risk of Miscarriage, A Case-Control Study among Women with A History of Spontaneous Abortion. International journal of fertility & sterility, 13(3), 184–189. https://doi.org/10.22074/ijfs.2019.5740
9. Stokkermans TJ, Havens SJ. Toxoplasma Retinochoroiditis. [Updated 2020 Jun 27]. In: StatPearls [Internet]. Treasure Island (FL): StatPearls Publishing; 2020 Jan-. Available from: https://www.ncbi.nlm.nih.gov/books/NBK493182/
10. Black, M. W., & Boothroyd, J. C. (2000). Lytic cycle of Toxoplasma gondii. Microbiology and molecular biology reviews : MMBR, 64(3), 607–623. https://doi.org/10.1128/mmbr.64.3.607-623.2000
11. Ahmed, N., French, T., Rausch, S., Kühl, A., Hemminger, K., Dunay, I. R., Steinfelder, S., & Hartmann, S. (2017). Toxoplasma Co-infection Prevents Th2 Differentiation and Leads to a Helminth-Specific Th1 Response. Frontiers in cellular and infection microbiology, 7, 341. https://doi.org/10.3389/fcimb.2017.00341
12. Kim, S. K., & Boothroyd, J. C. (2005). Stage-specific expression of surface antigens by Toxoplasma gondii as a mechanism to facilitate parasite persistence. Journal of immunology (Baltimore, Md. : 1950), 174(12), 8038–8048. https://doi.org/10.4049/jimmunol.174.12.8038
13. Sullivan, W. J., Jr, & Jeffers, V. (2012). Mechanisms of Toxoplasma gondii persistence and latency. FEMS microbiology reviews, 36(3), 717–733. https://doi.org/10.1111/j.1574-6976.2011.00305.x
14. Tiwari, A., Hannah, R., Lutshumba, J., Ochiai, E., Weiss, L. M., & Suzuki, Y. (2019). Penetration of CD8+ Cytotoxic T Cells into Large Target, Tissue Cysts of

Toxoplasma gondii, Leads to Its Elimination. The American journal of pathology, 189(8), 1594–1607. https://doi.org/10.1016/j.ajpath.2019.04.018

15. Neville, A. J., Zach, S. J., Wang, X., Larson, J. J., Judge, A. K., Davis, L. A., Vennerstrom, J. L., & Davis, P. H. (2015). Clinically Available Medicines Demonstrating Anti-Toxoplasma Activity. Antimicrobial agents and chemotherapy, 59(12), 7161–7169. https://doi.org/10.1128/AAC.02009-15
16. Ben-Harari, R. R., Goodwin, E., & Casoy, J. (2017). Adverse Event Profile of Pyrimethamine-Based Therapy in Toxoplasmosis: A Systematic Review. Drugs in R&D, 17(4), 523–544. https://doi.org/10.1007/s40268-017-0206-8
17. Dunay, I. R., Gajurel, K., Dhakal, R., Liesenfeld, O., & Montoya, J. G. (2018). Treatment of Toxoplasmosis: Historical Perspective, Animal Models, and Current Clinical Practice. Clinical microbiology reviews, 31(4), e00057-17. https://doi.org/10.1128/CMR.00057-17
18. Ruf, B., Schürmann, D., Bergmann, F., Schüler-Maué, W., Grünewald, T., Gottschalk, H. J., Witt, H., & Pohle, H. D. (1993). Efficacy of pyrimethamine/sulfadoxine in the prevention of toxoplasmic encephalitis relapses and Pneumocystis carinii pneumonia in HIV-infected patients. European journal of clinical microbiology & infectious diseases : official publication of the European Society of Clinical Microbiology, 12(5), 325–329. https://doi.org/10.1007/BF01964427
19. Jernberg, C., Löfmark, S., Edlund, C., & Jansson, J. K. (2010). Long-term impacts of antibiotic exposure on the human intestinal microbiota. Microbiology (Reading, England), 156(Pt 11), 3216–3223. https://doi.org/10.1099/mic.0.040618-0
20. Faucher, B., Moreau, J., Zaegel, O., Franck, J., & Piarroux, R. (2011). Failure of conventional treatment with pyrimethamine and sulfadiazine for secondary

prophylaxis of cerebral toxoplasmosis in a patient with AIDS. The Journal of antimicrobial chemotherapy, 66(7), 1654–1656. https://doi.org/10.1093/jac/dkr147

21. Flegr, J., & Horáček, J. (2020). Negative Effects of Latent Toxoplasmosis on Mental Health. *Frontiers in psychiatry*, *10*, 1012. https://doi.org/10.3389/fpsyt.2019.01012
22. Eissa, M. M., Barakat, A. M., Amer, E. I., & Younis, L. K. (2015). Could miltefosine be used as a therapy for toxoplasmosis?. Experimental parasitology, 157, 12–22. https://doi.org/10.1016/j.exppara.2015.06.005
23. Cope, J. R., Conrad, D. A., Cohen, N., Cotilla, M., DaSilva, A., Jackson, J., & Visvesvara, G. S. (2016). Use of the Novel Therapeutic Agent Miltefosine for the Treatment of Primary Amebic Meningoencephalitis: Report of 1 Fatal and 1 Surviving Case. Clinical infectious diseases : an official publication of the Infectious Diseases Society of America, 62(6), 774–776. https://doi.org/10.1093/cid/civ1021
24. Nau, R., Sörgel, F., & Eiffert, H. (2010). Penetration of drugs through the blood-cerebrospinal fluid/blood-brain barrier for treatment of central nervous system infections. *Clinical microbiology reviews*, *23*(4), 858–883. https://doi.org/10.1128/CMR.00007-10
25. Alday, P. H., & Doggett, J. S. (2017). Drugs in development for toxoplasmosis: advances, challenges, and current status. *Drug design, development and therapy*, *11*, 273–293. https://doi.org/10.2147/DDDT.S60973
26. McKie, J. H., Douglas, K. T., Chan, C., Roser, S. A., Yates, R., Read, M., Hyde, J. E., Dascombe, M. J., Yuthavong, Y., & Sirawaraporn, W. (1998). Rational drug design approach for overcoming drug resistance: application to pyrimethamine

resistance in malaria. *Journal of medicinal chemistry*, *41*(9), 1367–1370. https://doi.org/10.1021/jm970845u

27. Mukherjee, A., & Sadhukhan, G. C. (2016). Anti-malarial Drug Design by Targeting Apicoplasts: New Perspectives. Journal of pharmacopuncture, 19(1), 7–15. https://doi.org/10.3831/KPI.2016.19.001
28. Dittmar, A. J., Drozda, A. A., & Blader, I. J. (2016). Drug Repurposing Screening Identifies Novel Compounds That Effectively Inhibit Toxoplasma gondii Growth. mSphere, 1(2), e00042-15. https://doi.org/10.1128/mSphere.00042-15
29. Kucera, K., Koblansky, A. A., Saunders, L. P., Frederick, K. B., De La Cruz, E. M., Ghosh, S., & Modis, Y. (2010). Structure-based analysis of Toxoplasma gondii profilin: a parasite-specific motif is required for recognition by Toll-like receptor 11. Journal of molecular biology, 403(4), 616–629. https://doi.org/10.1016/j.jmb.2010.09.022
30. Sanford, A. G., Schulze, T. T., Potluri, L. P., Watson, G. F., Darner, E. B., Zach, S. J., Hemsley, R. M., Wallick, A. I., Warner, R. C., Charman, S. A., Wang, X., Vennerstrom, J. L., & Davis, P. H. (2018). Derivatives of a benzoquinone acyl hydrazone with activity against Toxoplasma gondii. International journal for parasitology. Drugs and drug resistance, 8(3), 488–492. https://doi.org/10.1016/j.ijpddr.2018.11.001
31. Pajouhesh, H., & Lenz, G. R. (2005). Medicinal chemical properties of successful central nervous system drugs. NeuroRx : the journal of the American Society for Experimental NeuroTherapeutics, 2(4), 541–553. https://doi.org/10.1602/neurorx.2.4.541
32. Field, M. C., Horn, D., Fairlamb, A. H., Ferguson, M. A., Gray, D. W., Read, K. D., De Rycker, M., Torrie, L. S., Wyatt, P. G., Wyllie, S., & Gilbert, I. H. (2017). Anti-trypanosomatid drug discovery: an ongoing challenge and a continuing

need. Nature reviews. Microbiology, 15(4), 217–231. Advance online publication. https://doi.org/10.1038/nrmicro.2016.193

33. Kerns, E. H., Di, L., & Carter, G. T. (2008). In vitro solubility assays in drug discovery. Current drug metabolism, 9(9), 879–885. https://doi.org/10.2174/138920008786485100
34. Bohnert, T., & Gan, L. S. (2013). Plasma protein binding: from discovery to development. Journal of pharmaceutical sciences, 102(9), 2953–2994. https://doi.org/10.1002/jps.23614
35. Masimirembwa, C. M., Bredberg, U., & Andersson, T. B. (2003). Metabolic stability for drug discovery and development: pharmacokinetic and biochemical challenges. Clinical pharmacokinetics, 42(6), 515–528. https://doi.org/10.2165/00003088-200342060-00002
36. McFarland, M. M., Zach, S. J., Wang, X., Potluri, L. P., Neville, A. J., Vennerstrom, J. L., & Davis, P. H. (2016). Review of Experimental Compounds Demonstrating Anti-Toxoplasma Activity. Antimicrobial agents and chemotherapy, 60(12), 7017–7034. https://doi.org/10.1128/AAC.01176-16
37. Martens, M. C., Won, M. M., Won, H. I., Schulze, T. T., Judge, A. K., Neville, A. J., Vennerstrom, J. L., & Davis, P. H. (2020). In vitro selection implicates ROP1 as a resistance gene for an experimental therapeutic benzoquinone acyl hydrazone in Toxoplasma gondii. Antimicrobial agents and chemotherapy, AAC.01040-20. Advance online publication. https://doi.org/10.1128/AAC.01040-20
38. Sidik, S. M., Huet, D., Ganesan, S. M., Huynh, M. H., Wang, T., Nasamu, A. S., Thiru, P., Saeij, J., Carruthers, V. B., Niles, J. C., & Lourido, S. (2016). A

Genome-wide CRISPR Screen in Toxoplasma Identifies Essential Apicomplexan Genes. Cell, 166(6), 1423–1435.e12. https://doi.org/10.1016/j.cell.2016.08.019

39. Wang, J. L., Huang, S. Y., Behnke, M. S., Chen, K., Shen, B., & Zhu, X. Q. (2016). The Past, Present, and Future of Genetic Manipulation in Toxoplasma gondii. Trends in parasitology, 32(7), 542–553. https://doi.org/10.1016/j.pt.2016.04.013
40. Sirotkin K. (1986). Advantages to mutagenesis techniques generating populations containing the complete spectrum of single codon changes. Journal of theoretical biology, 123(3), 261–279. https://doi.org/10.1016/s0022-5193(86)80242-9
41. Zhai, B., He, J. J., Elsheikha, H. M., Li, J. X., Zhu, X. Q., & Yang, X. (2020). Transcriptional changes in Toxoplasma gondii in response to treatment with monensin. Parasites & vectors, 13(1), 84. https://doi.org/10.1186/s13071-020-3970-1
42. Zhu, J., Zhao, Q., Katsevich, E., & Sabatti, C. (2019). Exploratory Gene Ontology Analysis with Interactive Visualization. Scientific reports, 9(1), 7793. https://doi.org/10.1038/s41598-019-42178-x
43. McGovern, K. E., & Wilson, E. H. (2013). Dark side illuminated: imaging of Toxoplasma gondii through the decades. Parasites & vectors, 6(1), 334. https://doi.org/10.1186/1756-3305-6-334
44. Liu, S., Du, Y., Ma, H., Liang, Q., Zhu, X., & Tian, J. (2019). Preclinical comparison of regorafenib and sorafenib efficacy for hepatocellular carcinoma using multimodality molecular imaging. Cancer letters, 453, 74–83. https://doi.org/10.1016/j.canlet.2019.03.037
45. Spangenberg, T., Burrows, J. N., Kowalczyk, P., McDonald, S., Wells, T. N., & Willis, P. (2013). The open access malaria box: a drug discovery catalyst for

neglected diseases. PloS one, 8(6), e62906. https://doi.org/10.1371/journal.pone.0062906

46. Randrianarivelojosia, M., Harisoa, J. L., Rabarijaona, L. P., Raharimalala, L. A., Ranaivo, L., Pietra, V., Duchemin, J. B., Rakotomanana, F., Robert, V., Mauclere, P., & Ariey, F. (2002). In vitro sensitivity of Plasmodium falciparum to amodiaquine compared with other major antimalarials in Madagascar. Parassitologia, 44(3-4), 141–147.
47. Walsh, S. E., Maillard, J. Y., Russell, A. D., Catrenich, C. E., Charbonneau, D. L., & Bartolo, R. G. (2003). Activity and mechanisms of action of selected biocidal agents on Gram-positive and -negative bacteria. *Journal of applied microbiology*, *94*(2), 240–247. https://doi.org/10.1046/j.1365-2672.2003.01825.x
48. Macsics, R., Hackl, M. W., Fetzer, C., Mostert, D., Bender, J., Layer, F., & Sieber, S. A. (2020). Comparative Target Analysis of Chlorinated Biphenyl Antimicrobials Highlights MenG as a Molecular Target of Triclocarban. Applied and environmental microbiology, 86(16), e00933-20. https://doi.org/10.1128/AEM.00933-20
49. Halden, R. U., Lindeman, A. E., Aiello, A. E., Andrews, D., Arnold, W. A., Fair, P., Fuoco, R. E., Geer, L. A., Johnson, P. I., Lohmann, R., McNeill, K., Sacks, V. P., Schettler, T., Weber, R., Zoeller, R. T., & Blum, A. (2017). The Florence Statement on Triclosan and Triclocarban. Environmental health perspectives, 125(6), 064501. https://doi.org/10.1289/EHP1788
50. Ingram-Sieber, K., Cowan, N., Panic, G., Vargas, M., Mansour, N. R., Bickle, Q. D., Wells, T. N., Spangenberg, T., & Keiser, J. (2014). Orally active antischistosomal early leads identified from the open access malaria box. PLoS neglected tropical diseases, 8(1), e2610. https://doi.org/10.1371/journal.pntd.0002610

51. Wu, J., Wang, C., Leas, D., Vargas, M., White, K. L., Shackleford, D. M., Chen, G., Sanford, A. G., Hemsley, R. M., Davis, P. H., Dong, Y., Charman, S. A., Keiser, J., & Vennerstrom, J. L. (2018). Progress in antischistosomal N,N'-diaryl urea SAR. Bioorganic & medicinal chemistry letters, 28(3), 244–248. https://doi.org/10.1016/j.bmcl.2017.12.064

52. Leas D, Sanford A., Wu J., Jianbo C., Maricel K., Wittlin S., Hemsely, R., Darner, E., Lui, L., Davis, P., Vennesrtrom J. (2021). Diaryl Ureas as an Antiprotozoal Chemotype. *ACS Infectious Diseases*. Submitted for Publication.

53. Barna, F., Debache, K., Vock, C. A., Küster, T., & Hemphill, A. (2013). In vitro effects of novel ruthenium complexes in Neospora caninum and Toxoplasma gondii tachyzoites. *Antimicrobial agents and chemotherapy*, *57*(11), 5747–5754. https://doi.org/10.1128/AAC.02446-12

54. Martins-Duarte, É. S., Carias, M., Vommaro, R., Surolia, N., & de Souza, W. (2016). Apicoplast fatty acid synthesis is essential for pellicle formation at the end of cytokinesis in Toxoplasma gondii. *Journal of cell science*, *129*(17), 3320–3331

55. Kennedy, K., Crisafulli, E. M., & Ralph, S. A. (2019). Delayed Death by Plastid Inhibition in Apicomplexan Parasites. *Trends in parasitology*, *35*(10), 747–759. https://doi.org/10.1016/j.pt.2019.07.010

56. Li, Z. H., Ramakrishnan, S., Striepen, B., & Moreno, S. N. (2013). Toxoplasma gondii relies on both host and parasite isoprenoids and can be rendered sensitive to atorvastatin. *PLoS pathogens*, *9*(10), e1003665. https://doi.org/10.1371/journal.ppat.1003665

57. Ramakrishnan, S., Docampo, M. D., Macrae, J. I., Pujol, F. M., Brooks, C. F., van Dooren, G. G., Hiltunen, J. K., Kastaniotis, A. J., McConville, M. J., & Striepen, B. (2012). Apicoplast and endoplasmic reticulum cooperate in fatty acid biosynthesis in apicomplexan parasite Toxoplasma gondii. *The Journal of*

biological chemistry, *287*(7), 4957–4971. https://doi.org/10.1074/jbc.M111.310144

58. McLeod, R., Muench, S. P., Rafferty, J. B., Kyle, D. E., Mui, E. J., Kirisits, M. J., Mack, D. G., Roberts, C. W., Samuel, B. U., Lyons, R. E., Dorris, M., Milhous, W. K., & Rice, D. W. (2001). Triclosan inhibits the growth of Plasmodium falciparum and Toxoplasma gondii by inhibition of apicomplexan Fab I. *International journal for parasitology*, *31*(2), 109–113. https://doi.org/10.1016/s0020-7519(01)00111-4
59. Imlay, L., & Odom, A. R. (2014). Isoprenoid metabolism in apicomplexan parasites. *Current clinical microbiology reports*, *1*(3-4), 37–50. https://doi.org/10.1007/s40588-014-0006-7
60. Uddin, T., McFadden, G. I., & Goodman, C. D. (2017). Validation of Putative Apicoplast-Targeting Drugs Using a Chemical Supplementation Assay in Cultured Human Malaria Parasites. *Antimicrobial agents and chemotherapy*, *62*(1), e01161-17. https://doi.org/10.1128/AAC.01161-17
61. Li, Z. H., Ramakrishnan, S., Striepen, B., & Moreno, S. N. (2013). Toxoplasma gondii relies on both host and parasite isoprenoids and can be rendered sensitive to atorvastatin. *PLoS pathogens*, *9*(10), e1003665. https://doi.org/10.1371/journal.ppat.1003665
62. Portes, J., Netto, C. D., da Silva, A. J., Costa, P. R., DaMatta, R. A., dos Santos, T. A., De Souza, W., & Seabra, S. H. (2012). A new type of pterocarpanquinone that affects Toxoplasma gondii tachyzoites in vitro. *Veterinary parasitology*, *186*(3-4), 261–269. https://doi.org/10.1016/j.vetpar.2011.11.008
63. Martins-Duarte, E., de Souza, W., & Vommaro, R. C. (2008). Itraconazole affects Toxoplasma gondii endodyogeny. *FEMS microbiology letters*, *282*(2), 290–298. https://doi.org/10.1111/j.1574-6968.2008.01130.x

64. Abdelbaset, A. E., Fox, B. A., Karram, M. H., Abd Ellah, M. R., Bzik, D. J., & Igarashi, M. (2017). Lactate dehydrogenase in Toxoplasma gondii controls virulence, bradyzoite differentiation, and chronic infection. *PloS one*, *12*(3), e0173745. https://doi.org/10.1371/journal.pone.0173745

65. Nare, B., Allocco, J. J., Liberator, P. A., & Donald, R. G. (2002). Evaluation of a cyclic GMP-dependent protein kinase inhibitor in treatment of murine toxoplasmosis: gamma interferon is required for efficacy. *Antimicrobial agents and chemotherapy*, *46*(2), 300–307. https://doi.org/10.1128/aac.46.2.300-307.2002

66. Sullivan, W. J., Jr, & Jeffers, V. (2012). Mechanisms of Toxoplasma gondii persistence and latency. *FEMS microbiology reviews*, *36*(3), 717–733. https://doi.org/10.1111/j.1574-6976.2011.00305.x

67. Huskinson-Mark, J., Araujo, F. G., & Remington, J. S. (1991). Evaluation of the effect of drugs on the cyst form of Toxoplasma gondii. *The Journal of infectious diseases*, *164*(1), 170–171. https://doi.org/10.1093/infdis/164.1.170

68. Isabelle Coppens, Cyrille Botté, Chapter 8 - Biochemistry and metabolism of Toxoplasma gondii: lipid synthesis and uptake, Editor(s): Louis M. Weiss, Kami Kim, Toxoplasma gondii (Third Edition), Academic Press, 2020, Pages 367-395, ISBN 9780128150412, https://doi.org/10.1016/B978-0-12-815041-2.00008-6.

69. Bottova, I., Sauder, U., Olivieri, V., Hehl, A. B., & Sonda, S. (2010). The P-glycoprotein inhibitor GF120918 modulates Ca2+-dependent processes and lipid metabolism in Toxoplasma gondii. *PloS one*, *5*(4), e10062. https://doi.org/10.1371/journal.pone.0010062

70. Nolan, S. J., Romano, J. D., Kline, J. T., & Coppens, I. (2018). Novel Approaches To Kill Toxoplasma gondii by Exploiting the Uncontrolled Uptake of Unsaturated Fatty Acids and Vulnerability to Lipid Storage Inhibition of the

Parasite. *Antimicrobial agents and chemotherapy*, *62*(10), e00347-18. https://doi.org/10.1128/AAC.00347-18

71. Coppens I. (2013). Targeting lipid biosynthesis and salvage in apicomplexan parasites for improved chemotherapies. *Nature reviews. Microbiology*, *11*(12), 823–835. https://doi.org/10.1038/nrmicro3139
72. Escoll, P., Rolando, M., Gomez-Valero, L., & Buchrieser, C. (2013). From amoeba to macrophages: exploring the molecular mechanisms of Legionella pneumophila infection in both hosts. *Current topics in microbiology and immunology*, *376*, 1–34. https://doi.org/10.1007/82_2013_351